NEDC-23856-2
December 1978

OXYGEN SUPPRESSION IN BOILING WATER REACTORS

QUARTERLY REPORT 3

April 1 to June 30, 1978

Contract EY-C-02-2985

Prepared by E. L. Burley

for the Commonwealth Research Corp.

Reviewed: M. Siegler
M. Siegler, Manager
Chemical Testing

Reviewed: John D. Wiley for
W. R. DeHollander, Manager
Chemical and Radiological
Engineering

Approved: B E Foster acting for
D.R. Wilkins, Manager
Plant Design and Analysis

Program Manager For Commonwealth Research Corp.: J. C. Blomgren

Program Manager For D.O.E.: P. J. Pettit

NUCLEAR ENERGY ENGINEERING DIVISION • GENERAL ELECTRIC COMPANY
SAN JOSE, CALIFORNIA 95125

GENERAL ELECTRIC

REA

DISCLAIMER

LEGAL NOTICE

This report was prepared by the General Electric Company (GE) as an account of work sponsored by the Department of Energy (DOE). Neither DOE, members of DOE, nor GE, nor any person acting on behalf of either, including Commonwealth Research Corporation:

a. *Makes any warranty or representation, express or implied, with respect to the accuracy, completeness, or usefulness of the information contained in this report, or that the use of any information, apparatus, method, or process disclosed in this report may not infringe privately owned rights; or*

b. *Assumes any liabilities with respect to the use of, or for damages resulting from the use of, any information, apparatus, method, or process disclosed in this report.*

TABLE OF CONTENTS

LIST OF ILLUSTRATIONS

LIST OF ILLUSTRATION (continued)

LIST OF TABLES

1. INTRODUCTION

Boiling water reactors (BWR's) generally use high purity, no-additive feedwater. The primary recirculating coolant is neutral pH and contains 100 to 300 ppb oxygen and stoichiometrically related dissolved hydrogen. However, oxygenated water increases austenitic stainless steel susceptibility to intergranular stress-corrosion cracking (IGSCC) when other requisite factors such as stress and sensitization are present. Thus, reduction or elimination of the oxygen in BWR water may preclude cracking incidents. One approach to reduction of the BWR coolant oxygen concentration is to adopt alternate water chemistry (AWC) conditions using an additive(s) to suppress or reverse radiolytic oxygen formation. Several additives are available to do this but they have seen only limited and specialized application in BWR's. This program is to perform an in-depth engineering evaluation of the potential suppression additives supported by critical experiments where required to resolve substantive uncertainties. On the basis of the engineering evaluation, the optimum oxygen suppression technique will be selected and a specific BWR plant recommended for an extended (3-year) plant demonstration experiment.

The program is funded by the United States Department of Energy (DOE) and managed by The Commonwealth Research Corporation. The preliminary engineering evaluations and related test work as described in this progress report are being done by The Nuclear Engineering Division of the General Electric Company.

2. SUMMARY

2.1 HYDROGEN FLOW SHEET

The data correlations from five test reactors used to calculate the hydrogen addition flow sheet[1] were compared with results recently received from the Studsvik reactor in Sweden. Direct application of the Swedish data is misleading; but, when translated into a form applicable to the BWR configuration, agreement is good.

2.2 AMMONIA FLOW SHEET

Studsvik tests of an ammonia flow sheet disagree significantly with calculations based on Atomic Energy of Canada, Limited (AECL) testing and experience. Because of the sizable extrapolations required to compare the two sets of data, and the depth and certainty of the Canadian data, the ammonia flow sheet formulated for this study will not be revised.

2.3 PRIMARY SYSTEM RADIATION LEVELS

The primary system dose rate measurement program at Dresden 2/3 was completed. Twelve remote area monitoring stations were used to follow system radiation levels as reactor power was varied from zero to full power; clean-up flows ranged from 2 to 5% of the feed water flow; and recirculation rates were adjusted between 40 and 100% of full recirculation flow. Although reactor power was the primary determining factor, minor but significant effects of varying flow rates were also observed.

2.4 TURBINE BUILDING RADIATION LEVELS

Source terms for the steam activity to be used in the calculation of turbine building full-power radiation levels were set at: 23.5 μ Ci of N-16/g, 11.5 μ Ci of C-15/g and 2.2 μ Ci of O-19/g.

2.5 OFF-GAS SYSTEM STUDIES

Preparations were continued to measure trace impurities in the Nine Mile Point offgas.

2.6 COOLANT LEAKAGE MONITORING

An in-line sodium monitor using a specific-ion electrode has been received and set up for laboratory standardization and testing. A similar low-level chloride-ion monitor is also expected to be received in the near future for testing and evaluation.

2.7 CONSTANT EXTENSION RATE MATERIALS TESTS

The main thrusts of the constant extension rate tests (CERTs) completed this quarter were to establish base line failure data and to devise an adequately sensitive CERT test to discriminate between the small differences in materials performance which are anticipated. The test specimen design will have a circumferential 0.033 cm (0.013-in.)-deep notch. Base line failure data were obtained in dry argon and in pure water with varying amounts of oxygen present.

2.8 STRAINING ELECTRODE TESTS

The first of three planned experiments was completed. The sample of Type-304 stainless steel welded and low temperature sensitized, was tested at an imposed potential of -0.75V to simulate the hydrogen additive environment. Failure was ductile with no evidence of IGSCC. In future experiments an actual hydrogen additive environment will determine the potential, and tests will be run with and without the normal added electrolyte to obtain comparative data for the three different test conditions.

2.9 DEMINERALIZER PERFORMANCE

Demineralizer performance in the ammonia-additive system is poor in comparison to current non-additive, neutral BWR's. In a deep-bed condensate

treatment system, for example, cation capacity is reduced to 5% of the current value, anion capacity to 10%, regenerant chemical concentrations must be doubled, and an additional ammonia wash is required during regeneration.

2.10 RADWASTE SYSTEM IMPACT

Operation of a radwaste system using an ammonia additive flow sheet and standard GE criteria for maximum tolerable cooling water leakage are clearly incompatible. System size and radwaste volume become intolerable because of the frequent regenerations and strength of chemicals required. Additional system constraints on leakage rate and composition are being formulated to determine whether any system with realistic allowable leakage and, at the same time, manageable radwaste volume, can be devised.

2.11 HYDROGEN ADDITION SYSTEM

Preliminary design of a hydrogen addition system has begun. Hydrogen gas will be dissolved in a side stream of feedwater which will then be returned to the main feedwater system in the vicinity of the reactor feed pumps.

2.12 OPERATIONAL CONSIDERATIONS

Standard industrial practices, precautions and hazards involved in handling hydrogen, ammonia, and hydrazine have been summarized.

2.13 ADDITIVE CONSUMPTION

The cost and availability of the three primary additives (exclusive of capital costs) are:

	Consumption kg/s	Consumption (lb/Day)	Cost ($/Day)	Availability
Hydrogen	2.6×10^{-3}	500	700	Readily available as bulk liquid.
Ammonia	0.13	24,000	1,200	Readily available as anhydrous liquid.
Hydrazine	0.13	24,000	44,000	Not presently available at this rate.

2.14 HYDROGEN RECYCLE

Off-gas recycle as a source of hydrogen is not feasible without hydrogen separation (from nitrogen) and purification. To help clarify the economics of such a purification and recycle process, a typical swing-cycle adsorption system has been defined.

3. DISCUSSION

3.1 TASK A. O_2 CONTROL – ADDITIVE CONCENTRATION REQUIREMENTS (T. L. Wong)

Objective. This task establishes the basic primary system flow sheets for the additives being considered. Optimum additive levels will be selected to allow a reasonable operating control range, prevent excessive and wasteful use of the chemical, and yet assure that minimum concentration requirements are always met.

Existing test information on the addition of hydrogen, ammonia and hydrazine to suppress oxygen formation has been used to predict mass balances for the GE BWR. In general, the results reported in the literature cannot be applied directly because the test equipment and conditions were significantly different from those for the BWR. The results from several different tests were used to develop methods of extrapolating the test data to the BWR conditions.

3.1.1 Hydrogen Flow Sheet Confirmation

The previously developed correlation for hydrogen addition to control oxygen level in the reactor water was compared with test data reported by ASEA-Atom on hydrogen addition experiments performed in the Studsvik reactor.[2] The major conclusion of this study is that the effect of adding hydrogen to the reactor water, when the hydrogen concentration in the steam from the test section is greater than 10 mℓ/kg, may be described by: $[H_2]^a[O_2]$ = constant, where a = 6. In a previous study at the heavy boiling water reactor (HBWR), a value of 2 for "a" correlated the experimental data.[3]

Initial interpretation of the ASEA-Atom data would be that oxygen concentration in the reactor water could be readily suppressed with a low quantity of hydrogen addition. However, it should be noted that the sixth power relationship only holds when hydrogen concentrations in the steam from the test section are greater than 10 mℓ/kg (890 ppb). Below 10 mℓ/kg, hydrogen had no distinguishable effect on the suppression of oxygen.

A comparison of the ASEA-Atom data and the previously developed correlation on hydrogen addition requirements (based on data from five test reactors as shown in Figure 3-1) can be made by comparing the hydrogen addition required to maintain 10 ppb oxygen in the reactor water. If an oxygen distribution factor of 100 is assumed for the steam and liquid, the ASEA-Atom data show that a hydrogen concentration at the inlet to the test section of ∿180 ppb is required. The experiments were conducted at 6.4 MPa (63 atm.). The power density was estimated by determining the energy required to produce the steam in the test section and the tests were conducted at subcooled inlet conditions. Using these values for the pressure and power density, the $[H_2]\ [P]^{1/2}$ and $[\text{Power Density}]^{1/2}$ terms for the ASEA-Atom data are 4.6×10^5 ppb $[Pa]^{1/2}$ (∿5500 ppb-$psi^{1/2}$) and 10 $(kw/\ell)^{1/2}$, respectively. There is good agreement between these values and the hydrogen-addition correlation. The differences are not significant enough to alter the existing flow sheets for hydrogen.

Burns and Moore[4] have conducted an analytical study on the radiation chemistry of the water coolant in a fuel channel of a pressure tube type BWR. Their predictions indicate that the outlet oxygen concentration decreases by a factor of 10 by having 2 STP cm^3/kg (180 ppb) hydrogen at the inlet. This value is in good agreement with the hydrogen addition requirement predicted by the previously developed correlation.

To date, the hydrogen addition correlation presented in the March 1978 quarterly report[1] is consistent with the experimental and analytical results reported in the open literature. Other information will be reviewed when available. The next logical step in evaluating the hydrogen addition correlation is to perform hydrogen addition experiments under conditions which are fairly representative of conditions in a BWR such as Dresden 2.

The major objective of these experiments would be to demonstrate that hydrogen addition does suppress the oxygen formation in the reactor water at the predicted levels. Initially, a base line test (no hydrogen addition) would be performed to identify core inlet and exit conditions such as, pressures, temperatures, flow rates and hydrogen and oxygen concentrations in both the vapor and liquid phases. Subsequently, hydrogen addition tests would be conducted to determine the effectiveness of added hydrogen in suppressing the radiolysis of water. The amount of

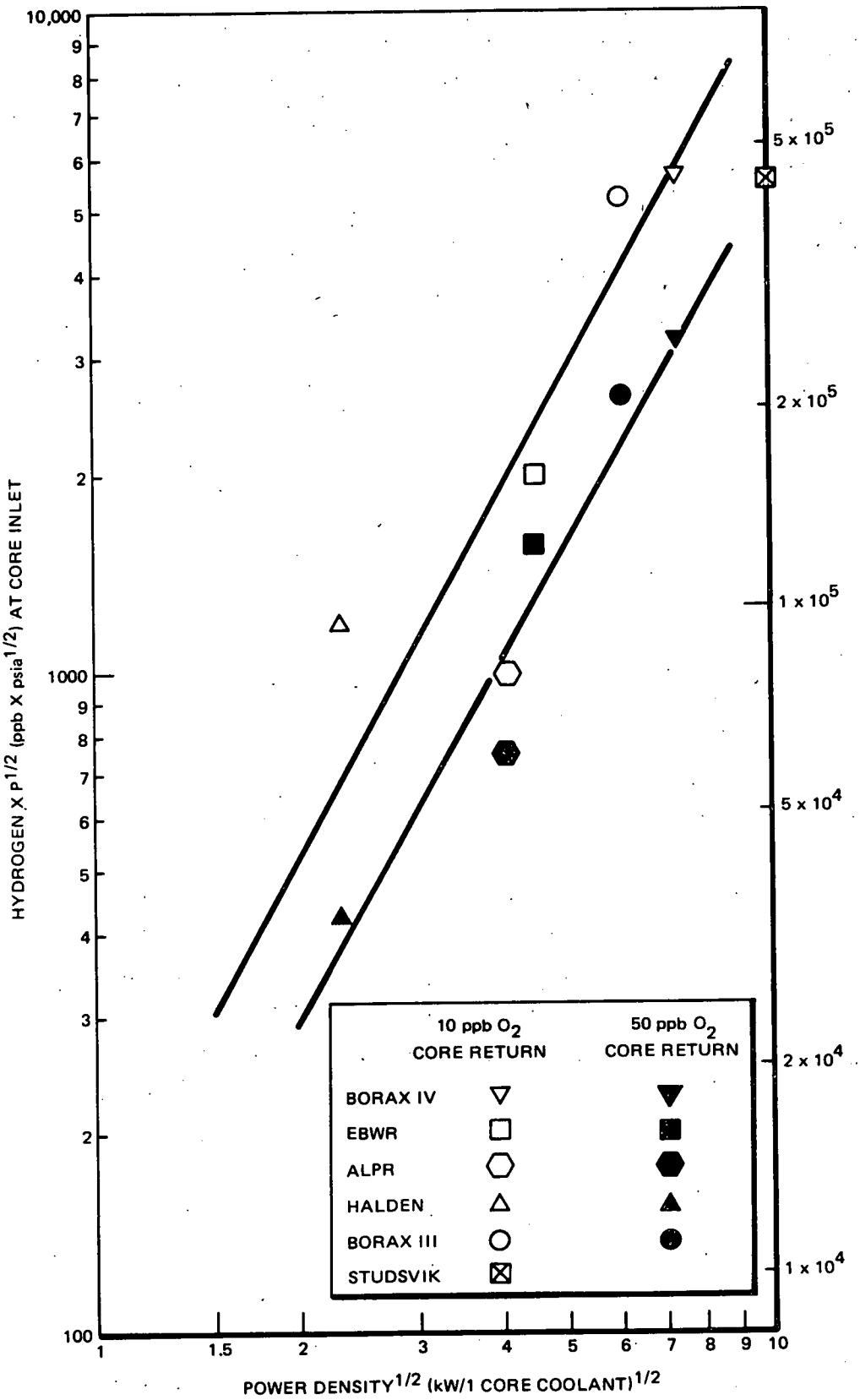

Figure 3-1. $[H_2]P^{1/2}$ Versus Power Density$^{1/2}$

hydrogen to be added is governed by the hydrogen concentration to be maintained at the core inlet. The equation (curve fit of Figure 3-1) for calculating the core inlet hydrogen concentration required to maintain 10 ppb oxygen in the core exit water is:

$$\ln [(H_2)\ P^{1/2}] = 5.0397 + 1.8048 \ln (P_D^{1/2})$$

where

P_D = core coolant power density (kW/ℓ of core coolant)

P = absolute pressure, Pascals x 0.145×10^{-3}, (psia)

$[H_2]$ = hydrogen concentration at core inlet (ppb)

For the hydrogen addition tests, the core inlet and exit conditions are again measured to provide a comparison with the base line test. Other test variables to be considered are core coolant power density and pressure.

3.1.2 Ammonia Flow Sheet Comparison

In addition to the hydrogen addition tests, ASEA-Atom also conducted tests with ammonia addition. The tests were performed for ammonia concentrations from 0.18 to 1.3 mg/kg for the test section inlet and with hydrogen addition at these low ammonia concentrations to prevent nitrite and nitrate formation. The tests were made at low ammonia concentrations because the Al-brass condensor tubes normally used in Sweden are sensitive to corrosion in media containing ammonia.

The ammonia radiolytic decomposition rate for Dresden 2 was estimated by using the ASEA-Atom $G(-NH_3)$ values for pure liquid and for the boiler section at $[H_2]$ = 270 ppb and $[NH_3]$ = 1 ppm. The decomposition rate was then corrected to the higher ammonia concentrations by using the Halden[3] ammonia decomposition correlation. The estimated ammonia addition required for Dresden 2 to maintain the ammonia concentration in the core exit water at 10 ppm is approximately a factor of 6 higher than the value reported in the March 1978 quarterly report.[1]

The estimation based on the ASEA-Atom data is questionable because extrapolation of the ASEA-Atom test results at low ammonia concentrations to the high concentrations for the BWR case is very great and may not be appropriate.

3.2 TASK B-1. N-16 DOSE RATE (G. F. Palino, H. R. Helmholz)

Objective. The primary source of radioactivity in the steam from a BWR is N-16 from the O-16 (n,p) reaction. The N-16 is formed in the water phase within the reactor core and then partitioned between the reactor water and steam during the phase separation. With standard BWR water chemistry, the bulk of the N-16 formed is quickly converted to relatively non-volatile anionic species, primarily NO_2^- or NO_3^-. Only a small amount of the N-16 formed in the core goes into the steam. As the oxidizing potential of the coolant is reduced by oxygen suppression additives, the proportion of the N-16 converted to relatively volatile, cationic (NH_4^+) species markedly increases and the fraction released to the steam rises commensurately. Measurements at the experimental boiling water reactor (EBWR)[5] showed a factor of 10 increase in steam radiation level. All three potential additives, i.e., H_2, NH_3, and N_2H_4, appear to act similarly in increasing the N-16 activity in the steam; however, the exact relationships need to be verified quantitatively so that the impact on turbine building shielding and/or operator-environment dose rates can be evaluated.

3.2.1 Measurement Program

Assessment of the impact of addition of chemical additives to suppress oxygen production in the BWR primary system demands reasonable estimates of the current non-additive BWR N-16/C-15 production rates and steam carryover, and of the primary system radiation levels. Consequently, base line studies were performed in January and February 1978 at Dresden 2 to obtain much of the required base line data. During May 1978 these measurements were completed, following installation of the necessary temporary instrumentation in Dresden 3.

3.2.2 Radiation Level Measurements

Recording radiation detection instrumentation was installed in the Dresden 3 turbine building to follow the radiation levels of selected components during operation. Installation was performed according to GE procedure TP 268.0306, Rev. A.

This phase of the program was to measure the partitioning of N-16 in the reactor and to determine whether or not this partitioning is dependent upon the reactor power and recirculation flow.

Twelve Remote Area Monitors (RAMs)+ were installed in the locations listed in Table 3-1.

Table 3-1
LOCATION OF RAMs+ INSTALLED AT DRESDEN 3

Location	RAM No.
Inlet to clean-up (CU) System Regenerative Heat Exchanger (A Side)	1,3
Inlet to CU System Non-Regenerative Heat Exchanger (A Side)	4
Outlet of CU System Non-Regenerative Heat Exchange (A Side)	2
"B" Steam Line - X Area	5,6
"A" Moisture Separator Drain	8
"B" Moisture Separator Vent Line	9
"A/B" Moisture Separator Steam Line to Low Pressure Turbines	10
"C" Steam Line - Turbine Building	7
Condenser Wall	12
"B" Steam Jet Air Ejector (SJAE) Discharge Line to Recombiner	11

The locations of the detectors on the particular systems were recorded photographically and reference distances were taken and recorded.

+Remote Area Monitor Systems; Eberline Instrument Corporation, Santa Fe, New Mexico.

The RAMs were connected in sets of six. The readout unit for the set in the reactor building was in a metal shed near the hatch on the mezzanine floor of Unit 2. The readout unit for the set in the turbine building was in the Unit 3 turbine building on the mezzanine level directly behind the turbine building sample sink. The block diagram for the electronics is presented in Figure 3-2. Each detector has been calibrated at the Vallecitos Nuclear Center (VNC) instrument calibration facility according to approved procedures.*

The basic premise of the data collection is that the output of the linear rate meter is directly proportional to the input count rate. Periodic reference calibration points were taken utilizing the scaler/timer. These calibration points were used as reference points for the interpretation of the graphical data.

In May, a trip to the Dresden site was made to ensure that the RAMs were installed to specification, to verify the instrument performance, to obtain background radiation level data, and to obtain radiation level data during the start up phase. Test plans were to follow reactor startup until the reactor was above the 50% power level, and then to leave the instruments in the remote data collection mode during the slow ascent to near 100% power.

All of the initial objectives were satisfied. Installation, although slow, was completed in time to connect and check out all instruments prior to startup. All instruments performed to specifications. Instrument performance was verified by activation of the check source and by comparing the check source net cpm with the check source net cpm observed at the time of calibration.

Reactor startup began May 10. By May 14 the unit thermal power was 1330 MW. At this point, data collection devices were put in the automatic collection mode while a search for and repair of a serious air leak were carried out. Close monitoring of radiation levels was begun again after the leak had been corrected.

*"Calibration of Eberline EC-3/DA-3CS Remote Area Monitor System", DRF A-00-268, Reactor Chemistry Unit Procedures.

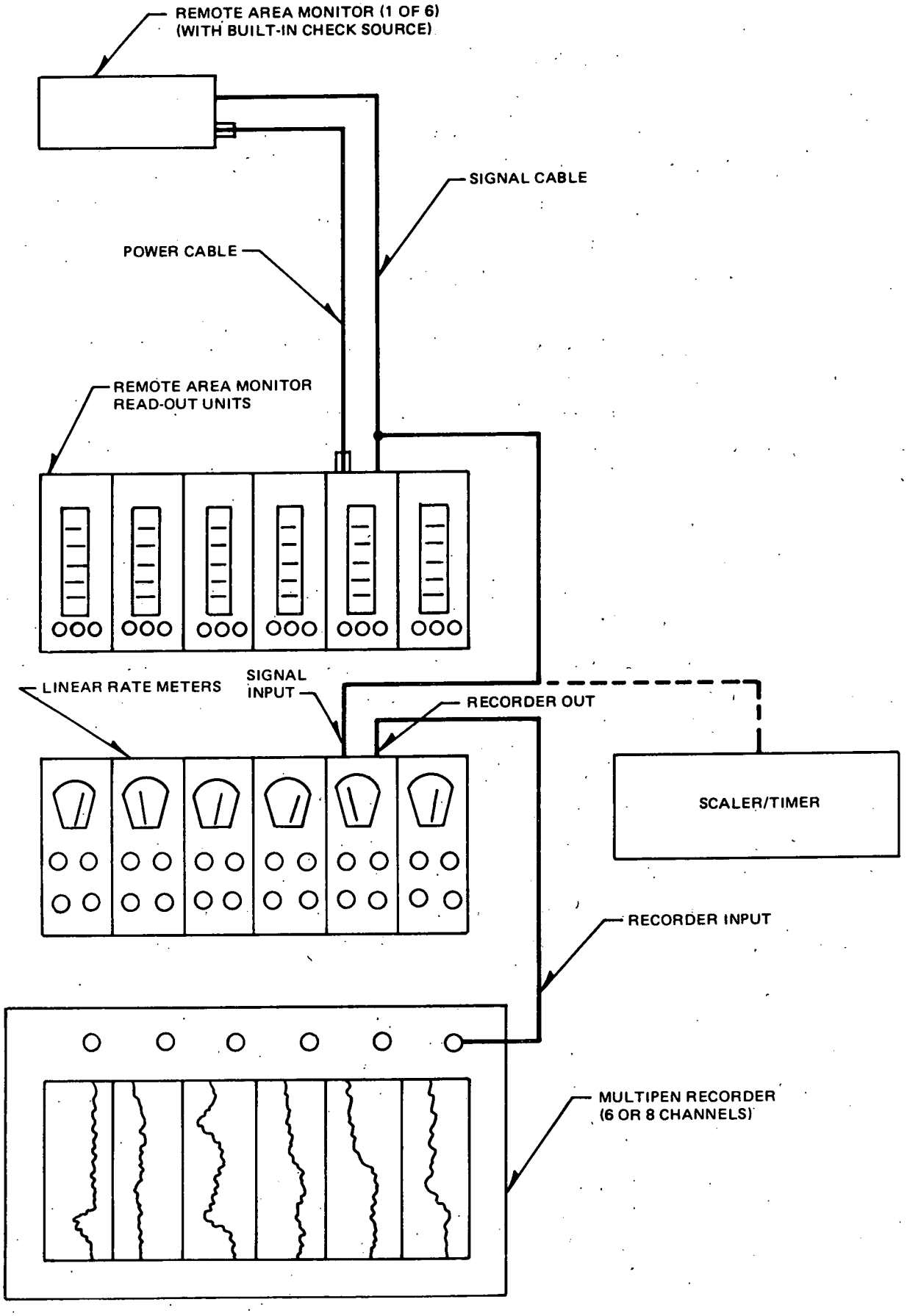

Figure 3-2. Remote Area Monitor Installation

On June 2, 1978, a return visit was made to The Dresden Site to obtain radiation level data during a scheduled power maneuver and to obtain follow-up chemistry data on Dresden 2. During the performance of the chemical measurements, radiation level data on Dresden 3 were taken continuously on the strip chart recorders and periodically using the scaler-timer.

The scaler-timer data were sufficient to obtain radiation level versus reactor power for all of the components surveyed. These data are summarized graphically in Figures 3-3 through 3-14. With the exception of the data on the steam-jet air ejector (SJAE) and on the reactor clean-up (CU) system (where radiation levels were not always power dependent due to flow variations) the data form a set of smooth curves, and dose rates vary rather consistently with reactor power.

3.2.3 Dependence of Primary System Radiation Levels Upon Recirculation Flow

During May 1978, a formal request was made to the Dresden operations staff to obtain radiation level measurements, using the existing installed RAMs, on the primary system components at two widely different recirculation flows, but at near identical thermal power. The measurements were made to obtain additional data on N-16 partitioning.

The test involved running the reactor down the 100% recirculation flow-power curve to near minimum flow, inserting a number of control rods, and increasing the recirculation flow to bring the unit back to the power level prior to the rod insertion. Radiation level data were taken for all of the RAMs prior to the fast flow drop test, at the end of the fast flow drop test, and after rod insertion and recovery to the low power point. These radiation data and relevant plant data are summarized in Table 3-2.

Table 3-2

RADIATION LEVEL MEASUREMENTS AT DRESDEN 3.
DEPENDENCE OF PRIMARY SYSTEM RADIATION
LEVELS UPON RECIRCULATION FLOW

Location	Test Condition: RAM No.	No. 1 Net (mR/h)	No. 2 Net (mR/h)	No. 3 Net (mR/h)	Δ%[a]
Inlet to Regenerative Heat Exchanger	1	967	584	596	+ 2.06
Outlet of Non-Regenerative Heat Exchanger	2	863	707	631	-10.67
Inlet to Regenerative Heat Exchanger	3	813	535	509	- 4.91
Inlet to Non-Regenerative Heat Exchanger	4	443	341	289	-15.44
"B" Steam Line - X Area	5	1060	545	515	- 5.40
"B" Steam Line - X Area	6	1105	549	521	- 5.10
Steam Line Turbine Building	7	1100	298	285	- 4.59
"A" Moisture Separator Drain	8	1718	458	448	- 2.08
"B" Moisture Separator Vent Line	9	1507	420	394	- 6.14
Steam Line from A/B Moisture Separator	10	951	258	241	- 6.48
"B" SJAE Discharge Line	11	16897	9332	8928	- 4.33
Condenser Wall	12	284	97	91	- 5.88
Operating Conditions					
Reactor Power (MW_t)		2395	1288	1281	
Reactor Power (MWe)		788	406	402.7	
Feedwater Flow (mlb/h)		9.27	4.71	4.68	
Core Flow (mlb/h)		97.66	40.36	55.19	
Recirc. Flow (mlb/h)		34.11	11.45	17.85	
Clean-up Flow (mlb/h)		0.285	9.285	0.2859	
Reactor Water Level (in.)		28.6	29.76	29.44	
Reactor Pressure (psig)		1018	936	963	

[a] $\Delta\% = \frac{[(2) - (3)]}{(2)} \times 100$

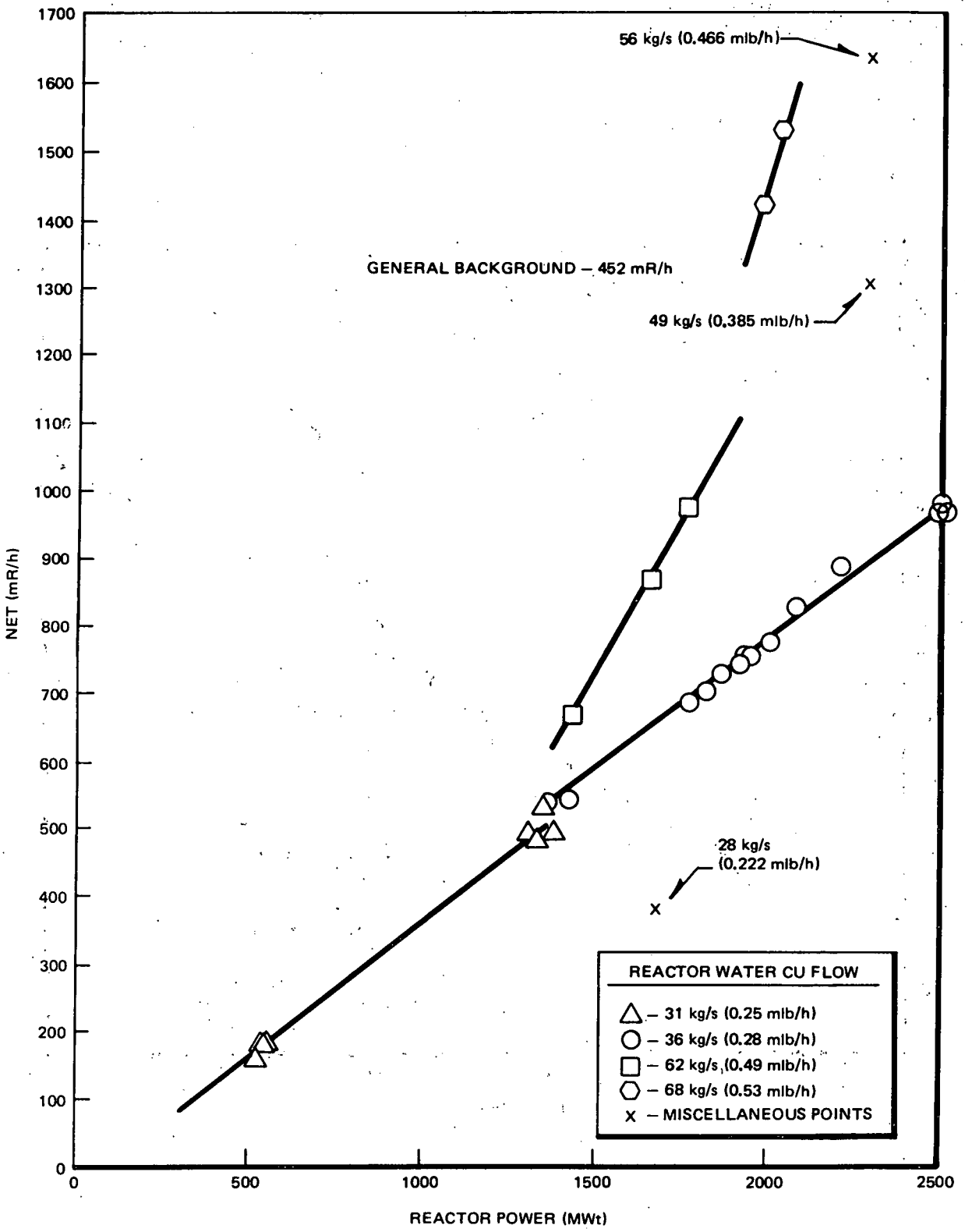

Figure 3-3. Inlet to Regenerative Heat Exchanger (A Side), Sensor No. 1

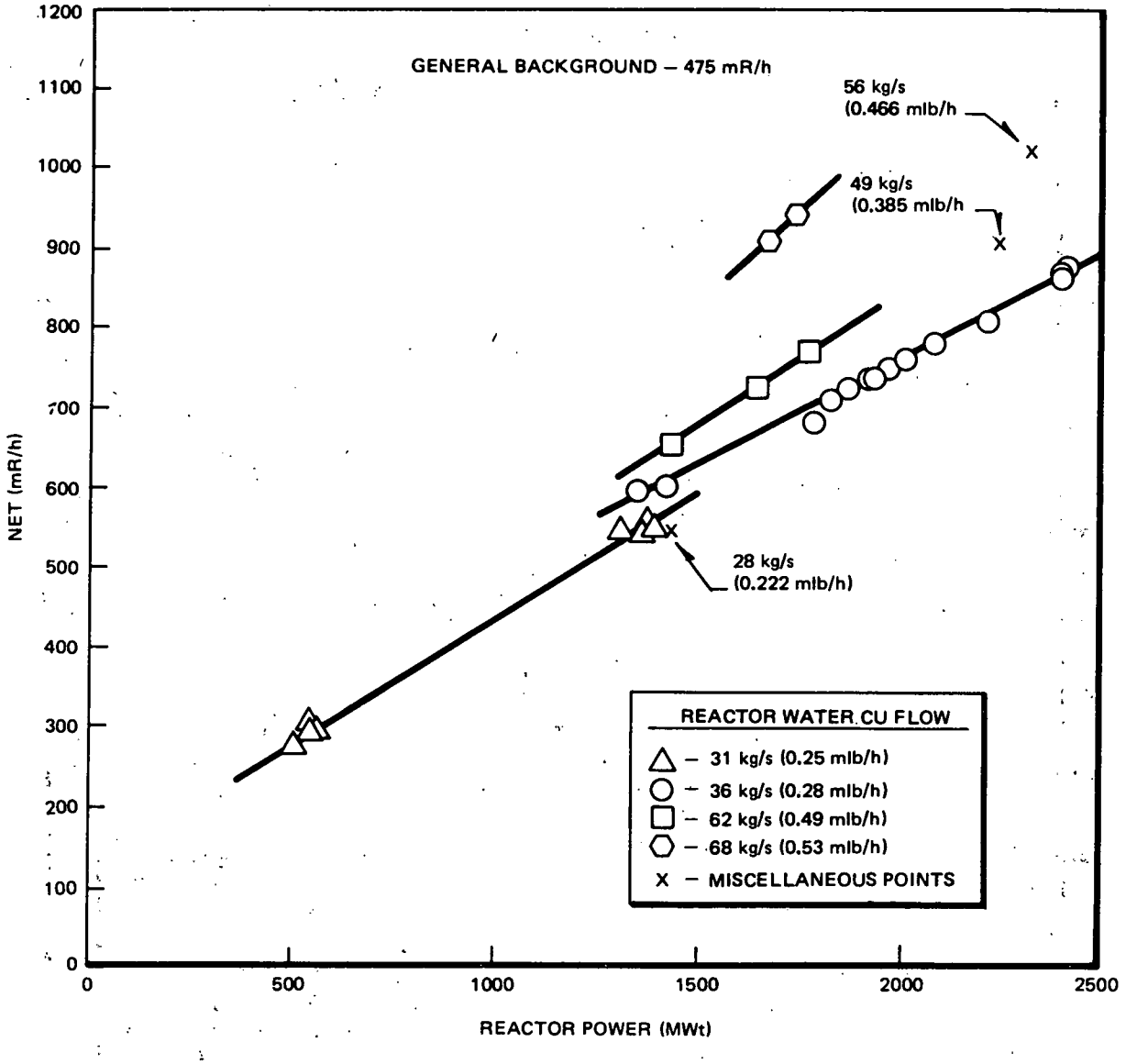

Figure 3-4. Outlet of Non-Regenerative Heat Exchange, Sensor No. 2

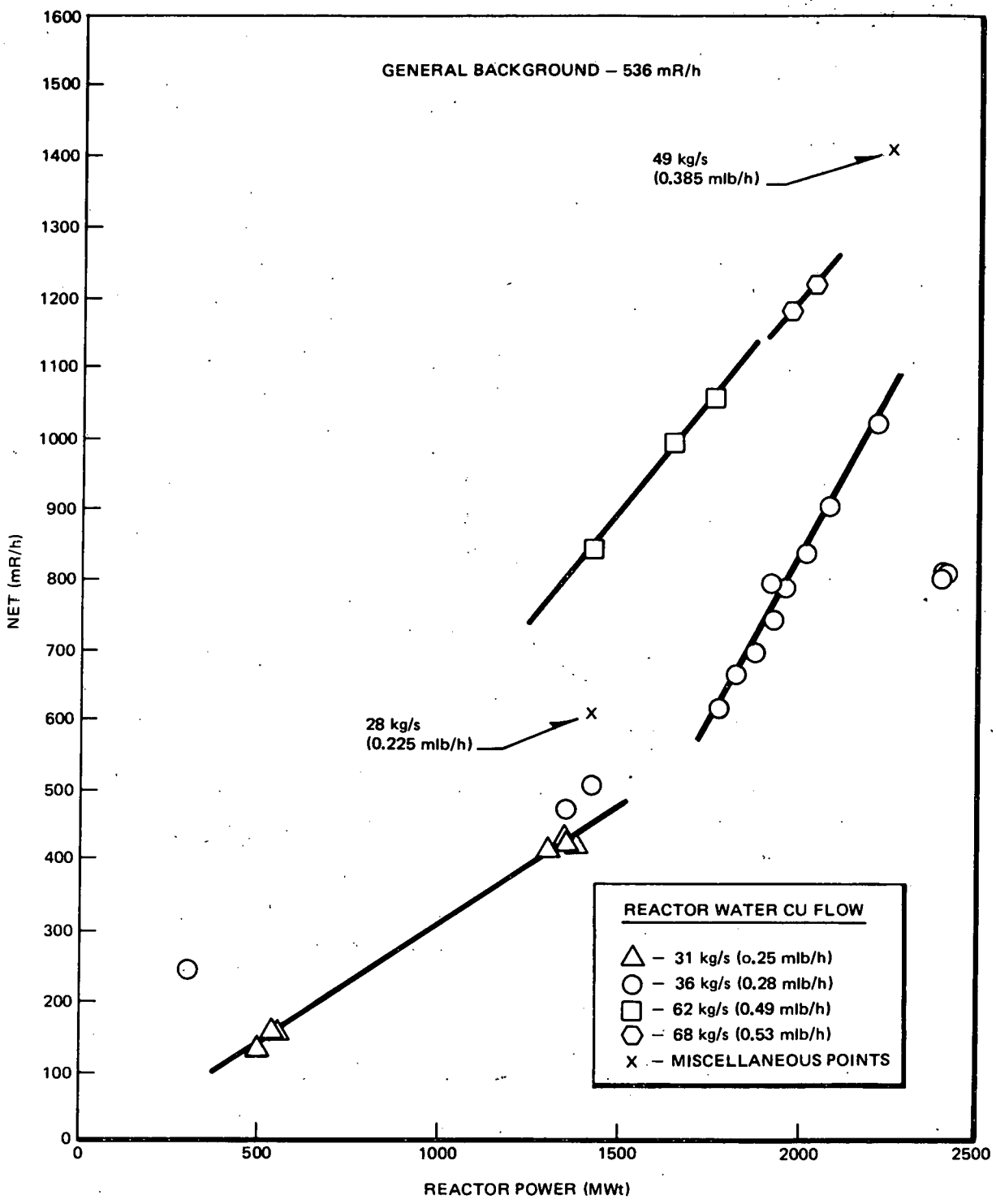

Figure 3-5. Inlet to Regenerative Heat Exchanger (A Side), Sensor No. 3

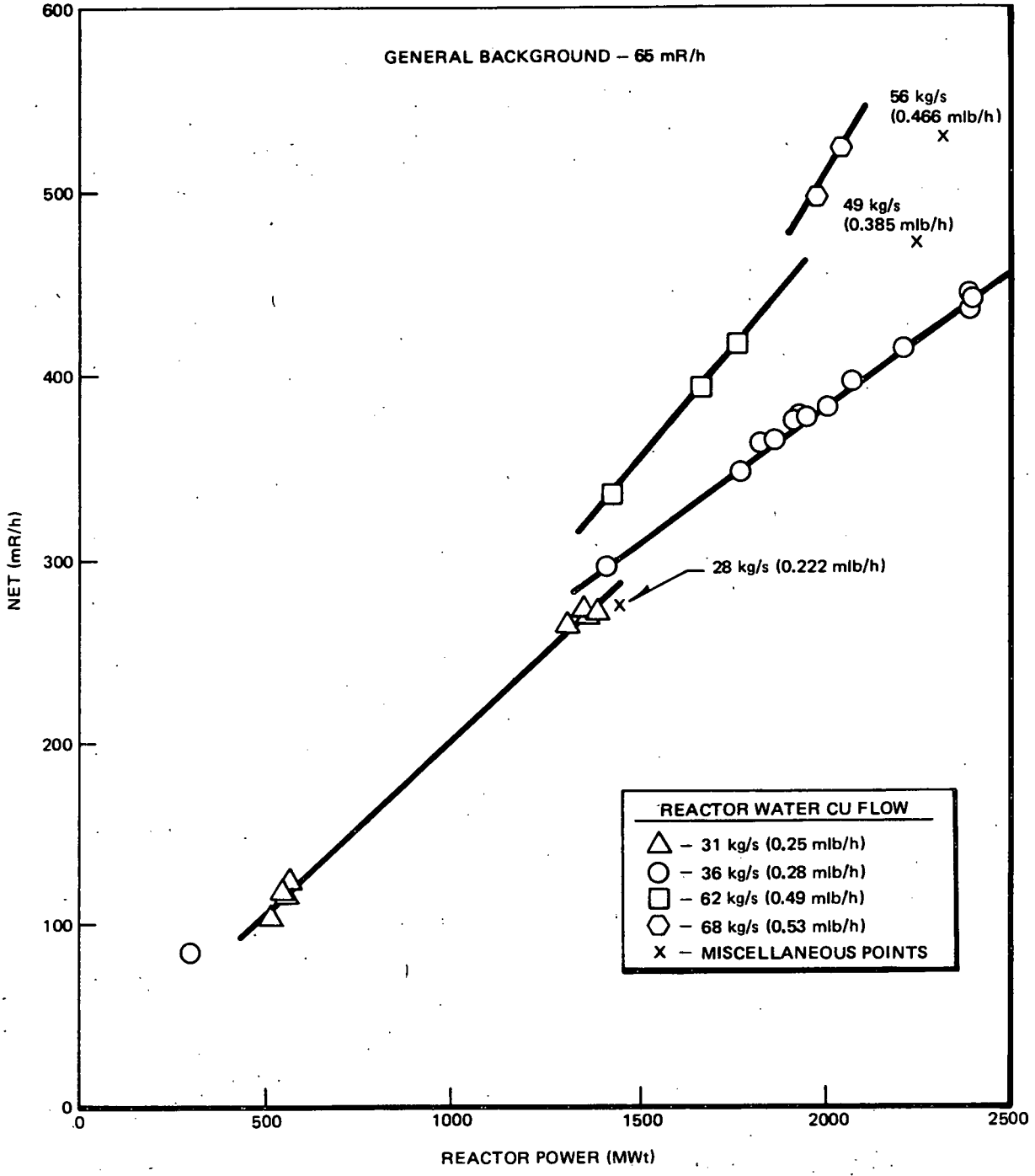

Figure 3-6. Inlet to Non-Regenerative Heat Exchanger, Sensor No. 4

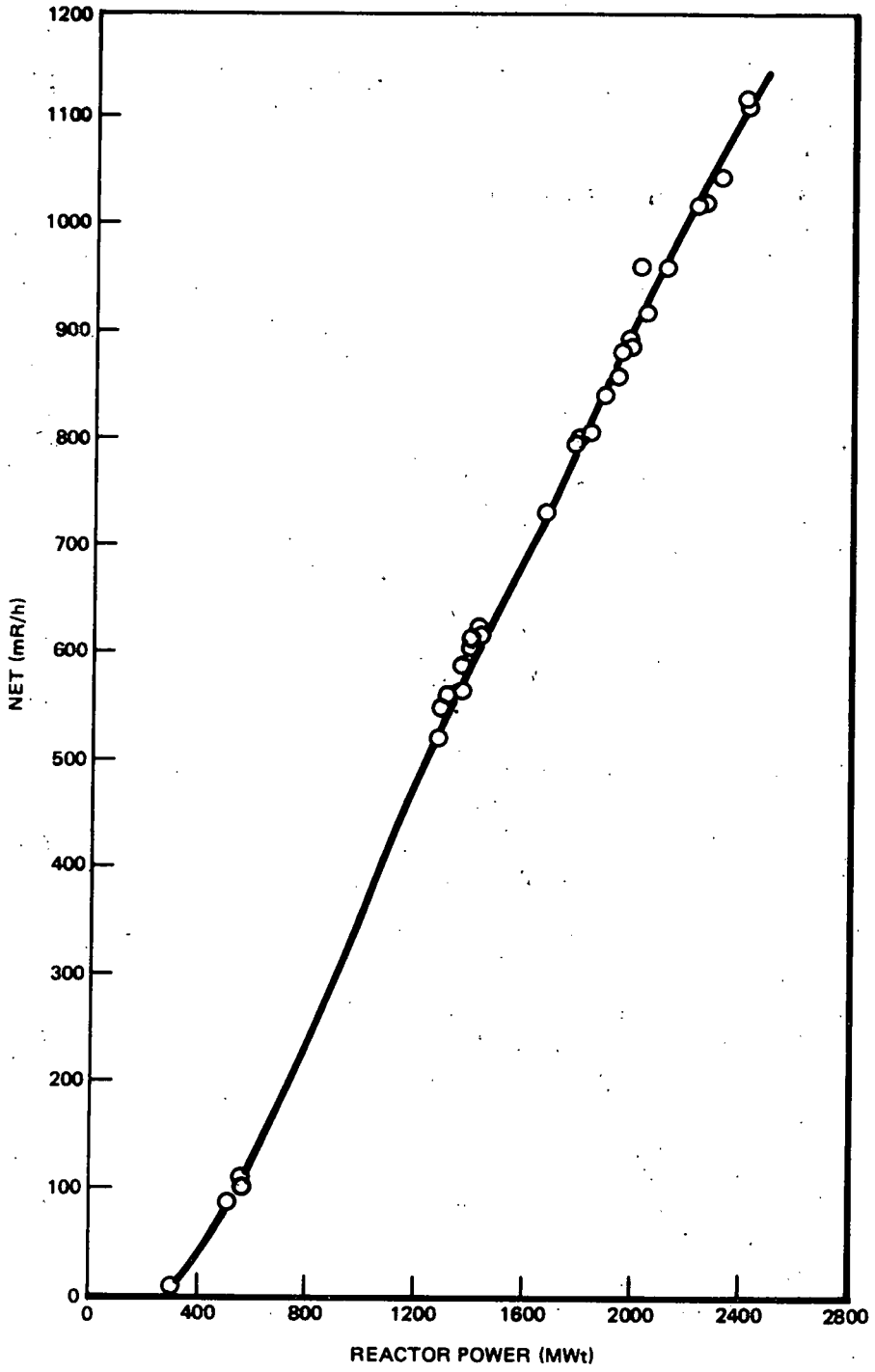

Figure 3-7. "B" Steam Line - X Area, Dresden 3, RAM No. 5

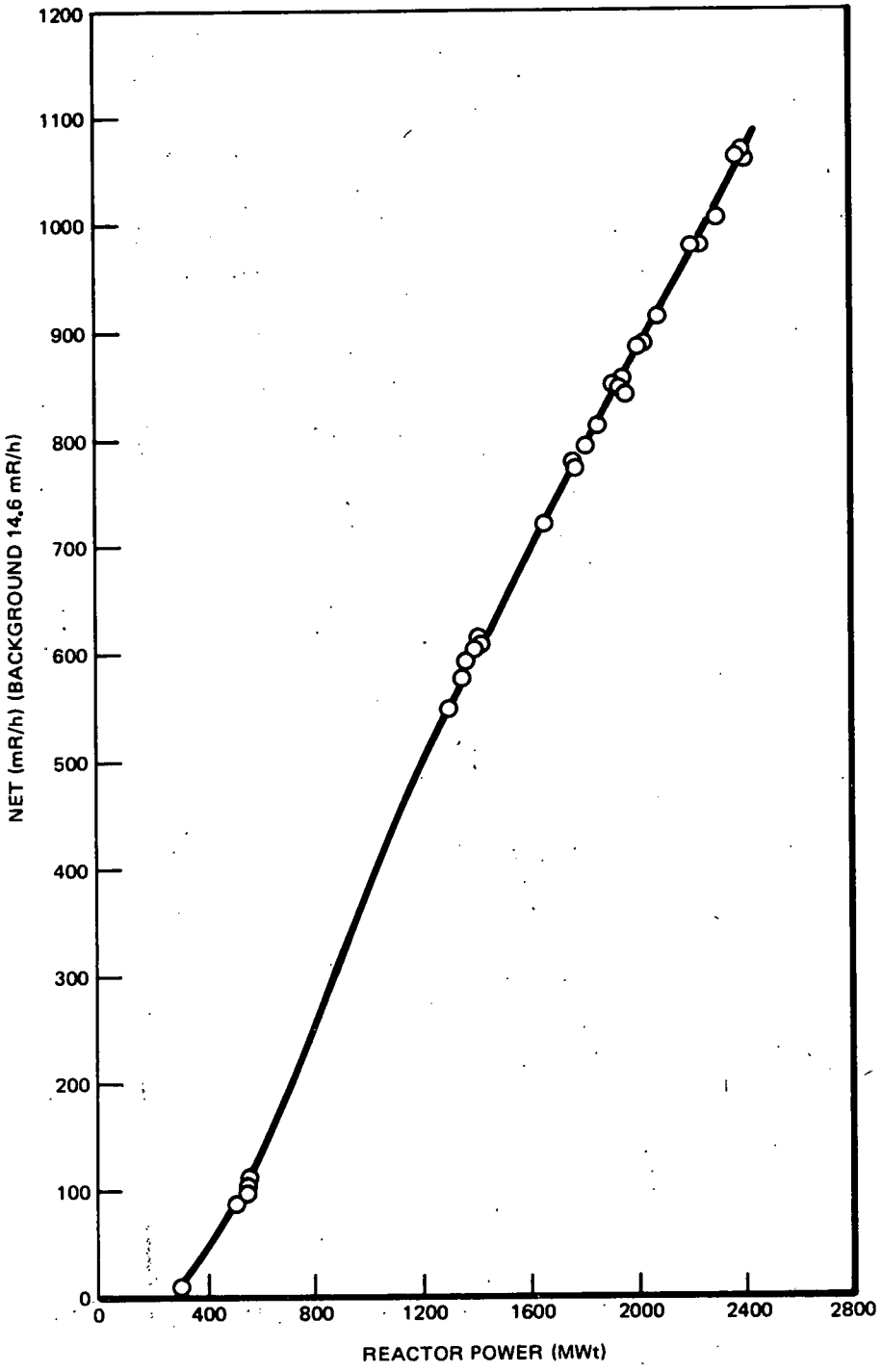

Figure 3-8. "B" Steam Line - X Area, Dresden 3, RAM No. 6

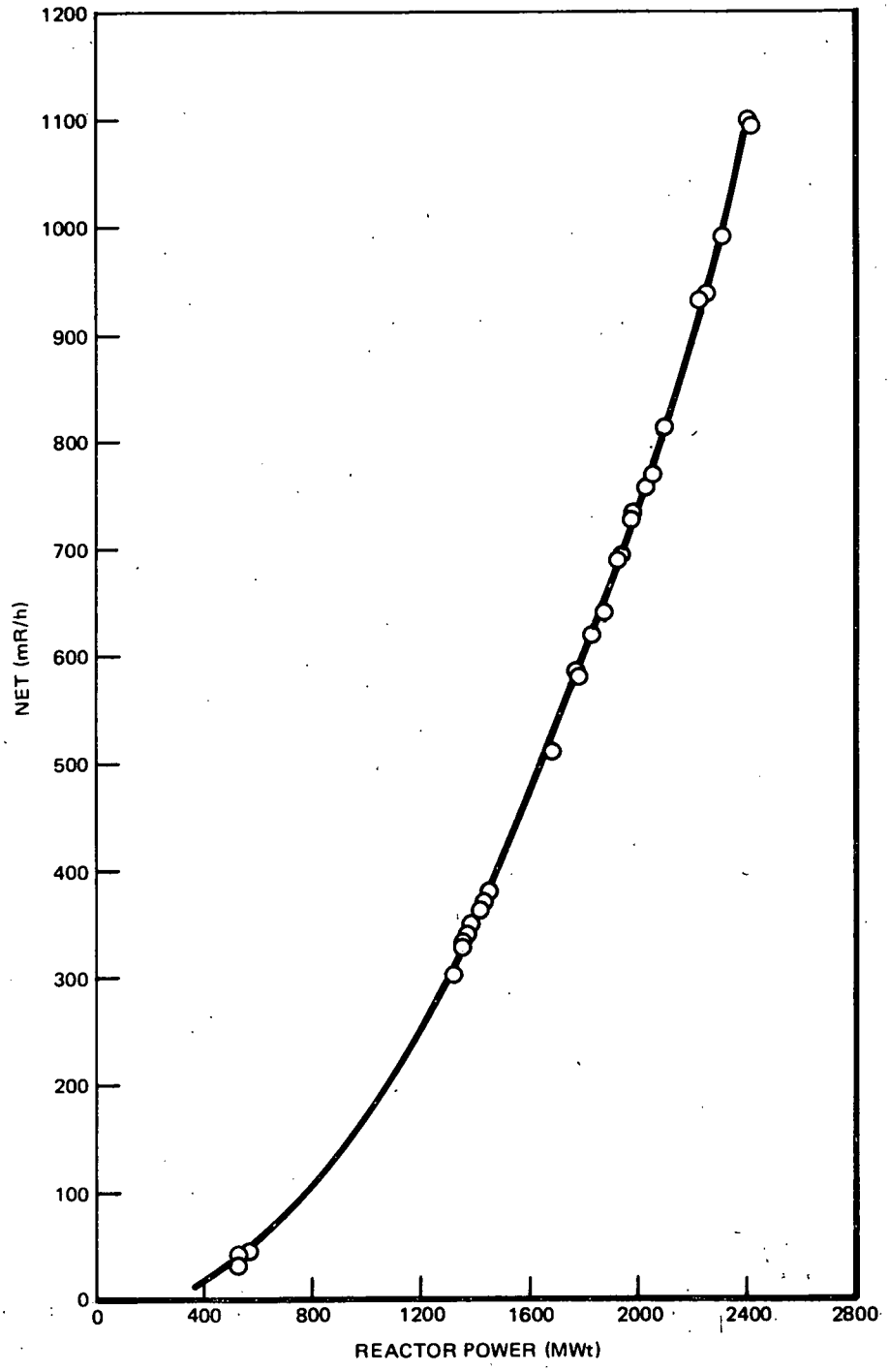

Figure 3-9. Steam Line - Turbine Building, Dresden 3, RAM No. 7

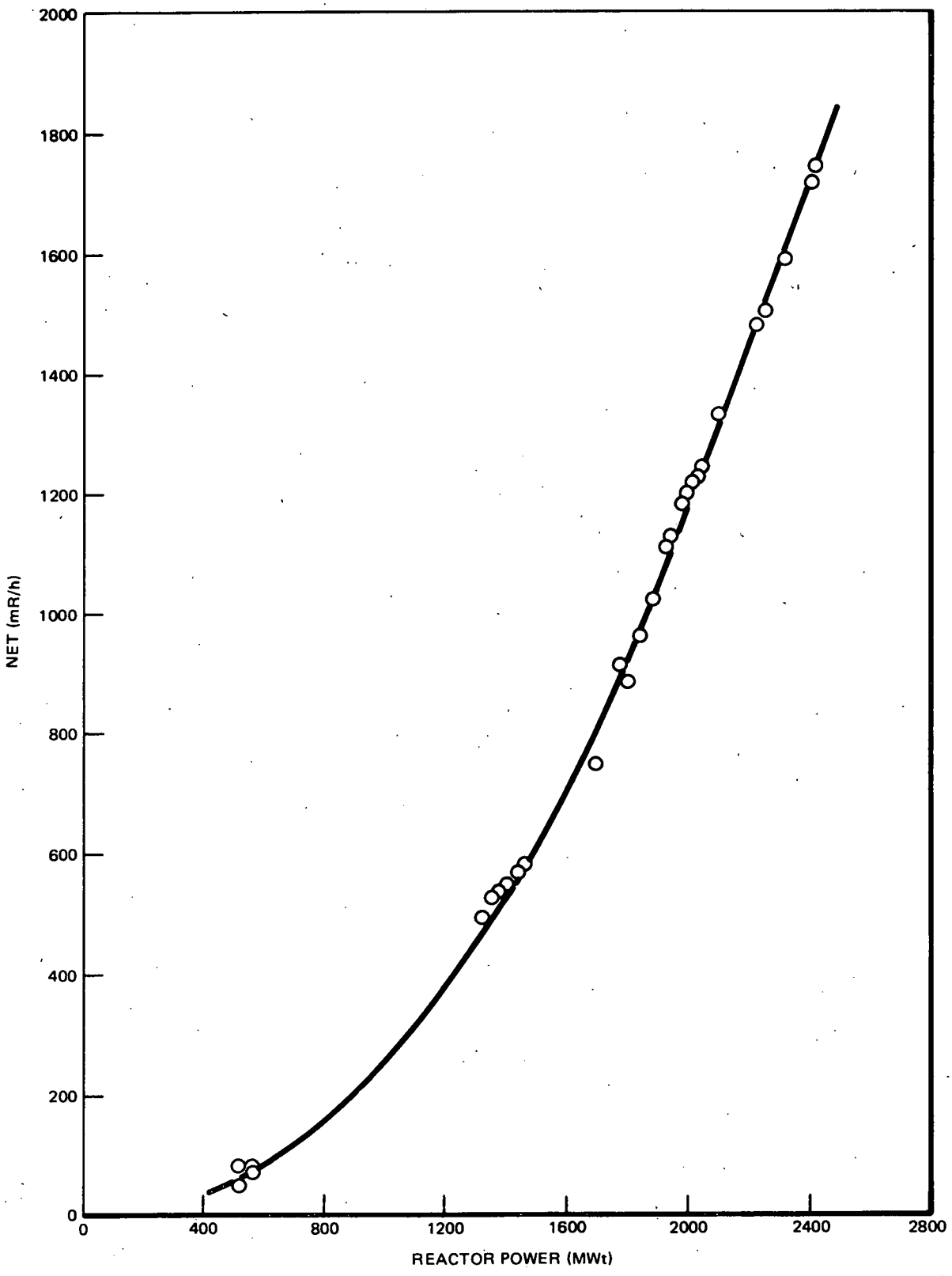

Figure 3-10. "A" Moisture Separator Drain Dresden 2, RAM No. 8

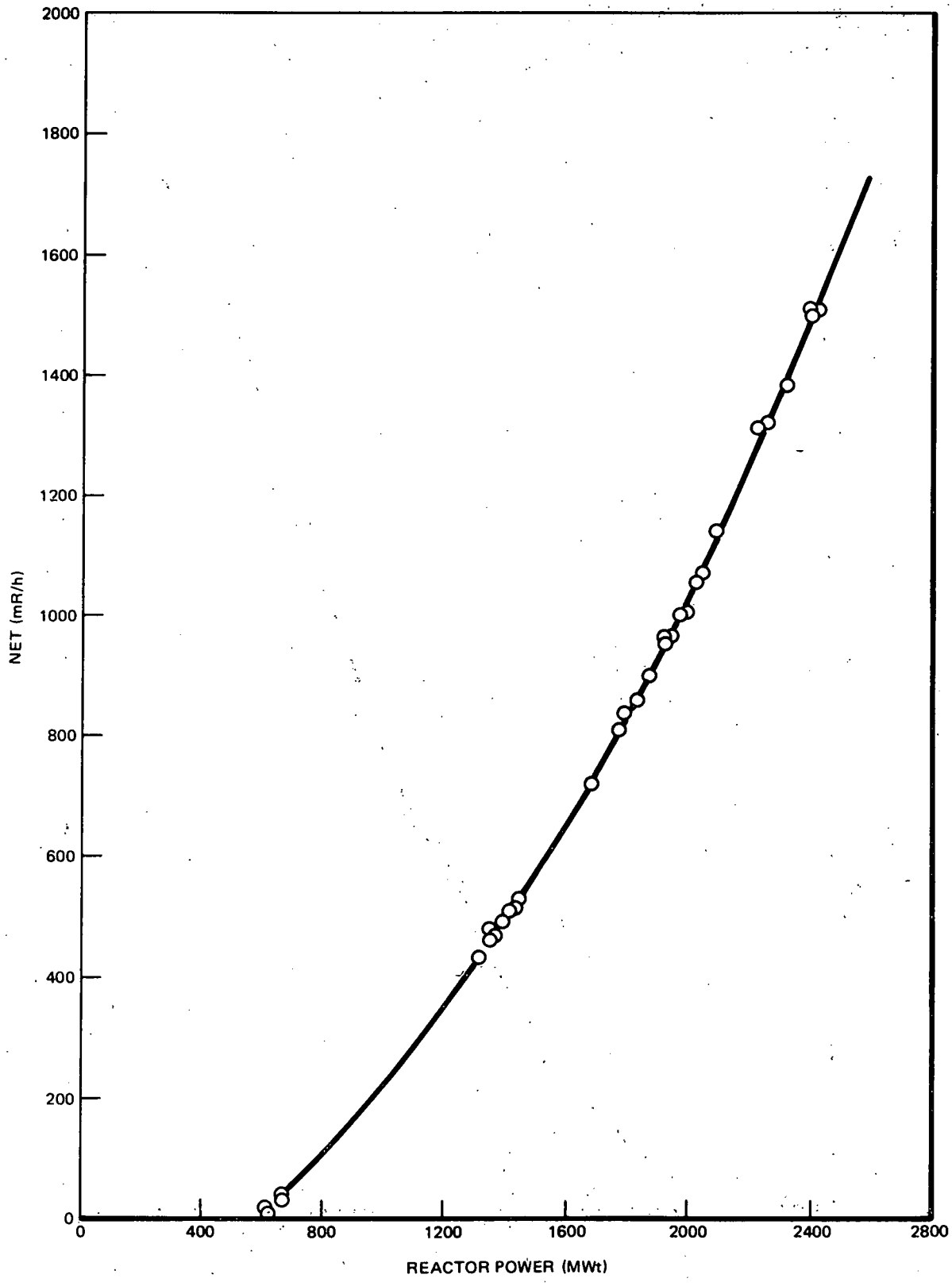

Figure 3-11. "B" Moisture Separator Vent Line Dresden 3, RAM No. 9

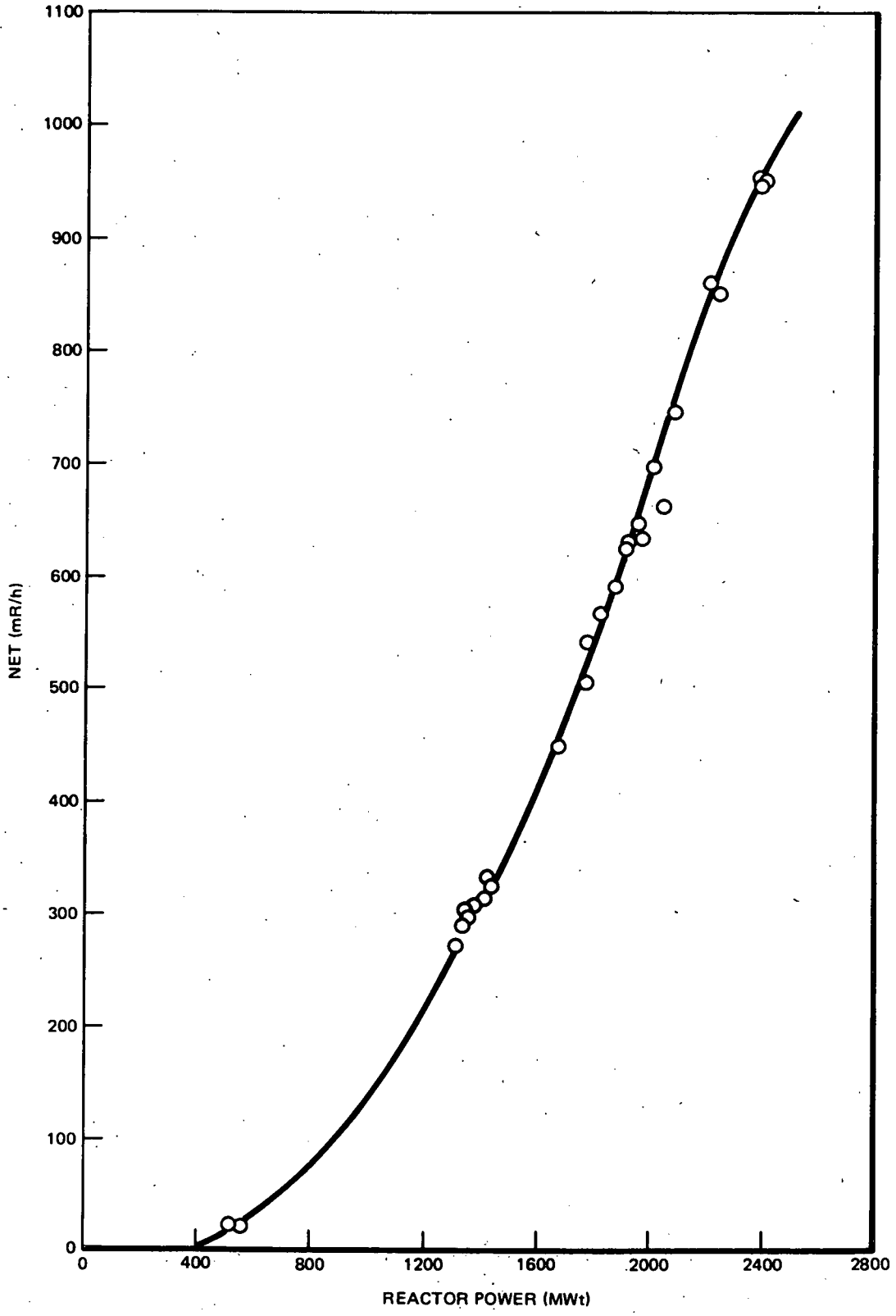

Figure 3-12. Steam Line from A/B Moisture Separator to Low Pressure Turbine Dresden 3, RAM No. 10

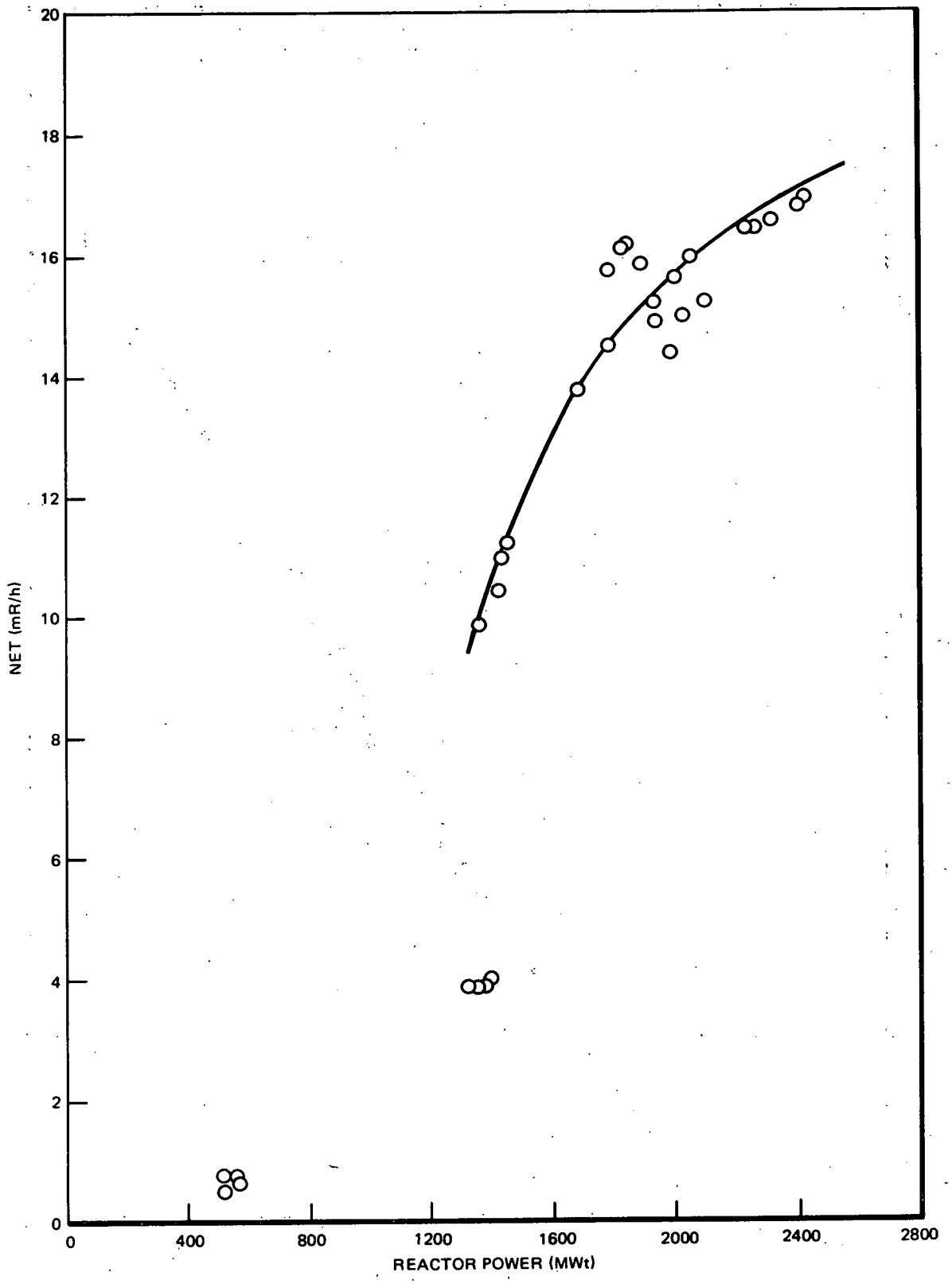

Figure 3-13. "B" SJAE Discharge Line to Recombiner Dresden 3, RAM No. 11

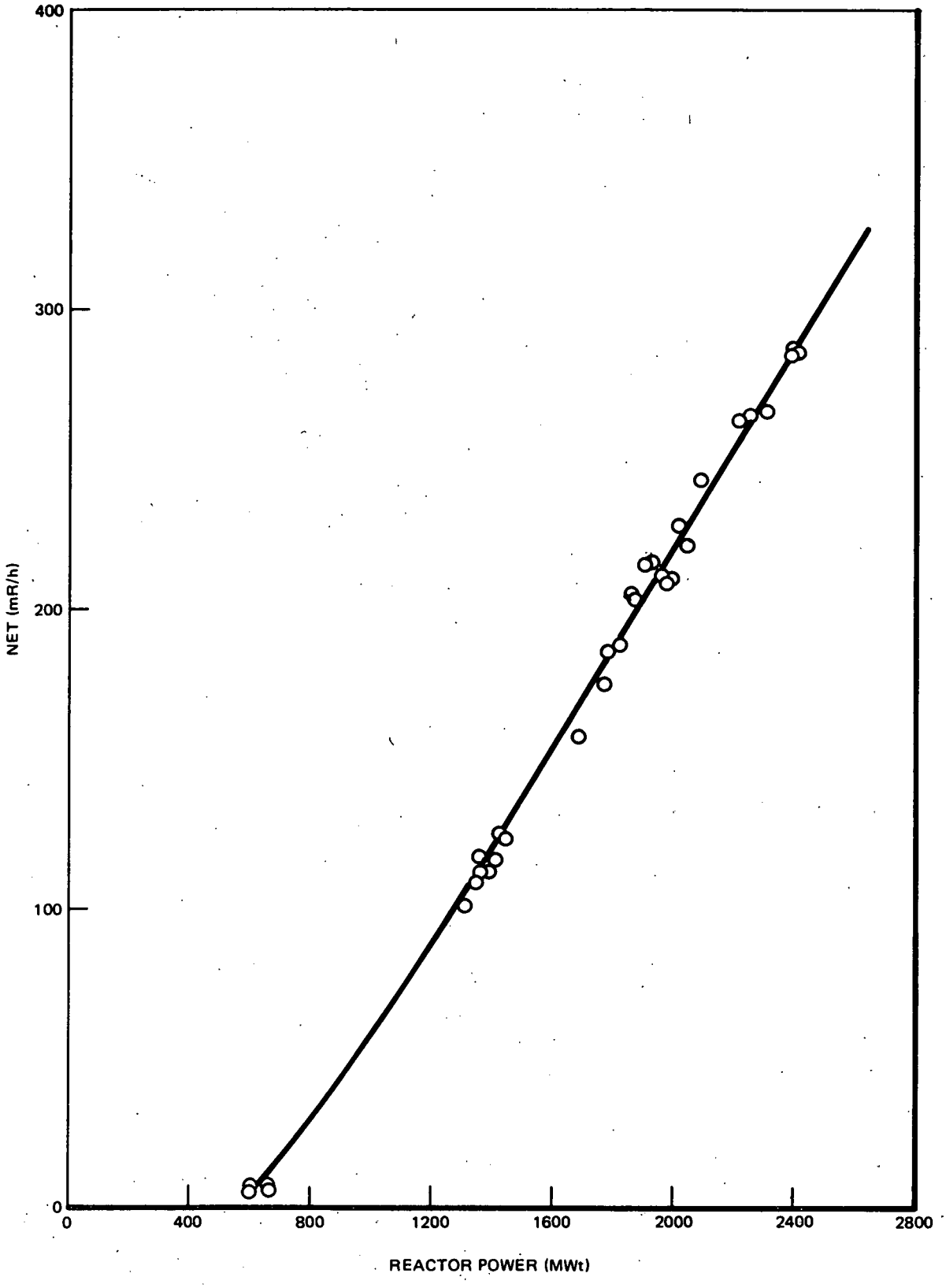

Figure 3-14. Condenser Wall - Turbine Building, Dresden 3, RAM No. 12

3.2.4 Turbine Building Radiation Levels

Turbine building radiation levels were measured to provide base data for the modeling of the radiation field about the building and environs.

The data for surveys of the Dresden 3 turbine are summarized in Table 3-3.

The data for a survey of the Dresden 2 turbine are summarized in Table 3-4.

A radiation survey was also performed along the south shield wall of the Dresden 3 turbine. The results of this survey are presented in Table 3-5. The shield wall is 0.61 m (2-ft) thick and 3.7 m (12-ft) high.

In addition to the above, radiation surveys were performed exterior to the turbine building. A survey was made on top of the Dresden 3 turbine building roof along the turbine axis. These data are presented in Table 3-6.

The LiF thermoluminescent dosimenters (TLDs) were suspended at 3-meter intervals from the north exterior wall of the turbine building at approximately the centerline of the high pressure (HP) turbine hood for 3 days. During this interval the thermal power level of Dresden 3 varied from 1592 to 2288 MW with the average power at 2089 MW. The results of this measurement are presented in Table 3-7.

3.2.5 Dose Rate Calculations (H. H. Paustian)

3.2.5.1 Steam Activity

One set of basic values which have been established is the radioactive source terms in the high-pressure steam. Based on gross gamma measurements made on the Dresden 2 main steam lines with the Victoreen 470 Panoramic Survey Meter and the LiF TLD's and on the proportions of N-16, C-15, and O-19 measured by the Ge(Li) detector, activities in the steam at the measurement point were calculated to be 8.7×10^8 Bq/kg (23.5 μCi/g) of N-16, 4.3×10^8 Bq/kg (11.5 μCi/g) of C-15, and 0.81×10^8 Bq/kg (2.2 μCi/g) of O-19.

Table 3-3

DRESDEN 3 TURBINE RADIATION LEVELS[a]

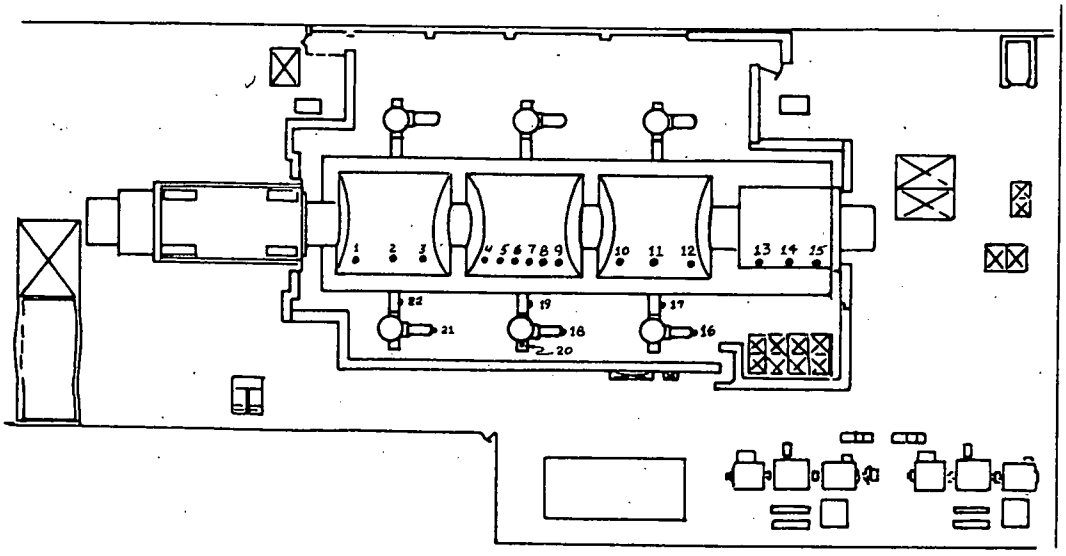

Date	5/13/78	5/14/78	6/14/78
Time	1105	1030	1543
Reactor Power (MWt)	568	1334	2002
Surveyed Position[b]	Exposure Rate (mR/h)		
1. "C" LP Hood (W. End)	2.7	39.5	50
2. "C" LP Hood (Center)	---	---	85
3. "C" LP Hood (E. End)	---	---	55
4. "B" LP Hood (W. End)	---	---	60
5. "B" LP Hood (W. End)	3.3	50	50
6. "B" LP Hood (Center)	---	---	80
7. "B" LP Hood (Center)	---	---	90
8. "B" LP Hood (E. End)	---	---	100
9. "B" LP Hood (E. End)	---	---	60
10. "A" LP Hood (W. End)	3.3	33	75
11. "A" LP Hood (Center)	---	49	100
12. "A" LP Hood (E. End)	---	---	62
13. HP Hood (3 ft from W. End)	5.5	54	100
14. HP Hood (Center)	---	168	400
15. HP Hood (3 ft from E. End)	---	---	130
16. CIV Inlet; "A" LP Turbine	---	175	415
17. CIV Outlet; "A" LP Turbine	10.5	124	300
18. CIV Inlet; "B" LP Turbine	11.5	163	410
19. CIV Outlet; "B" LP Turbine	11.2	120	290
20. CIV Casing, "B" LP Turbine	---	---	150
21. CIV Inlet, "C" LP Turbine	---	148	400
22. CIV Outlet, "C" LP Turbine	10.2	117	275

[a] Contact measurements using Victoreen 470A Panoramic Survey Meter, s/n-1094. Measurements made on turbine hoods made at elevation of 3 ft above deck level. Measurements on CIV made at the centerline of the pipe, approximately 1 ft above floor level.

[b] LP = low pressure
HP = high pressure
CIV = control and intermediate value

Table 3-4

DRESDEN 2 TURBINE RADIATION LEVELS

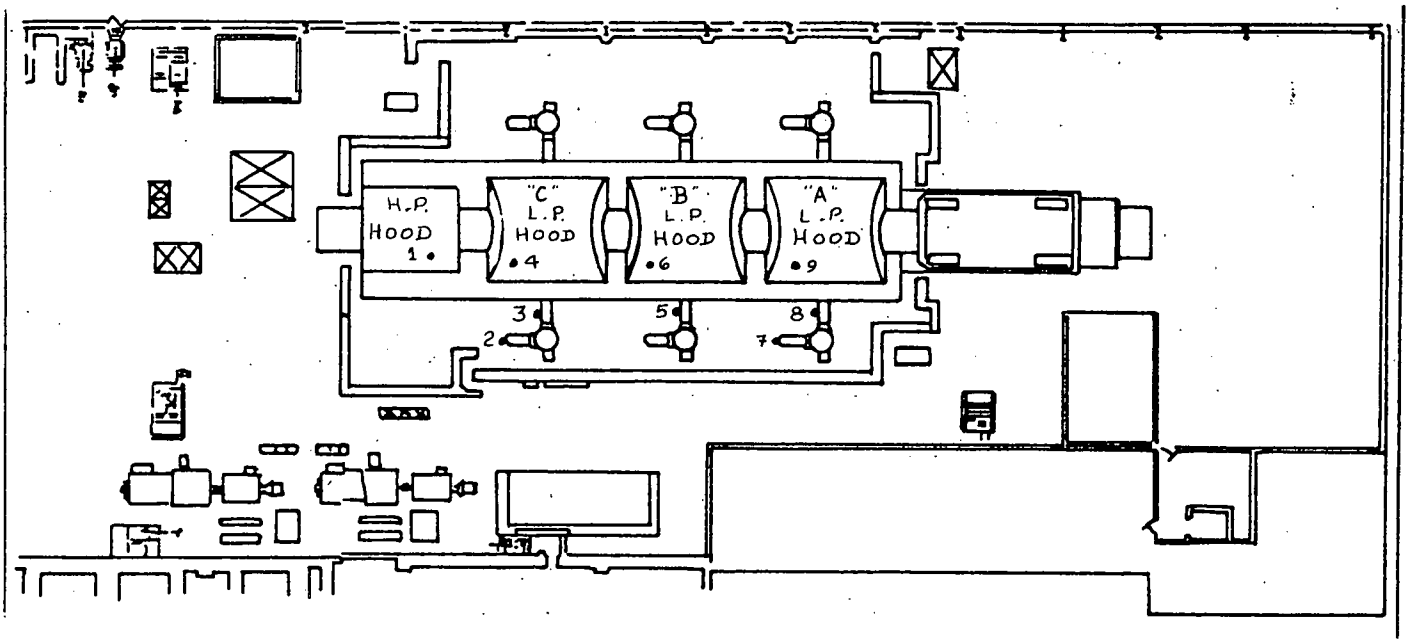

Date	5/13/78
Time	1125
Reactor Power (MWt)	2413

Surveyed Position	Exposure Rate (mR/h)
1. HP Hood (6 ft from E. End)	183
2. CIV Inlet, "C" LP Turbine	505
3. CIV Outlet, "C" LP Turbine	380
4. "C" LP Hood (W. End)	136
5. CIV Outlet, "B" LP Turbine	370
6. "B" LP Hood (W. End)	138
7. CIV Inlet, "A" LP Turbine	445
8. CIV Outlet, "A" LP Turbine	340
9. "A" LP Hood (W. End)	118

Table 3-5

SURVEY OF DRESDEN 3 TURBINE BUILDING SHIELD WALL

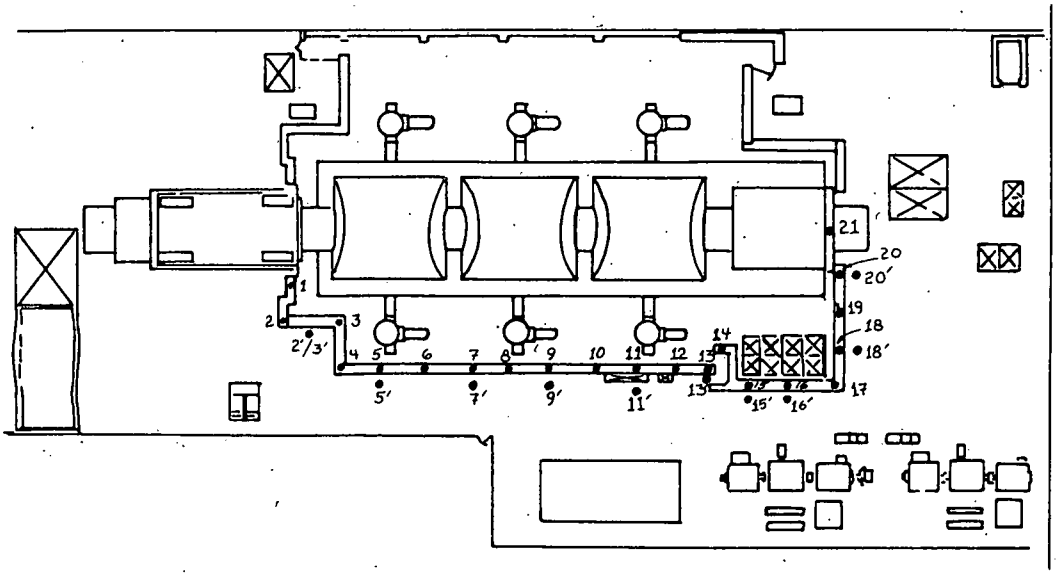

Survey Position[a]	Exposure Rate[b] (mR/h)	Survey Position	Exposure Rate (mR/h)
1	9.0	12	38.0
2	5.0	13	43.5
3	12.5	13'	0.35
2'-3' prime	<0.1	14	32.0
4	13.0	15	12.5
5	19.8	15'	0.12
5'	0.15	16	12.5
6	40.0	16'	0.14
7	31.0	17	10.8
7'	0.12	18	20.5
8	29.0	18'	0.20
9	40.0	19	30.0
9'	0.33	20	15.2
10	33.5	20'	0.20
11	31.5	21	41.0
11'	0.15		

[a] Survey positions 4-17 are spaced at 10-ft intervals along the south shield wall. Survey positions 17-20 are spaced at 10-ft intervals along the east wall. The primed numbers denote survey positions near contact with the outside shield wall at an elevation 5-ft above the turbine building main floor. The normal numbers represent positions at the elevation of the top of the shield wall vertical with the inner surface.

[b] Victoreen 470A Panoramic Survey Meter, s/n-1094.

Table 3-6

SURVEY OF DRESDEN 3 TURBINE BUILDING ROOF[a]

Date	6/13/78
Time	1550
Reactor Power MWt	2002

Distance From[b] West Wall (m)	Exposure Rate (mR/h)	Distance From West Wall (m)	Exposure Rate (mR/h)
0	0.50	40	9.3
3	0.65	43	9.9
6	0.55	46	11.5
9	0.60	49	7.0
13	0.60	52	12.0
15	1.10	55	12.0
19	2.7	58	9.8
22	2.2	62	9.5
25	4.3	65	4.4
28	5.1	68	6.5
31	7.8	71	5.8
33	7.6	74	3.8
37	8.4	77	3.8

[a] Measurements made 15 m from north wall. Traverse down centerline of turbine at 3.1 m intervals starting from inside edge of west parapet wall. Victoreen 470A Panoramic Survey Meter set upright on roof surface. Roof elevation 192 m. Turbine main floor elevation 173 m.

[b] ℄ "C" LP Hood = 33 m; ℄ "B" LP Hood = 43 m; ℄ "A" LP Hood = 54 m; ℄ HP Hood = 64 m. Cranes were located between the Unit-3 and Unit-2 turbines.

Table 3-7

DRESDEN 3 TURBINE BUILDING EXTERIOR EXPOSURE RATES
(NORTH WALL)[a]

Date	6/13-16/78
Average Reactor Power	2089 MWt

Elevation, m	Average[b] mR/h
175	1.5±0.2
178	6.0±0.4
181	8.0±0.3
184	6.0±0.3
187	8.5±0.4
190	8.2±0.8

[a]String of TLDs 3.1 m apart strung on north wall of Unit-3 turbine building at a position approximately at the centerline of the high pressure turbine.

[b]TLDs read by Radiation Detection Corporation, Sunnyvale, California

This N-16 concentration is about 30% higher than that obtained by other measurements for absolute concentration made by the VNC personnel at Dresden 2. It should be noted that a number of measurements at different distances from the steam lines were used in the calculations; good consistency among the source strengths calculated for each of the various locations was obtained, thereby lending more credence to these source terms. Consistency between the two detector types, survey meter and TLD, was also good. These source strengths are quite comparable to the results of measurements observed at three BWR/4s; although this is the first attempt to quantify the C-15 source term. The significance of the C-15 source is that because it is a significant fraction of the total steam source and it has a gamma energy nearly as high as N-16, any proposed alternate water chemistry must be evaluated based on affects not only on N-16 chemistry, but also on C-15 chemistry. Comparisons between the concentrations evaluated for Dresden 2 and concentrations that will result from a particular AWC will enable evaluation of the extent dose rates on the turbine operating floor and outside around the turbine building might change because of the AWC selected.

3.2.5.2 Turbine Building Dose Rates

A second major activity currently underway is calculation of dose rates at selected locations on the Dresden 2 operating floor. This requires estimation of activity inventories contained in the turbine equipment on the operating floor and estimation of the transit time from the reactor to the turbine equipment and through each of the various turbine components. The selected locations for dose rate calculations include one point inside the access shielding, two points outside the access shielding, and one point directly above LP hood "B" of the turbine at the elevation of the turbine building rooftop. These calculations are being done on a normalized source strength basis, so that when the concentrations (N-16 and C-15) corresponding to a possible AWC are determined, these dose rates need only be multiplied by a simple factor to determine expected dose rates on the operating floor of Dresden 2.

3.2.5.3 Site Dose Rates

A third consideration is the relative contributions to the environmental gamma radiation levels outside the Unit 2/3 turbine building at The Dresden site. The turbines for Units 2 and 3 include moisture separators beneath, rather than on, the operating floor. Because moisture separator-reheaters and the associated crossover piping are major radiation sources in turbine cycles where they're included, Units 2 and 3 of Dresden have significantly smaller activity inventories on the operating floor than do BWR plants with moisture separator-reheaters on the operating floor. In fact, Unit 1 is the major contributor to the environmental gamma levels outside the turbine buildings at Dresden. Note, there are also a number of waste storage tanks situated at various locations around the Dresden site which have significant readings at surface contact. Therefore, even a significant increase in the activity entering the main steam lines of Unit 2 might increase the dose rates on the Dresden 2 turbine operating floor appreciably but not have a significant effect in the environment surrounding the turbine building.

This same conclusion is not necessarily true when applied to a "BWR/6 standard plant turbine building." In this case, the inventory contained on the operating floor is significantly greater, both because the plant itself is considerably larger as well as because recent BWR plant designs often include moisture separator-reheaters and crossover piping on the operating floor. The application of an AWC that increases the activity in the steam may necessitate increased shielding or a larger site for a BWR/6.

3.3 TASK B-2. ADDITIVE VOLATILITY/DECOMPOSITION — OFF-GAS SYSTEM MODIFICATIONS (R.J. Law)

Objective. Each of the potential oxygen suppression additives and its volatile decomposition products will be continuously stripped into the steam phase in the reactor vessel. These volatile components are subsequently extracted from the condenser by the SJAE and, with any fission product gases present, constitute the inlet flow of the off-gas treatment system. The exact magnitude of the inlet

gas flow to the offgas for each additive must be determined. It is possible that the gas flow will be several times larger than that in the current, no-additive situation and will dictate an increase in the size of the system components and piping. In addition, the altered composition (including trace impurities) of the offgas may alter the recombiner performance, affect the hydrogen explosion hazard, and will be of special significance if hydrogen is to be recycled as the feedwater additive.

3.3.1 Impurity Measurements

Off-gas base line impurity studies are to be conducted to evaluate:

a. potential interactions of additives with impurities, and

b. modification requirements to proposed recovery and/or removal methods and equipment.

Effort on the off-gas base line impurity measurements was continued during this quarter. The analytical instruments proposed for the test as reported in the March 1978 quarterly report[1] have been refurbished. The analytical techniques for making the proposed impurity measurements have been developed.

The acceptable minimum detection limits for krypton, xenon, carbon monoxide, carbon dioxide and hydrocarbons have been determined on the TRACOR, Model MT 150, Gas Chromatograph. The Dynascience Air Pollution Monitor for the nitrogen-oxide measurements has been serviced. A standard wet-chemistry analysis for ozone measurements has been completed. Calibration procedures and standard operating procedures for each type of analysis have been prepared and approved.

3.3.2 Test Preparations

The test plan, test procedure and quality plan[6] for making these impurity measurements at Nine Mile Point 1 have been prepared, reviewed and approved. A design review of the proposed tests has also been conducted and approved.

3.4 TASK B-3. COOLANT LEAKAGE MONITORING (L. L. Sundberg)

Objective. Uncorrected condenser leakage can quickly exhaust the BWR full flow, condensate demineralizers and inject undesirable impurities, including chloride, into the reactor water. With dissociating additives such as NH_3 or N_2H_4, the condensate conductivity will rise to about 35 μS/cm and simple conductivity is no longer a sensitive leakage monitoring technique. An alternative leakage monitoring technique must be selected and evaluated.

3.4.1 Sodium Monitor

An in-line sodium monitor was ordered and received from Orion Research Corporation. It has been opened and inspected and is being set up for laboratory testing. The system operates at a flow rate of 50 mℓ/min (minimum) with an inlet gauge pressure of 0.10 MPa (15 psig) (minimum), and is temperature-compensated from 0 to 50°C. The Sample enters through a sample bypass valve, small cartridge filter, pressure regulator valve, rotometer, gas phase diffusion chamber, electrode chamber, and out to an atmospheric drain. Nernstian response (59 mV per decade of Na concentration) is expected. Adjustment of the pH to ca 10.5 (to decrease additive electrode response to H^+) is accomplished by passing the sample through 1.2 m of tubing immersed in liquid ammonia.

Calibration is accomplished by passing the sample at a known flow rate through a Barnstead ion-exchange column to produce sodium-free water. A standard of known concentration is injected into this stream at a known flow rate using a precision rack and pinion carriage block to force the standard through a syringe. With a constant flow rate of "sodium-free" water, the standard is injected at two unique flow rates which differ by a factor of 10. This yields a two-point calibration in the analytical range of interest, and a check on the Nernstian behavior of the system.

3.5 TASK B-4. PLANT MATERIALS COMPATIBILITY (B. M. Gordon, R. L. Cowan)

Objective. A primary concern in the application of an alternate water chemistry (AWC) to the BWR is the possibility of materials-coolant incompatibilities which might be introduced. This task, in addition to evaluating the necessary and limiting additive and oxygen concentrations necessary to mitigate stress-corrosion cracking tendencies in the primary coolant loops, will investigate the general corrosion behavior of normally encountered BWR materials in the proposed additive chemistry environment.

The tests in the program are specifically designed to not only demonstrate that the various AWC's do indeed prevent stress-corrosion cracking of typical BWR structural materials, but also do not in themselves produce any detrimental or unacceptable corrosion problems.

3.5.1 Turbine Materials

Discussions were held at the Large Steam Turbine-Generator (LSTG) Department concerning the logic and flow of the AWC program with particular emphasis on the possible corrosion effects on LST components. The primary concern of the LSTG Department is the effects of the additives on the chemistry of the steam entering the turbine. Therefore, a comparison table was constructed outlining the turbine steam chemistry for typical fossil and BWR plants and hydrogen and ammonia modified plants as shown in (Table 3-8):

Table 3-8
TURBINE STEAM CHEMISTRY

System	Oxygen	Hydrogen	Ammonia	pH
Typical Fossil	<10 ppb	<10 ppb	1 ppm	8.5 to 9.5
Typical BWR	20 to 30 ppm	2 to 4 ppm	-	7.2
Hydrogen Addition BWR	1 ppm	2 ppm	-	7.2
Ammonia Addition BWR	-	14 ppm	37 ppm	9.5 to 10.5

Both of the proposed additives result in a significant modification of the turbine steam chemistry.

The ammonia addition results in significant decreases in the oxygen content and increases in the hydrogen and ammonia content of the turbine steam. The higher hydrogen input could conceivably result in hydrogen embrittlement of susceptible turbine components such as Type-410 and Type-422 martensitic stainless steels. The higher pH due to the presence of ammonia could also result in stress corrosion cracking or accelerated general corrosion of the brass steam packings in the turbine.

Hydrogen addition results in less significant alternations in the turbine steam environment. The pH and hydrogen content of the steam remain basically unchanged; however, the decrease in oxygen content may have an adverse effect, according to LSTG, on the corrosion-erosion of carbon steel crossaround piping due to a loss in high oxygen-passivation kinetics at the neutral pH of the BWR steam. On the other hand, since 1 ppm oxygen is frequently considered "high oxygen" it may still be sufficient to promote the formation of an adherent protective oxide film.

Another concern regarding modification of BWR steam chemistry is the difficulty of predicting changes in the stress corrosion cracking and corrosion fatigue resistances of turbine components. Both of these corrosion phenomena are extremely complex, and are apparently very difficult to predict or experimentally verify at the LSTG. It was indicated, for example, that an extensive laboratory test program at LSTG failed to predict the corrosion-erosion experience by turbine crossaround piping and that efforts to simulate this phenomenon in the laboratory were unsuccessful.

The LSTG will consider further the implications of the modified steam chemistry on the behavior of turbine components and will transmit this information to GE San Jose.

3.5.2 Constant Extension Rate Tests (F. P. Ford, Corporate Research and Development Center, Schenectady)

3.5.2.1 Test Basis

The overall objective of this project is to investigate the feasibility of making chemical additions to BWR feedwater to reduce the probability of stress-corrosion cracking of weld-sensitized Type-304 stainless-steel in the radiolytically oxygenated coolant. Assuming that these additions lower the oxygen level to an acceptable value vis-à-vis cracking, it is the specific objective of this task to determine whether the presence of excess additive per se may give rise to an increased stress-corrosion cracking tendency. The amine additions originally considered for this study are given in Table 3-9. Since this choice was made, however, several additives have been relegated to secondary interest (for reasons other than stress-corrosion cracking considerations) with the result that only ammonia (mean 20 ppm) or hydrogen (mean 0.2 ppm) additions are being considered seriously.

Since it is suspected that these additions will have only a small effect on the stress-corrosion susceptibility the preliminary task of this investigation is to evolve a rapid stress-corrosion testing technique capable of resolving small changes in stress-corrosion susceptibility. The work described in this quarterly report covers this task, by examining how the sensitivity of the CERT technique to detect stress-corrosion cracking in sensitized Type-304 stainless steel varies with specimen notch geometry and solution oxygen content.

3.5.2.2 Experimental Procedures

The loop details were described in the previous quarterly report.[1] The Type-304 stainless steel used in these experiments was supplied by General Electric, San Jose (HT X14902) and had the following composition:

Cr	Ni	Mn	Si	Cu	Mo	P	S	C
18.4%	8.45%	1.65%	0.34%	0.30%	0.84%	0.038%	0.024%	0.063%

Table 3-9

SUGGESTED ADDITIONS TO BWR FEEDWATER

	Additive Concentration in Primary Water, (ppb)	
	Range	Initial Value to be Investigated
Ammonia	12 to 30	20
Hydrazine	0.4	0.4
Hydrazine + Morpholine	0.1 to 0.15 3 to 8	0.1 5.0
Ammonia + Hydrazine	0.3 to 1.5 0.05 to 1.0	1.0 0.5
Hydrogen	0.1 to 0.3	0.2

After rough maching into 1.27 cm-diameter x 10 cm-long bars, the material was solution annealed at 1100°C for 1/2 hour and water quenched. The specimens were then centerless ground to 0.64 cm-diameter gage diameter tensile bars (Figure 3-15) with a 30 degree angle notch (root radius 0.0025 cm) of varying depth at the midlength position of the 3.8 cm gauge section. The tensile bars were encapsulated in quartz, evacuated to 1.3×10^{-4} Pa, furnace sensitized at 650°C for 24 hours, air-cooled to room temperature, low temperature sensitized at 500°C for 24 hours, and air-cooled to room temperature.

These heat-treated tensile specimens were subjected to constant extension rate testing according to the following environment/notch depth matrix:

Environment	Notch Depth (cm):	0	0.033	0.066	0.132
			Specimen Number		
Argon		1A1	1A5	1A9	1A13
H_2O/8 ppm O_2		1A2	1A6	1A10	1A14
H_2O/0.2 ppm O_2		1A3	1A7	1A11	1A15
H_2O/0.01 ppm O_2		1A4/1A18	1A8	1A12	1A16

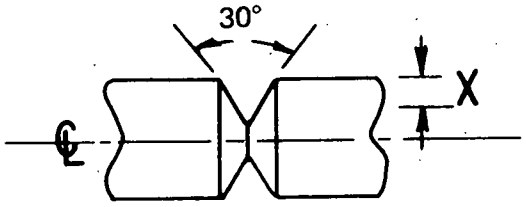

DETAIL 'A'

ROOT RADIUS 0.0025 cm

X,cm; 0, 0.033, 0.066, 0.132

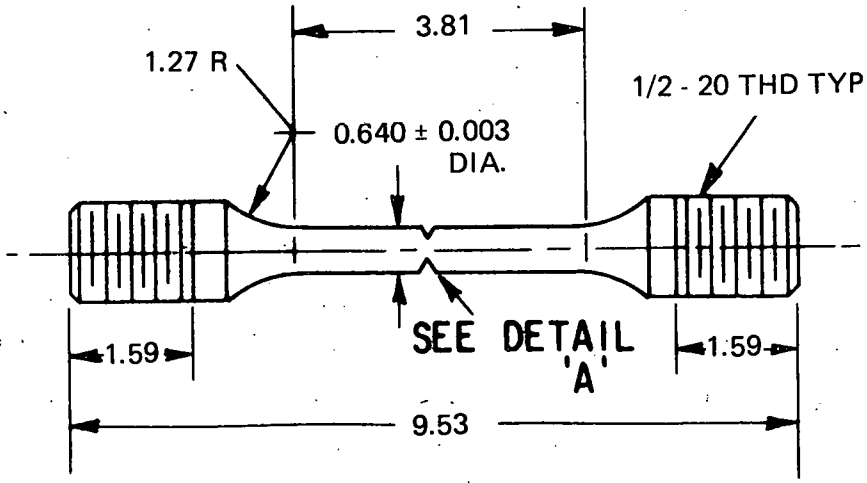

(DIMENSIONS IN cm)

Figure 3-15. Details of Tensile Bar and Notch Geometry

The testing chronology following alignment of the specimen in the autoclave was:

a. Saturate the water (conductivity <1 μs/cm) in the main reservoir with either air, argon plus 0.5% oxygen, or argon, to give respectively 8 ppm O_2, 0.2 ppm O_2, or 0.007 to 0.015 ppm O_2 in the water.

b. Pressurize autoclave with water to 10 MPa (1500 psig) and adjust flow to 20 cc/min.

c. Heat autoclave to 288°C.

d. Connect tie-rod to Instron cross-head and start extension at 8.5×10^{-6} cm/sec (2×10^{-4} in./min.). This corresponds to a nominal strain rate of 1.33×10^{-4} min^{-1}.

3.5.2.3 Results and Discussion

The nominal engineering stress/strain curves for testing in different oxygen contents are shown in Figure 3-16 (a-d) for various notch depths. The data for dry argon and 8 ppm O_2 in high temperature water (reported in the first quarterly report)[1] are included for comparison. In these figures the nominal engineering stress is defined as the load/cross-sectional area at notch root; the strain is defined as the instantaneous extension/initial gage length. Further data are given in Table 3-10, including the fracture morphologies. In contrast to the first quarterly report, crack "velocities" are defined in terms of maximum observed crack penetration/testing time.

As expected, increasing the oxygen content increases the stress-corrosion susceptibility for both notched and unnotched bars [Figure 3-16 (a through d)]. The crack velocities (defined above) decrease with decreasing oxygen content, the general relationship for unnotched specimens being similar to that observed by other authors[7] (Figure 3-17). In agreement with the latter work, the crack morphology changes from intergranular (IG) in 8 ppm O_2/H_2O (Figure 3-18) to completely transgranular (TG) in oxygen contents <0.02 ppm at 288°C (Figure 3-19); at the intermediate 0.2 ppm O_2 content, the cracks initiate in

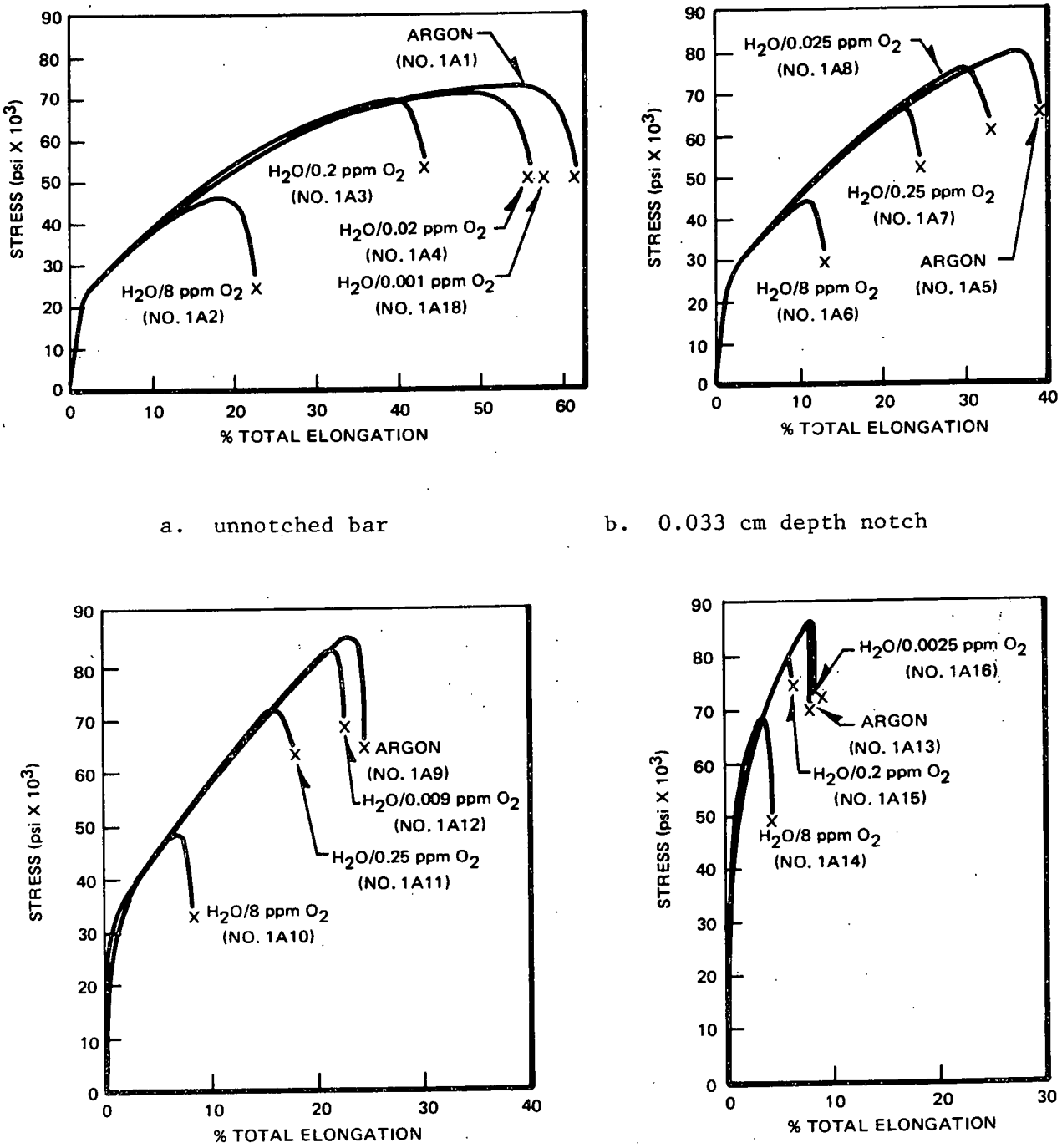

a. unnotched bar

b. 0.033 cm depth notch

c. 0.066 cm depth notch

d. 0.13 cm depth notch

Figure 3-16. Stress-Elongation Curves in Argon, and Water with Various Oxygen Contents, at 288°C. $\dot{\varepsilon} = 1.3 \times 10^{-4}$ min-1.

Table 3-10

SPECIMEN FAILURE DATA

Environment	Specimen	Nominal Notch Depth (in.)	Gage Length Diam. (in.)	Notch Root Diam. (in.)	Yield Stress (psi)	UTS[a] (psi)	% RA[b]	Total Elongation (in.)	Plastic Strain to Fracture (%)	% SCC TG	% SCC IG	Maximum Crack Penetration (in.)	Test Time (hr)	Maximum Crack Velocity (mils/day)	O_2 (ppm)
Argon	1A1	0	0.2515	0.2515	22,250	73,000	67	0.925	59	Ductile					
	1A5	0.013	0.2562	0.2288	23,105	80,000	46	0.585	37	Ductile					
	1A9	0.026	0.2532	0.2013	28,275	85,611	28	0.365	23	Ductile					
	1A13	0.052	0.2532	0.1525	43,790	87,575	12	0.115	7.6	Ductile					
H_2O/8 ppm O_2	1A2	0	0.2520	0.2520	17,500	46,300	22	0.338	22.4	-	65	0.123	28.16	105.0	8.0
	1A6	0.013	0.2593	0.2318	23,695	44,430	15	0.190	12.1	-	78	0.098	15.83	150.0	8.0
	1A10	0.026	0.2562	0.2013	23,390	48,540	6	0.119	6.2	-	78	0.049	9.98	120.0	8.0
	1A14	0.052	0.2562	0.1495	47,295	68,375	4	0.065	4.3	-	59	0.049	5.3	225.0	8.0
H_2O/0.2 ppm O_2	1A3	0	0.2518	0.2515	20,000	69,000	36	0.642	40.4	5	5	0.033	53.5	14.8	0.2-0.25
	1A7	0.013	0.2562	0.2288	23,710	66,875	27	0.365	23.4	28	15	0.029	30.41	23.0	0.15-0.2
	1A11	0.026	0.2562	0.2013	30.630	74,615	20	0.265	16.2	30	10	0.022	22.0	24.0	0.25
	1A15	0.052	0.2532	0.1464	39,515	84,965	8	0.118	7.1	32	-	0.017	9.8	42.0	0.2
H_2O/0.01 ppm O_2	1A4	0	0.2520	0.2520	19,500	71,000	54	0.846	54.5	23	-	0.017	70.5	6.0	0.02-0.025
	1A18	0	0.2517	0.2517	19,000	70,400	59	0.854	55.2	28	-	0.018	71.1	6.1	0.001-0.003
	1A8	0.013	0.2562	0.2288	23,105	77,945	38	0.508	33.0	12	-	0.005	42.2	2.8	0.025
	1A12	0.026	0.2562	0.2013	29,845	83,100	23	0.336	21.8	7	-	0.0036	28.0	3.1	0.009
	1A16	0.052	0.2562	0.1510	43,550	89,335	10	0.134	8.6	5	-	0.0033	11.2	7.1	0.0025

[a] UTS = ultimate tensile strength

[b] % RA = % reduction in area

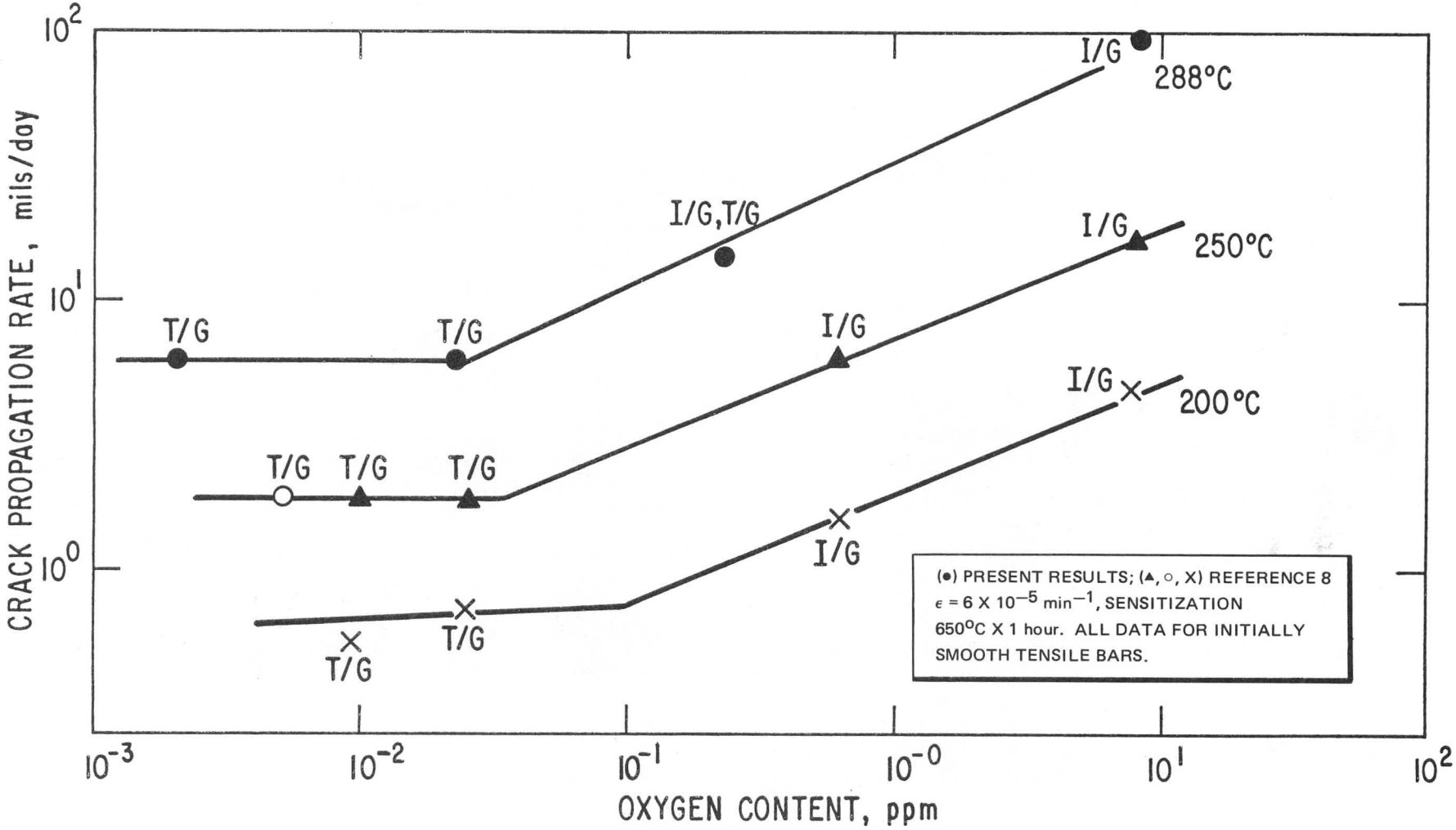

Figure 3-17. Relationship Between Oxygen Content and Crack-Propagation Rate in CERT for Sensitized No. 304 Stainless Steel.

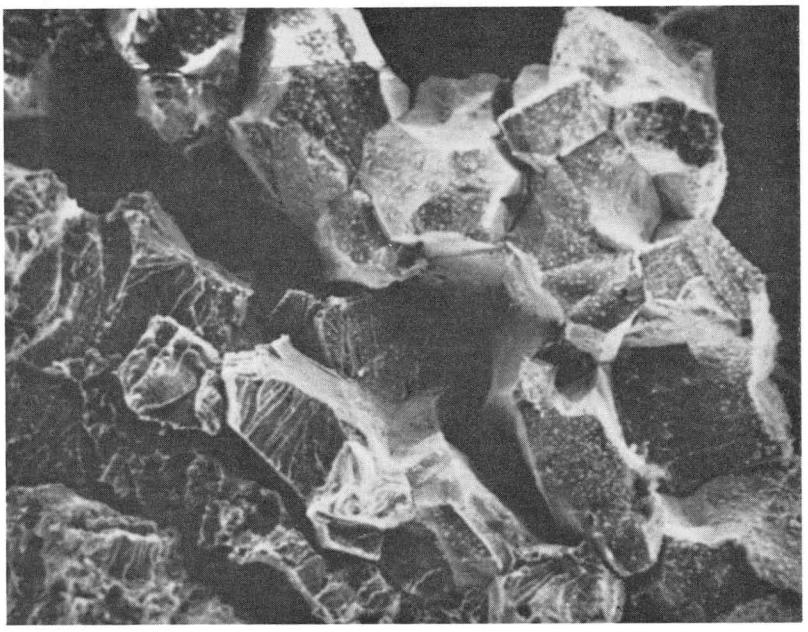

Figure 3-18. Integranular Fracture in 8 ppm O_2/H_2O, 288°C. (Specimen 1A14 x 200)

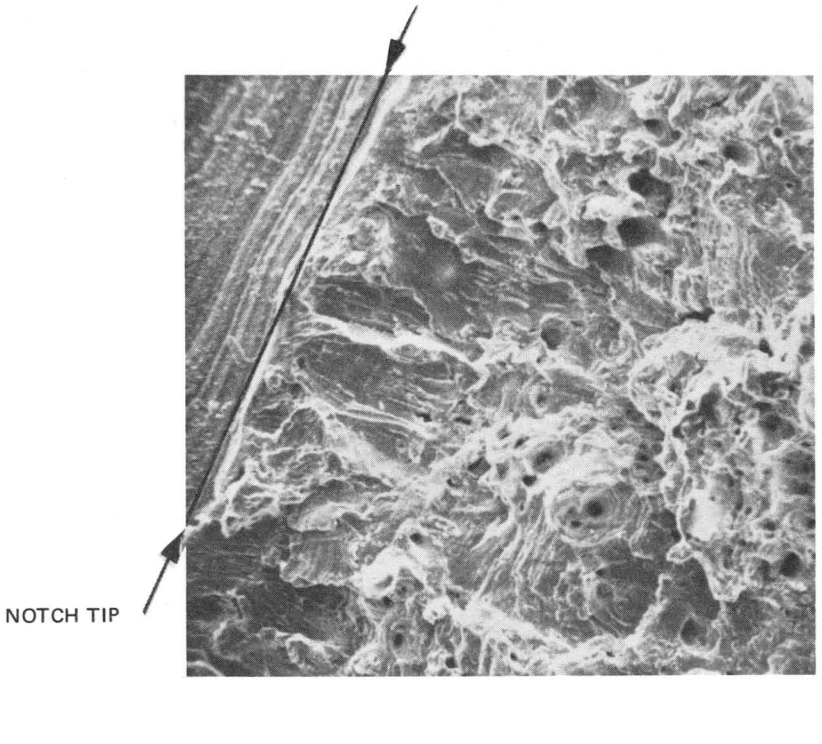

Figure 3-19. Transgranular Fracture on 0.025 ppm O_2/H_2O, 288°C. (Specimen 1A11 x 200)

the IG mode but change to TG as the crack deepens (Figure 3-20). This transition in crack morphology in 0.2 ppm O_2/H_2O is presumably related to a decrease in oxygen in solution due to the formation of (FeMnCr) oxides which precipitate (Figure 3-21) on the crack sides near the crack opening; thus for deeper cracks and initial notch size, the real oxygen content (and hence electrode potential at the crack tip) is different from that measured in the bulk solution.

An investigation of the reason for crack mode transition with oxygen content is being conducted in a separate contract. From a practical point of view, however, it should be noted that even deaerating the solution to 1 ppb will not stop stress corrosion cracking, once initiated in a dynamic straining test. The intergranular crack propagation rate at low oxygen contents should be independent of the degree of sensitization of the grain boundary as demonstrated by Ohio State University experiments conducted at lower temperatures[7] (250 and 200°C).

There is a change in crack nucleation density associated with the change in oxygen content. In high oxygen (8 ppm) solutions, the IG crack density (number of cracks/unit area) is relatively low, although the cracks are deep (Figure 3-22), whereas in the low oxygen solutions the transgranular crack density is high, albeit with shallow penetration (Figure 3-23). Also noted is the fact that the strain for nucleation of the two cracking modes is different; for instance, IG cracks are not observed on the relatively low strained surfaces adjacent to the notch opening, whereas TG cracks can be initiated in these regions. The magnitude of the difference in strain for initiation of the two cracking modes has not been determined.

Notching the tensile bar has the apparent effect of increasing the crack velocity during CERT (Figure 3-24). Note, however that this is an assumed effect since the velocity is calculated on one measured crack penetration value (the maximum observed on the fracture surface) and an assumed linear propagation rate over the whole testing time. A more realistic evaluation is shown in Figures 3-25 (a) and 3-25 (b); the criteria used in making these evaluations are as follows. For the 8 ppm O_2/H_2O solution (Figure 3-25 (a), one data point is known on a crack length/time plot for each specimen; it is assumed that at the point of final ductile fracture, the subcritical crack propagation

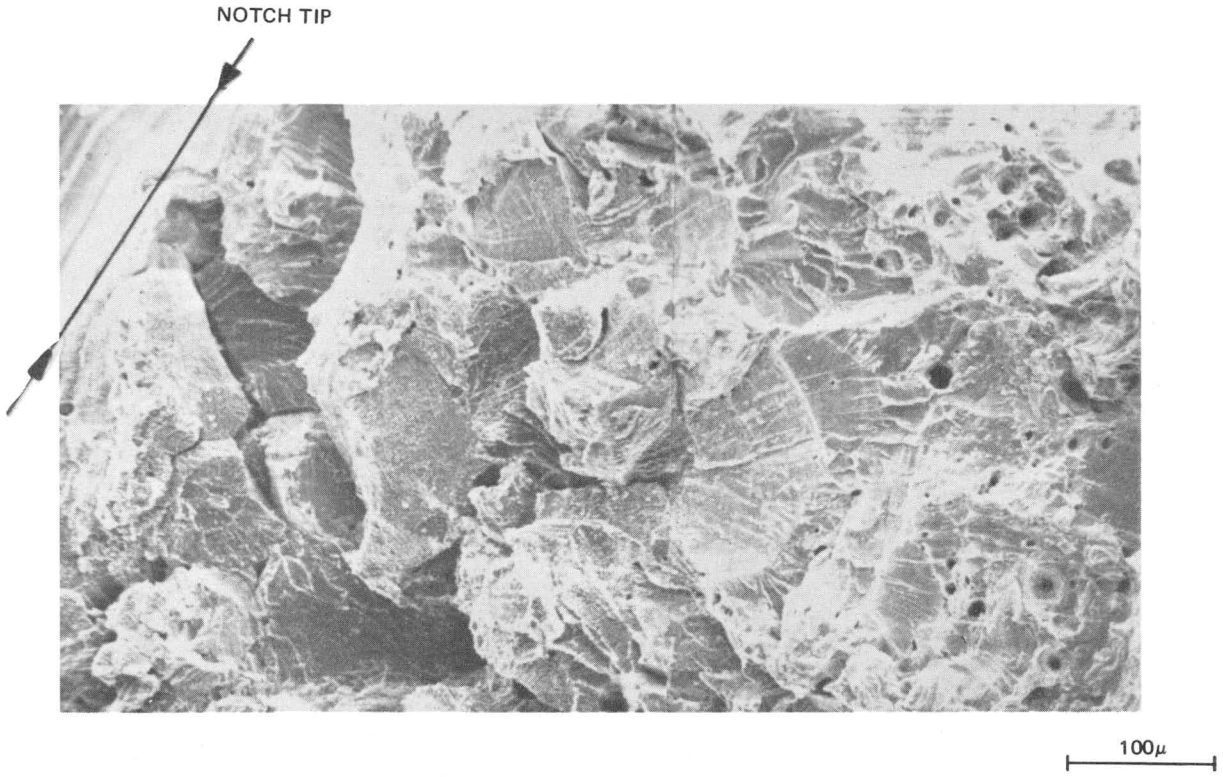

Figure 3-20. Transition From Intergranular to Transgranular Cracking in 0.2 ppm O_2/H_2O, 288°C. (Specimen 1A11 x 200.)

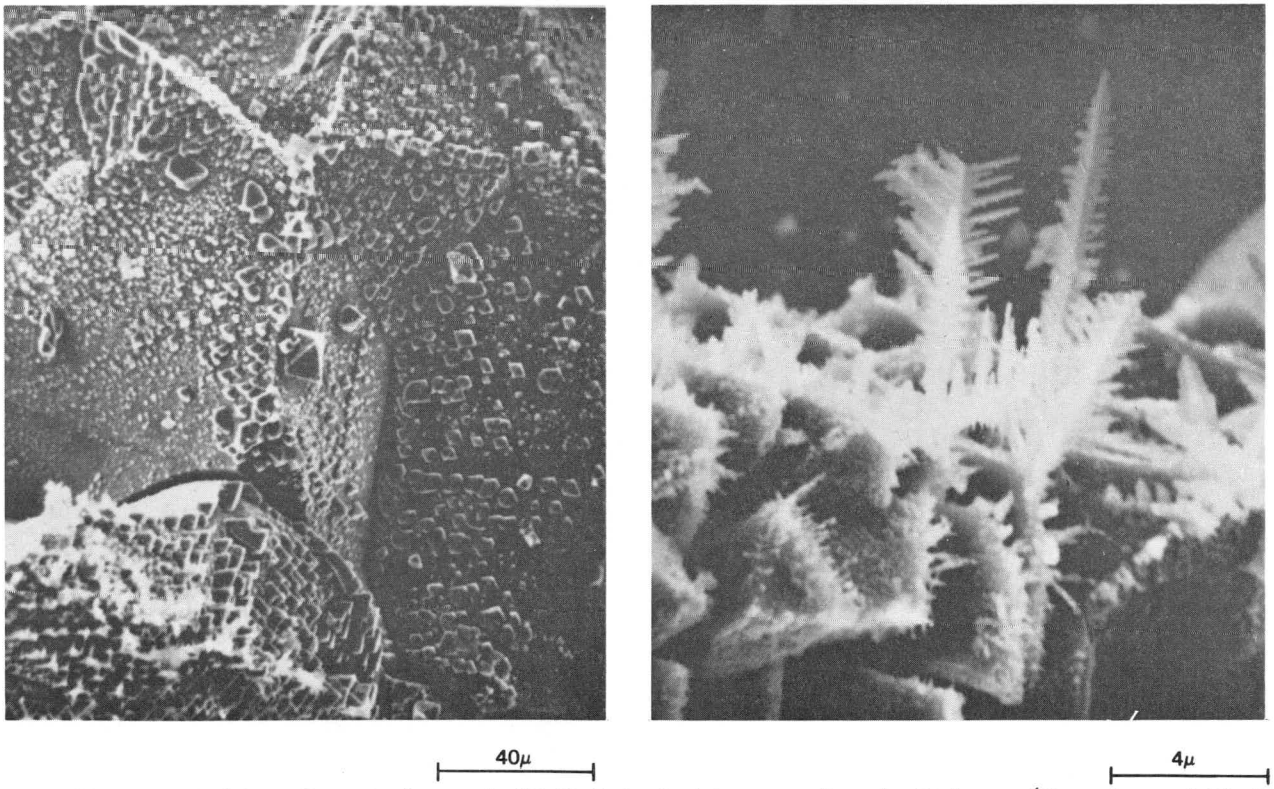

Figure 3-21. Precipitated (FeMnCr) Oxides on Crack Sides. (Specimen 1A6.)

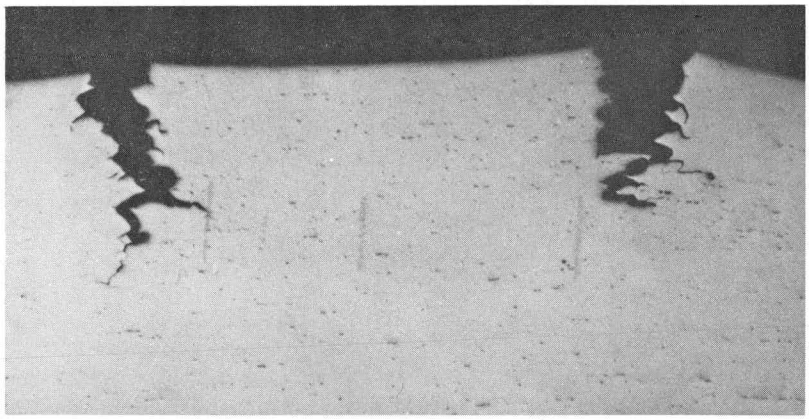

20X

Figure 3-22. Intergranular Crack Nucleation on Unnotched Specimen in 8 ppm O_2/H_2O. (Note that no initiation is observed on notched specimens in areas remote from the notch.)

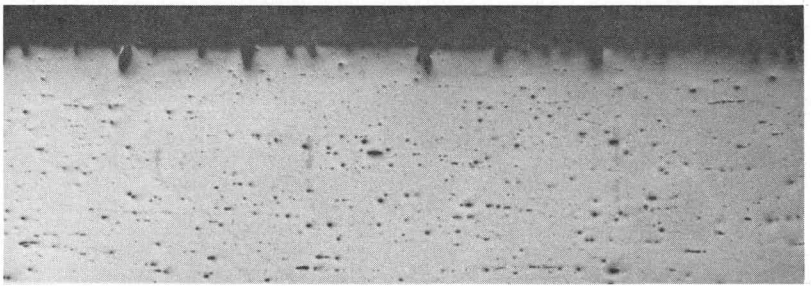

a. Transgranular crack nucleation on unnotched specimen (0.02 ppm O_2/H_2), x20)

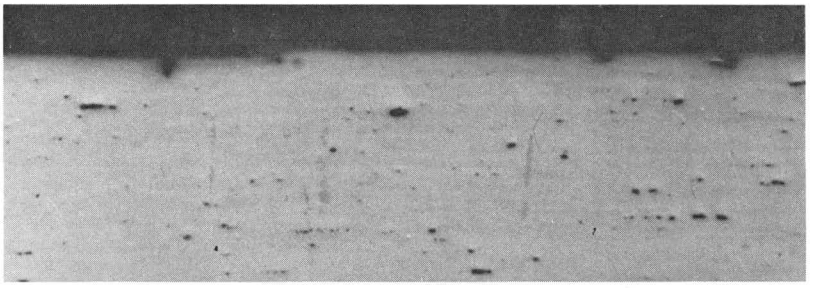

b. Transgranular crack nucleation on surface remote from notch in 0.025 ppm O_2/H_2O, x50

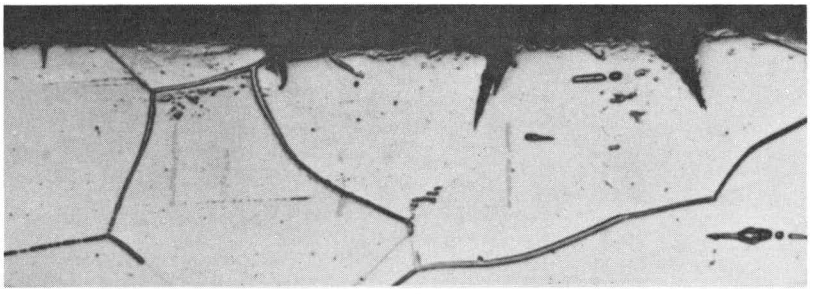

c. Transgranular crack nucleation on surface remote from notch in 0.025 ppm O_2/H_2O, x500

Figure 3-23. Transgranular Crack Nucleation On Unnotched Specimen

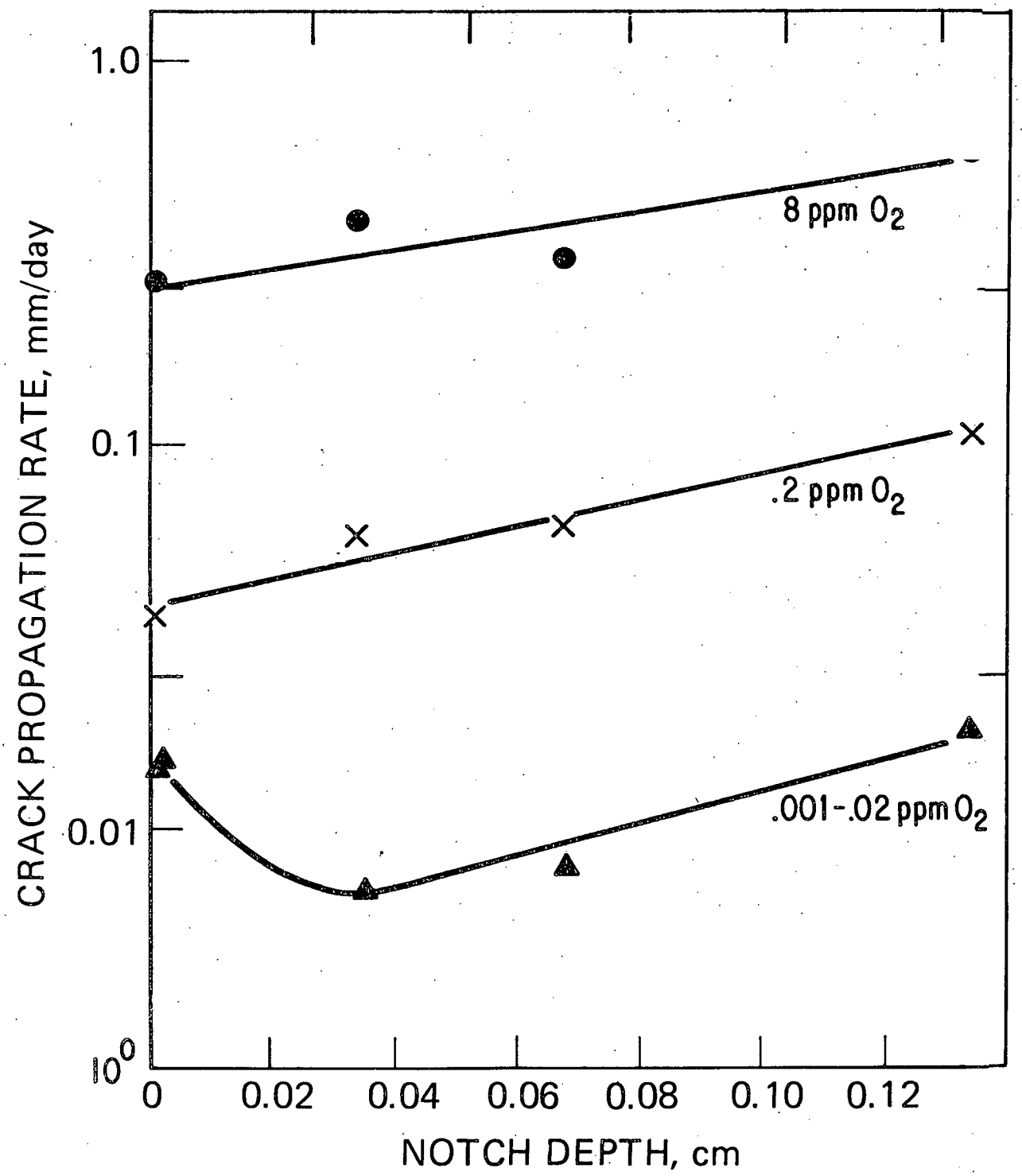

Figure 3-24. Relationship Between Crack Propagation Rate in CERT and Notch Depth for Various Oxygen Contents ($\dot{\varepsilon}$ = 1.3 x 10^{-4} min^{-1}, 288°C.)

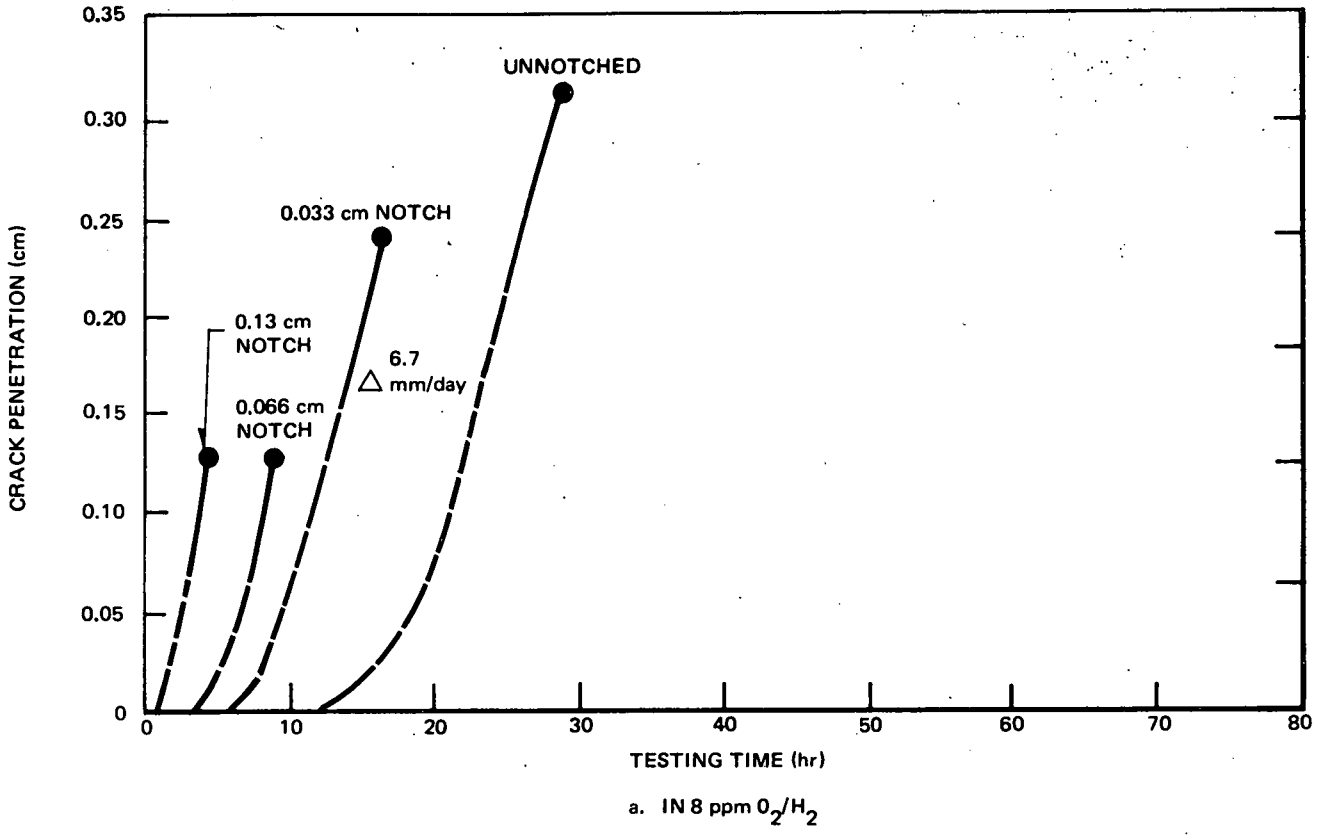

a. IN 8 ppm O_2/H_2

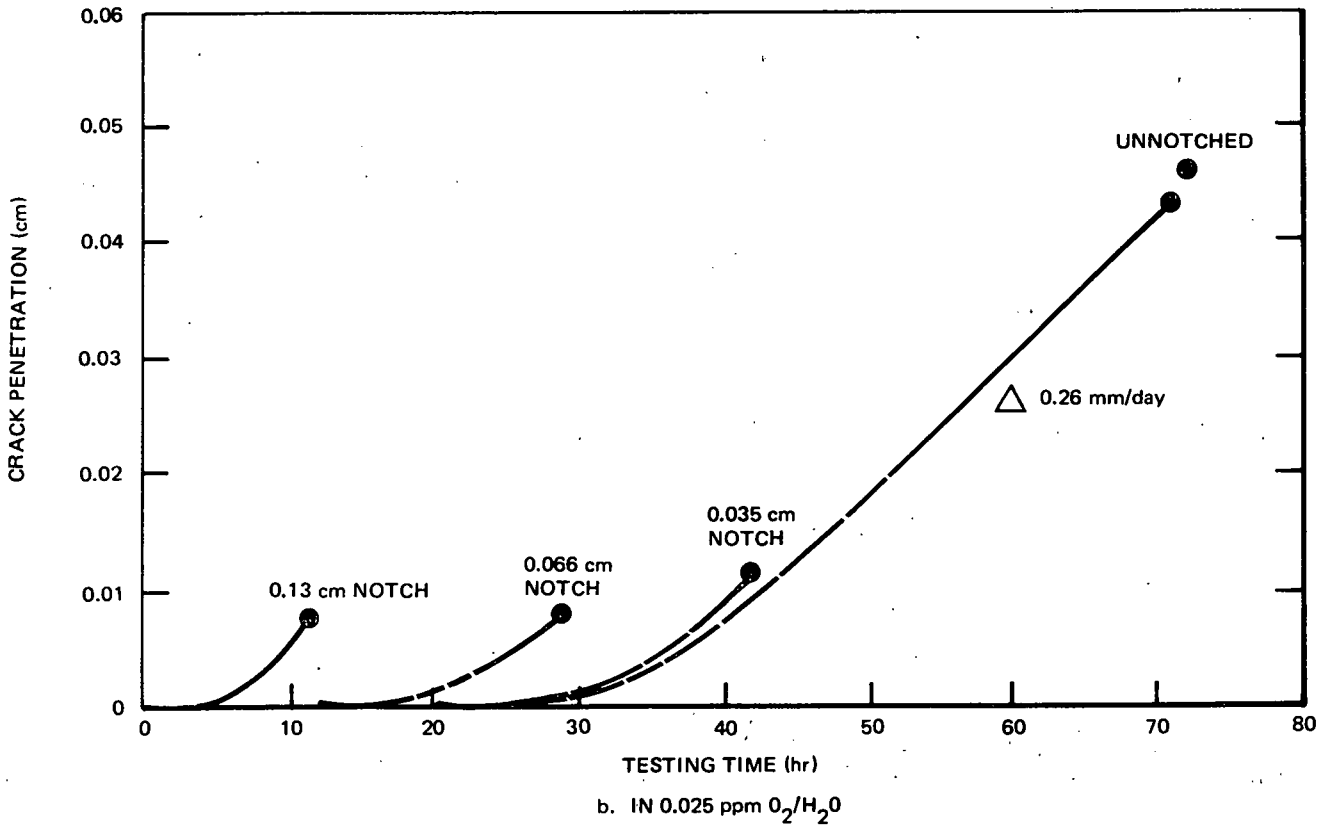

b. IN 0.025 ppm O_2/H_2O

Figure 3-25. Semiquantitative Crack Length-Time Relationship for Notched and Unnotched Specimens

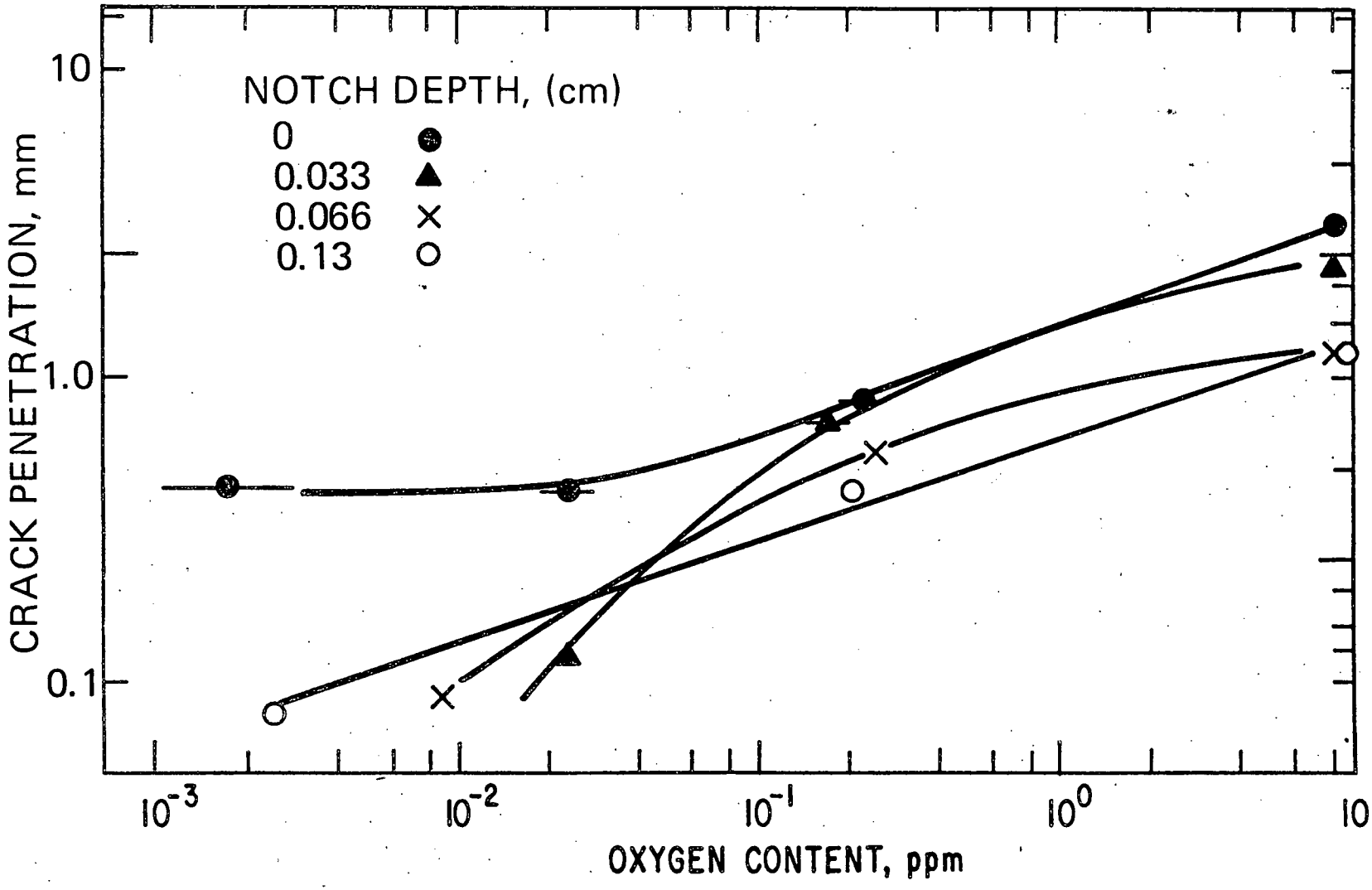

Figure 3-26. Variation of Maximum Crack Penetration During CERT ($\dot{\varepsilon} = 1.3 \times 10^{-4}$ min^{-1}) With Oxygen Content at 288°C

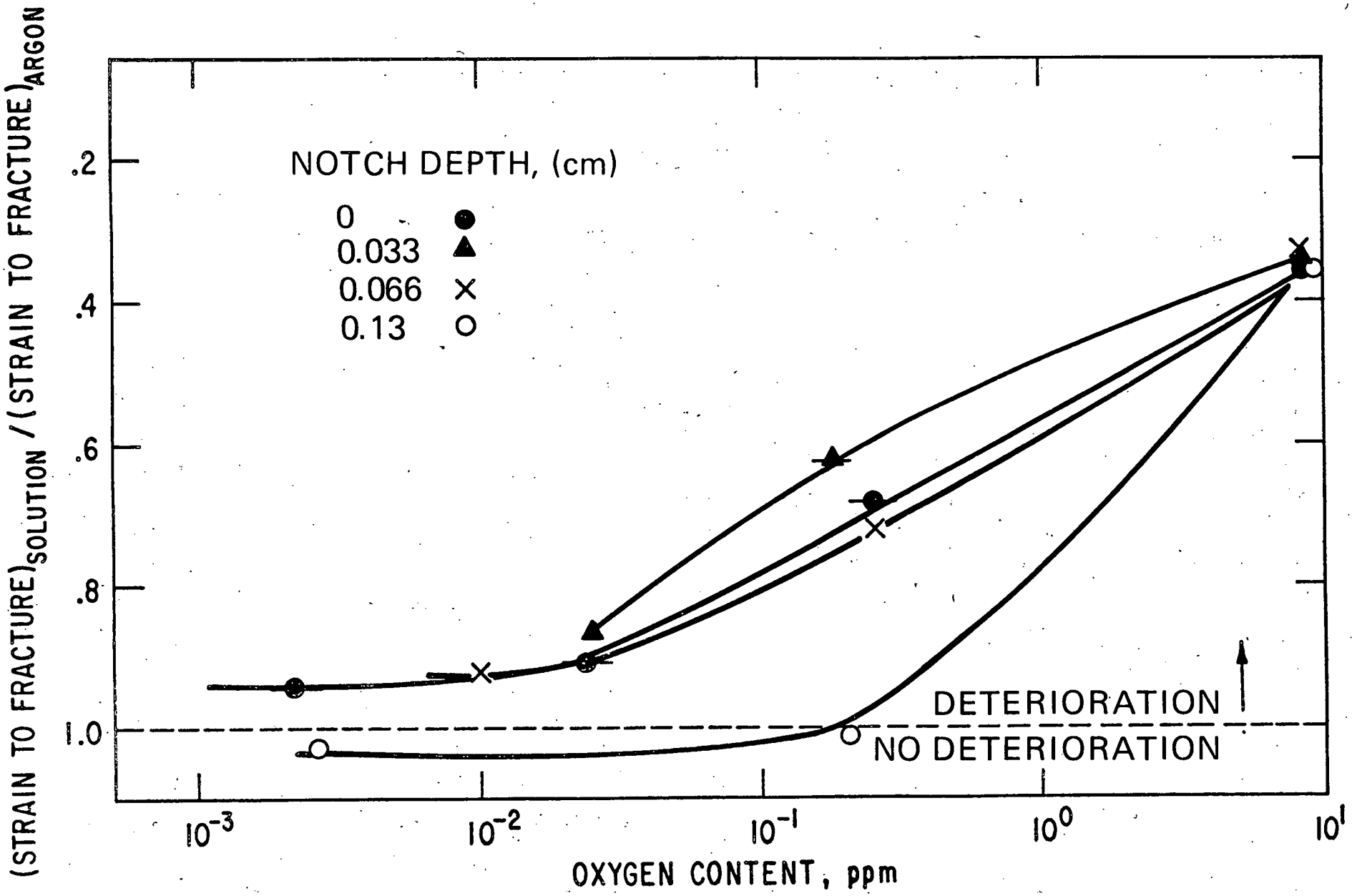

Figure 3-27. Variation of Ratio $\varepsilon_{f_{(solution)}} / \varepsilon_{f_{(argon)}}$ With Oxygen Content

rate is the same for all specimens (i.e., the stage II velocity); a rough calculation of the initiation time may be made via knowledge of the K_{ISCC} value for 8 ppm O_2 (in this case 0.33 $[MN/M^2]^{-3/2}$ (6 $ksi^{-3/2}$) has been used for the deepest notch and slightly higher- and elastically invalid-values for the shallower notches). Similar curves may be drawn for 0.01 ppm O_2/H_2O, making use of the fact that transgranular initiation seems to occur at relatively low strains (Figure 3-23).

Although the curves in Figure 3-25 (a and b) are only semiquantitative, they illustrate the hypothesis that the use of notched specimens should decrease the initiation period during the total testing time.

The basic objective of these preliminary tests is to evaluate the testing conditions to be used in subsequent investigations on the effect of amine and hydrogen additions on the stress-corrosion susceptibility. In the first quarterly report on stress-corrosion in 8 ppm O_2/H_2O it was shown that although some of the parameters usually quoted in CERT investigations (e.g., ratio of strain to fracture in solution to that in argon, GE stress-corrosion index, etc.) may mirror the observed stress-corrosion damage, the most foolproof method of examining the effect of environmental change was to measure the crack penetration directly on the fracture surface of the specimen. This conclusion is still applicable for the low oxygen solutions. For instance, crack penetration was observed fractographically in all oxygen-containing solutions (Figure 3-26) and although the ductility parameters extracted from the CERT data indicated a degradation in ductility with increasing oxygen content (Figures 3-27 and 3-28) they did not always give the required sensitivity to cracking - especially at low oxygen contents, e.g., see the data for the deep notched specimen in Figure 3-27 where no degradation of ductility is exhibited for the low oxygen solutions.

Consequently, in future experiments the measure of material degradation will be by fractographic examination. Tests will be conducted on circumferentially notched tensile bars, with a notch depth of 0.033 cm (0.013 in.). The notching is included since components will be flawed in service, and the test sensitivity (in terms of increment in crack penetration per change in oxidizing conditions) is greater for notched samples than smooth samples in low-oxygen solutions

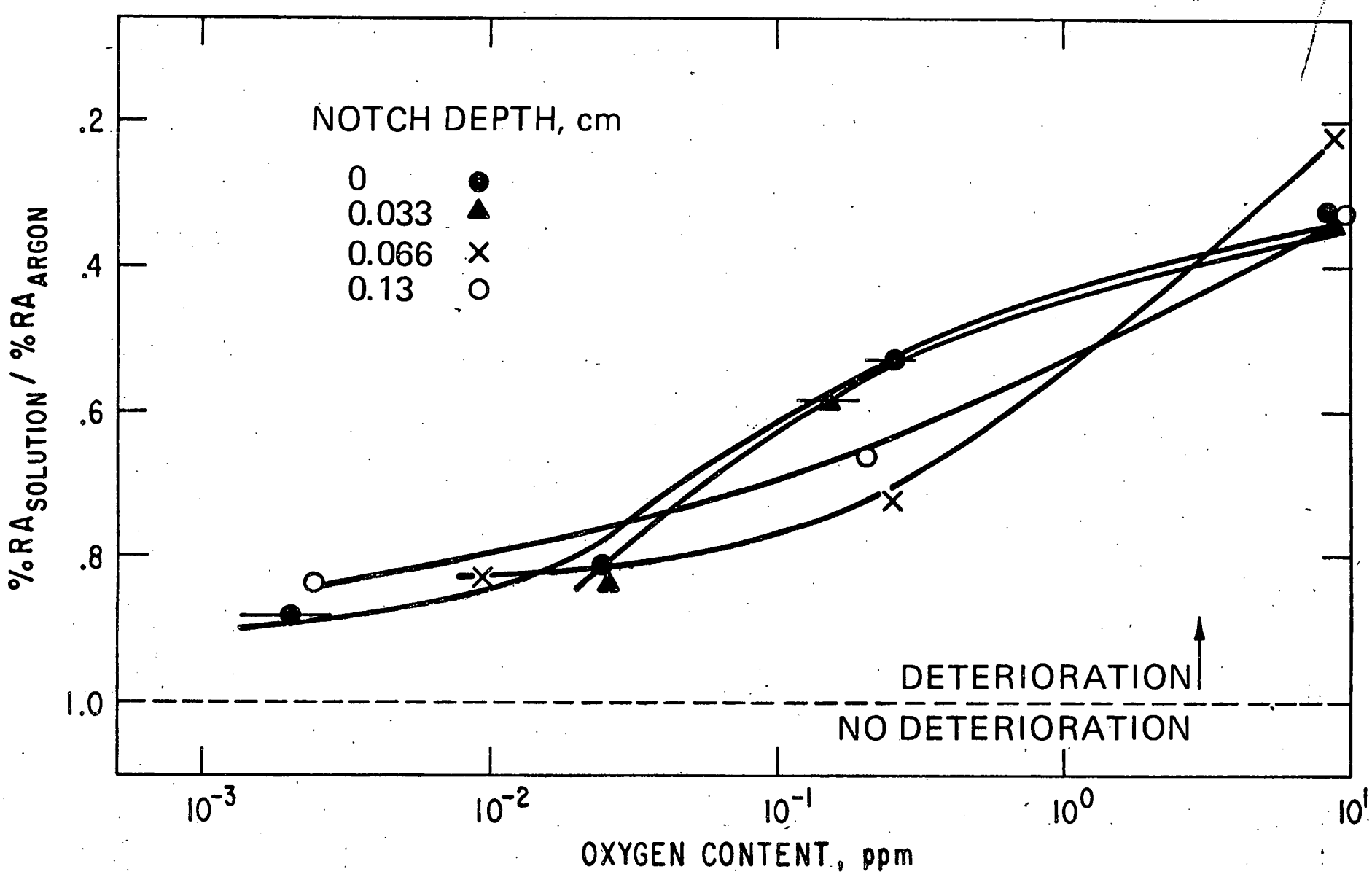

Figure 3-28. Variation of Ratio % RA (Solution)/% RA (Argon) with Oxygen Content at 288°C; $\dot{\varepsilon} = 1.3 \times 10^{-4}$ min^{-1}

(Figure 3-26). The choice of 0.033 cm notch depth allows a maximum testing time and hence a measurable penetration depth which can be examined for possible changes with ammonia or hydrogen additions.

The test matrix for future testing is given in Table 3-11. The program will be reviewed after test 1B13 to decide on the necessity for continuing with other amine additions.

Table 3-11

TEST MATRIX

		Reactor Water Concentration (ppm)		
Specimen	Notch Depth, cm	O_2	Additive	
1B1	0	0.01	-	
1B2	0	0.2	-	
1B3	0	0.2	20	NH_3
1B4	0	0.01	20	NH_3
1B5	0.033	0.01	20	NH_3
1B6	0.033	0.05	20	NH_3
1B7	0.033	0.2	20	NH_3
1B8	0.033	0.01	-	
1B9	0.033	0.05	-	
1B10	0.033	0.2	-	
1B11	0.033	0.01	0.2	H_2
1B12	0.033	0.05	0.2	H_2
1B13	0.033	0.2	0.2	H_2
1B14	0.033			
1B15	0.033	available for additional tests		
1B17	0.033			
1B18	0.033			

All tests at 288°C and $\dot{\varepsilon} = 1.3 \times 10^{-4}$ min^{-1}.

3.5.2.4 Conclusions

a. Stress-corrosion cracking can occur in sensitized Type-304 stainless steel in a dynamic CERT test at 288°C in water containing as little as 1 ppb oxygen. As the oxygen content decreases the crack propagation rate decreases also, and the crack morphology changes from intergranular to transgranular. The strain for transgranular crack initiation is probably lower than that for intergranular cracking and the nucleation density is higher in the former mode.

b. The sensitivity for detecting changes in crack penetration during CERT at low oxygen contents is improved by circumferentially notching the tensile bar specimens.

3.5.3 Straining Electrode Studies (M. E. Indig)

The addition of hydrogen to BWR primary coolant is a viable concept to eliminate the possibility of IGSCC of welded Type-304 stainless steel. From an electromechanical viewpoint, the presence of hydrogen with <10 ppb dissolved oxygen at 274°C should lower the corrosion potential of austenitic stainless steel to a value where welded and/or severely sensitized stainless steel would be immune to IGSCC. Previous testing has shown that as the potential of welded stainless steel is lowered, the susceptibility to IGSCC decreases. Figure 3-29 shows the combined effect of lowering the dissolved oxygen concentration on the potential of Type-304 stainless steel and the effect of the reduced potential on the susceptibility of welded Type-304 stainless steel to IGSCC. The stress corrosion data were obtained in straining electrode tests in an electrolyte of 0.01N Na_2SO_4 while the O_2/potential studies were conducted in pure water. To relate controlled potentials obtained in 0.01N Na_2SO_4 to the measured potentials in pure water, as was done in Figure 3-29, a correction factor of 0.150V was applied. The correction factor is necessary because at 274°C 0.01N sodium sulfate solution is more basic (pH 7.1) than pure water, (pH 5.75). The correction factor was calculated and then checked experimentally[8]. Using the correction factor and referring to Figure 3-29, $-0.400V_{SHE}$ in Na_2SO_4 at 274°C is equivalent to $-0.250V_{SHE}$ in pure water at 274°C. The

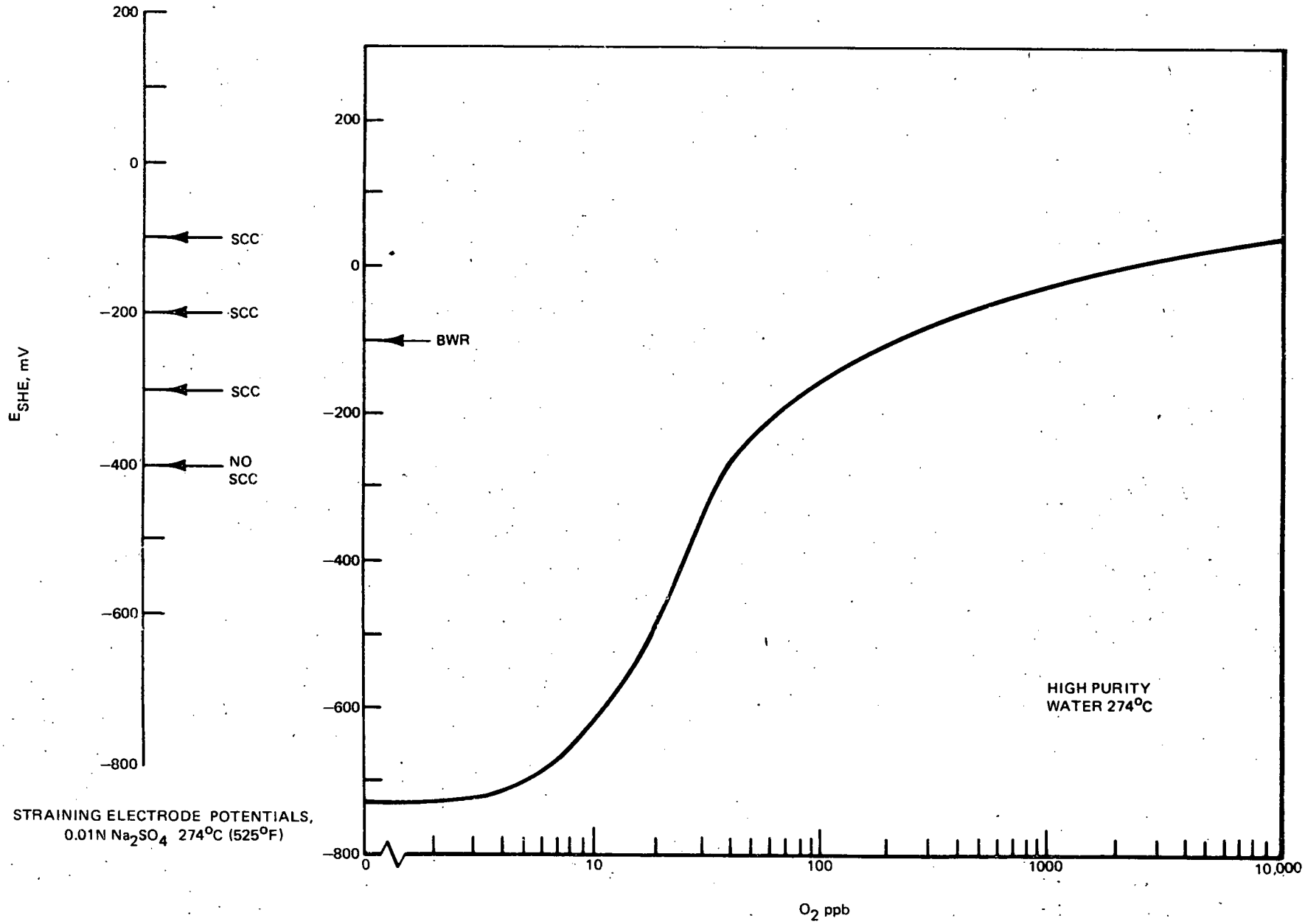

Figure 3-29. The Effect of Dissolved O_2 on the Corrosion Potential of T-304 Stainless Steel

latter potential is equivalent to a dissolved oxygen concentration of about 50 ppb at 274°C. The straining electrode experiments with welded stainless steel were performed with heat No. M7616. This particular heat is extremely susceptible to IGSCC in the as-welded condition.

In the series of experiments proposed to evaluate the effects of H_2 on stress corrosion, samples obtained from pipe welds (i.d. section preserved) were given a low temperature sensitization (LTS) treatment at 500°C for 24 hours, to further increase sensitization and susceptibility to IGSCC.

3.5.3.1 Planned Experiments

Three experiments are planned to determine the effects of hydrogen additions to water at 274°C on the IGSCC of welded +LTS Type-304 stainless steel. Figure 3-30 shows the three types of samples taken from portions of 10.16 cm (4 in.) diameter welded pipe. In the present studies the tensile sample with the weld centered in the gage section and the cylindrical electrode specimen were used. The first experiment, which has been concluded was a logical continuation of the series of straining electrode experiments performed at various controlled potential in 0.01N deaerated Na_2SO_4 at 274°C. The presence of hydrogen is simulated by an applied potential -0.75V from the corrosion potential. The cathodic potential is the electrochemical equivalent of about 4 ppm dissolved H_2 at 274°C. All experiments are performed in the straining electrode facility shown in Figure 3-31 at a strain rate of 2×10^{-5}/min.

The second experiment will be conducted in the same electrolyte, 0.01N Na_2SO_4, but with the potential controlled by the direct addition of hydrogen to the system rather than electrochemical control with a potentiostat. If required, a combination of chemical and potentiostatic control will be used.

The third experiment is to be performed in pure water at 274°C. In this experiment either pure H_2 or a mixture of H_2 and O_2 would be used to control the potential of the straining specimen. The potential of the straining

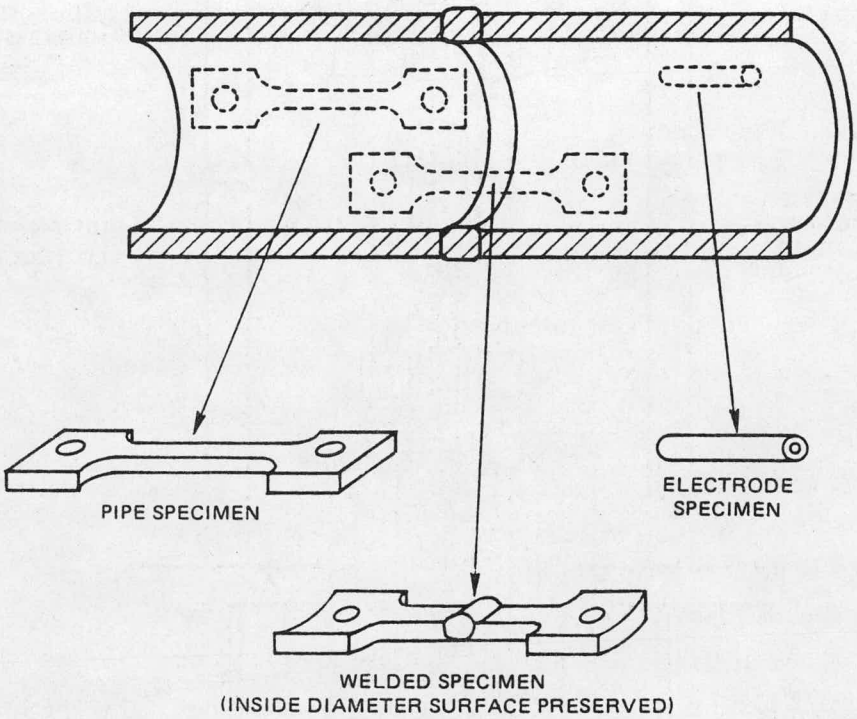

Figure 3-30. Test Specimens from Welded Schedule 80 Pipe

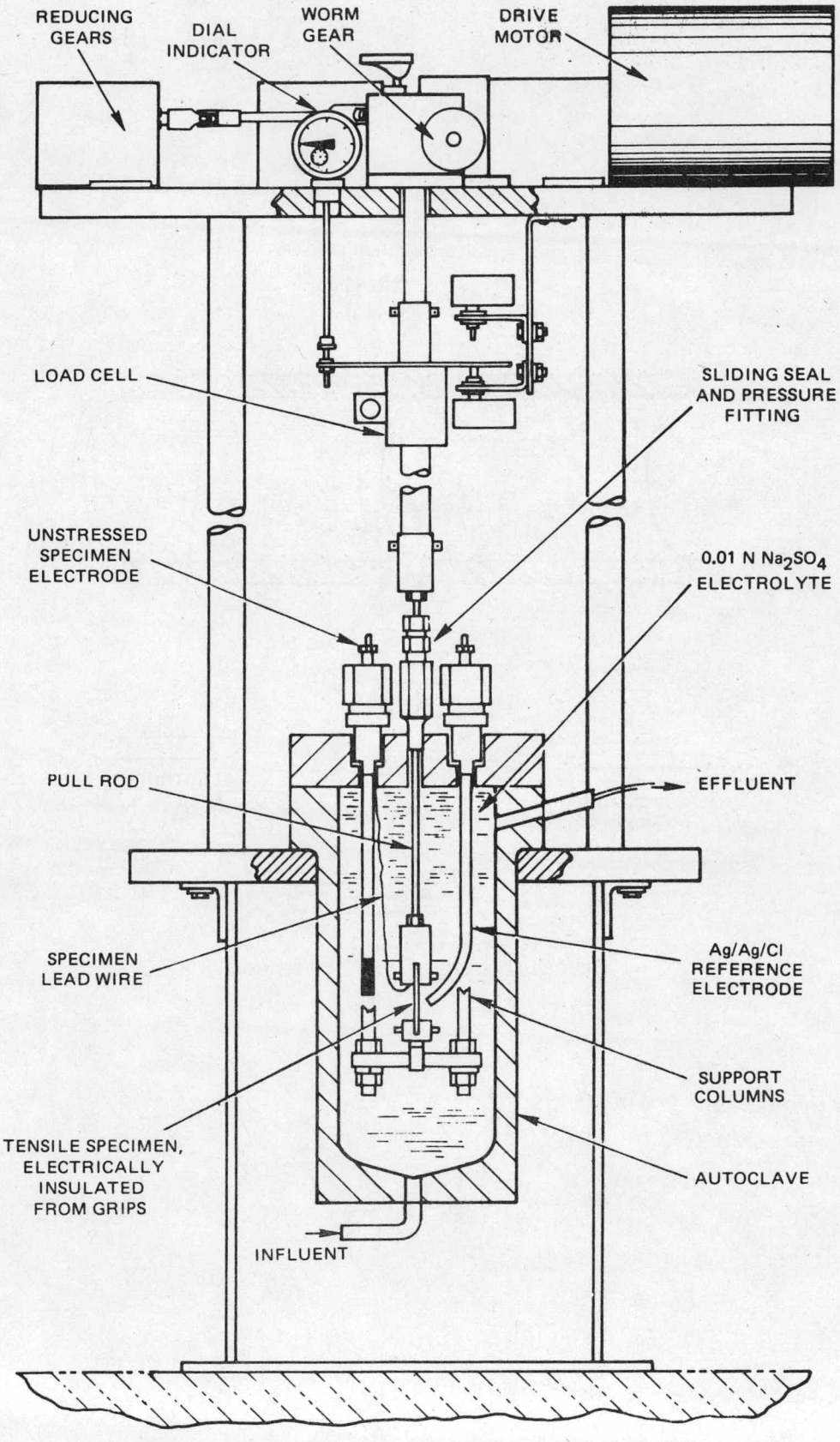

Figure 3-31. Straining Electrode Apparatus

specimen, an unstrained cylindrical electrode specimen of the same material (Type-304 stainless steel, heat No. M7616), and that of a platinum electrode would be monitored with a high temperature Ag/AgCℓ reference electrode.

3.5.3.2 Initial Results

The first of the three planned experiments has been completed. Post-test examination of the sample pulled to failure while under a control potential of -0.75 V_{SHE}, showed that the sample failed by ductile rupture, coalescence of microvoids, with no evidence of IGSCC. It should be noted that TG cracks occurred on all surfaces. These cracks are often associated with surface discontinuities and cold-worked areas, such as machined grooves on the i.d. section of the pipe. Previous studies in several laboratories have shown that these TG cracks can be expected to occur in constant extension rate or straining electrode testing. These cracks require considerable strain to initiate, (around 10%) and have no engineering significance. Figure 3-32 shows an example of such a TC crack at a machine groove. The deepest TG crack, Figure 3-33, about 0.25 mm, was located adjacent to the weld fusion line. The ductile nature of fracture located some distance from the heat affected zone is shown by scanning electron microscopy (SEM), Figure 3-34. Figure 3-35 and 3-36 show the general grain structure near the fracture and in the tab section of the sample. The elongated grains near the fracture are due to strain and the sensitized grain boundaries in both regions are clearly evident.

The mechanical properties obtained during test and in post-test examination are given in the bottom entries in Table 3-12. The other data in Table 3-12 were developed in earlier programs and show the effect of decreasing potential and the LTS heat treatment on IGSCC. The as-welded condition fails in a ductile manner at $-0.400V_{SHE}$ (equivalent to 50 ppb dissolved O_2) while the as-welded +LTS condition fails by IGSCC. At $-0.750V_{SHE}$ (H_2 simulation experiment) the mechanical properties indicate ductile failure for the as-welded +LTS condition.

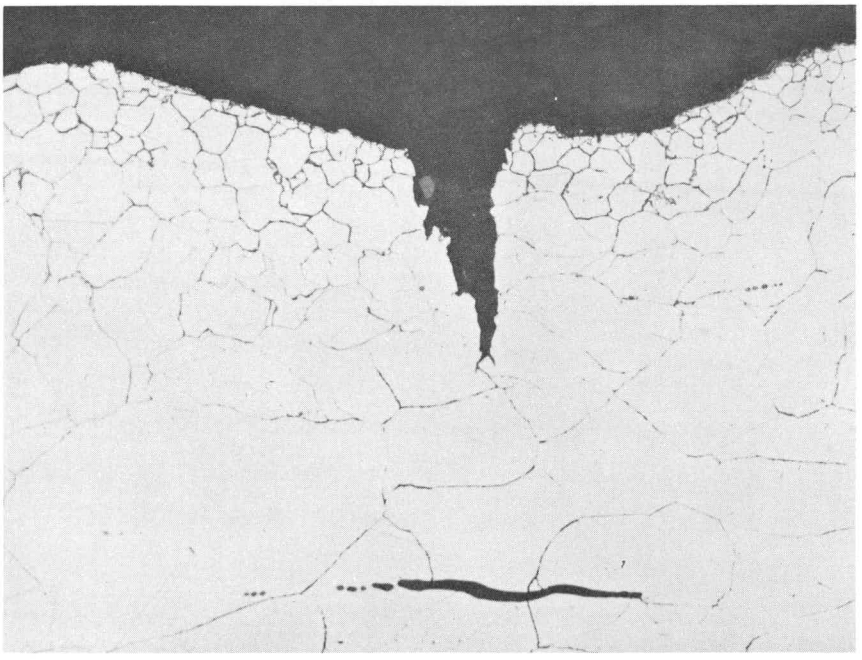

400X

Figure 3-32. Crack at Machine Groove

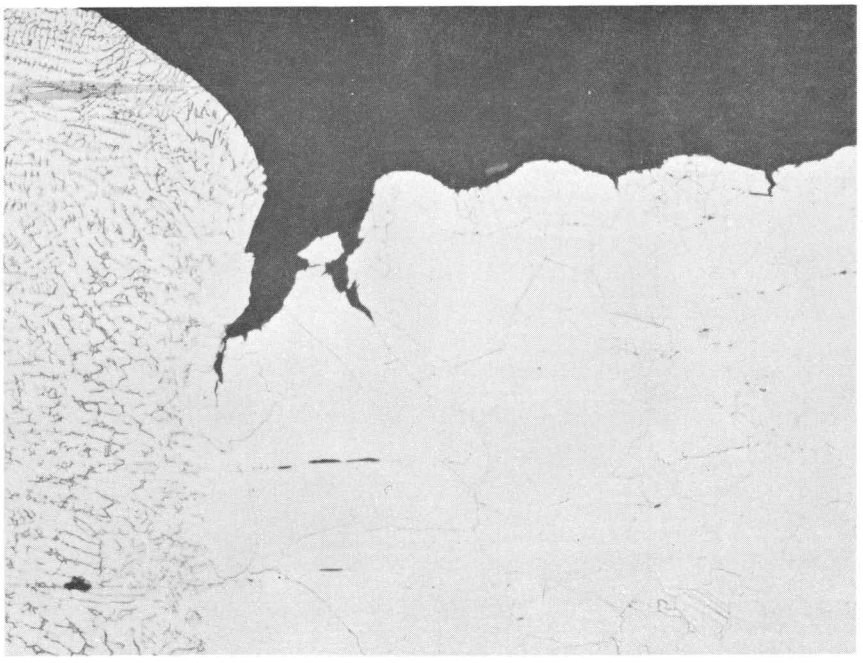

100X

Figure 3-33. Crack at Fusion Line

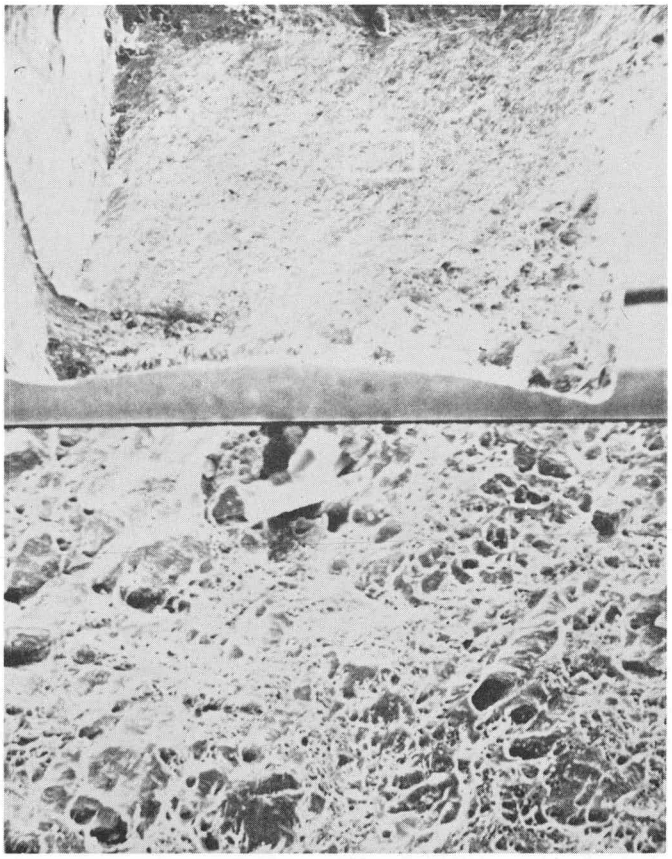

30/300X

Figure 3-34. SEM of Fracture

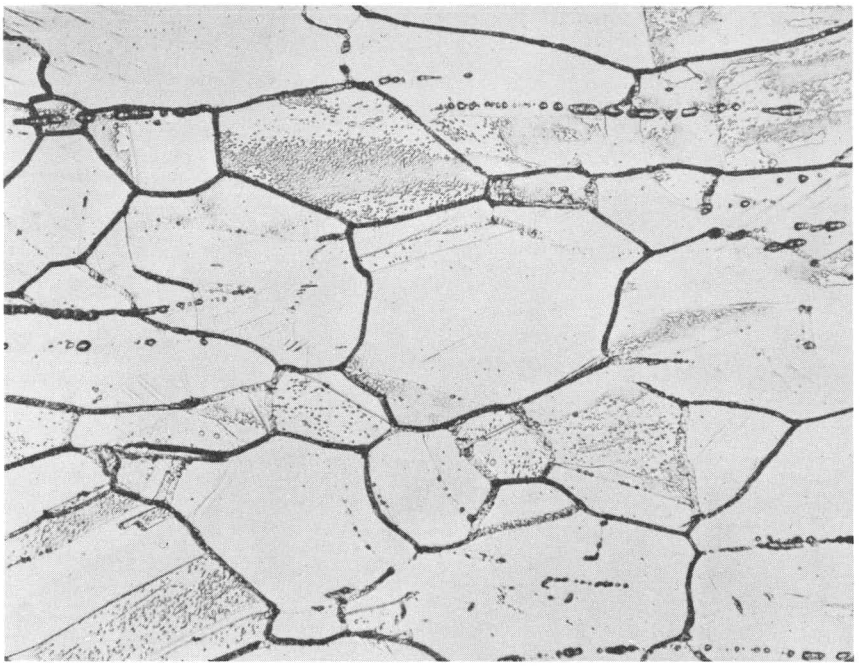

400X

Figure 3-35. General Microstructure Near Fracture

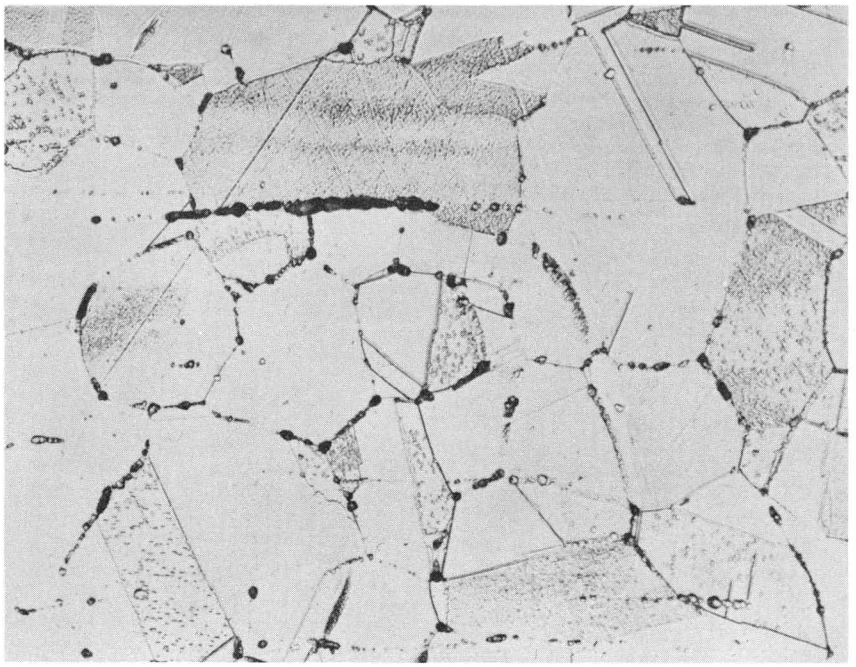

400X

Figure 3-36. General Microstructure in Tab Section

Table 3-12

STRAINING ELECTRODE[a] RESULTS FOR WELDED TYPE-304 STAINLESS STEEL (HEAT NO. 7616) AT 274°C IN 0.01N Na_2SO_4

Process Code[b]	Potential (SHE)	Fracture Stress (MPa)[c]	(ksi)	UTS[d] (MPa)	(ksi)	T_f[e] (H)	RA[f] (%)	Elong[g] (%)	Failure Morphology
W	-0.100	421	(61)	372	(54)	78	11.5	4.1	IGSCC
W	-0.300	614	(89)	448	(65)	161	26.7	10.4	0.7 IGSCC[h] 0.3 Ductile
W	-0.400	862	(125)	483	(70)	262	44.2	14.7	Ductile
W	-0.400	814	(118)	531	(77)	255	38.9	15.6	Ductile
W+grd+LTS	-0.100	317	(46)	276	(40)	39	5.0	1.6	IGSCC
W+LTS	-0.400	310	(45)	303	(44)	64	2.5	4.5	IGSCC
W+LTS	-0.450	545	(79)	455	(66)	234	26.7	7.9	IGSCC, Some Ductile
W+LTS	-0.750	669	(97)	489	(71)	216	26.6	13.6	Ductile, minor transgranular SCC

[a] Strain Rate of 2×10^{-5} min^{-1}

[b] W - Welded
grd - Ground
LTS - Low Temperature Sensitization (500°C for 24 hours)

[c] Maximum load/failure cross section. MPa = mega Pascal.

[d] Ultimate tensile strength - maximum load/original cross section

[e] Time to failure

[f] Reduction in area

[g] Elongation

[h] Initiated by short transgranular crack on i.d. machined surface.

3.5.3.3 Expected Results

The electrochemical measurements and the mechanical properties obtained during test and by post-test examination will be compared for the three proposed tests. With the foundation of previous testings and the results of the future tests, plans are to develop a potential/H_2 equivalency criteria to provide an environmental parameter where IGSCC could be avoided for severely sensitized austenitic stainless steel.

3.6 DEMINERALIZER PERFORMANCE (W. L. Lewis)

Objective. Current BWR practice is to employ hydrogen form (i.e., acid regenerated) cation exchange resin for the clean-up and condensate demineralizers. This practice can be continued when using hydrogen as the AWC additive; however, the cation resin will have to be changed to the ammonia form if NH_3 or N_2H_4 is the additive. Use of ammonia-form resins instead of the acid form reduces the demineralizer efficiency for ionic impurity removal. The impact of this reduced efficiency and any other accompanying performance change on both normal operational and shutdown clean-up system capability must be evaluated.

3.6.1 Hydrogen Additive

If hydrogen additive is used to suppress oxygen formation, the condensate will contain no new ionic species, and the currently used [H^+ - OH^-] cycle demineralizers will continue to be used. No change in performance would be expected.

3.6.2 Ammonia-Dosed Condensate Treatment

Calculations, for deep-bed ion exchangers, show that ammonia and hydrazine addition have highly deleterious effects upon ion-exchange capacity, efficiency, and regeneration requirements for both the cation and anion resins. These effects may be traced to: (a) the high ammonia loading of the condensate and

reactor water clean-up streams, (b) the high pH involved, and (c) the ionic species used for calculation. A brief summary of how the resins are affected is:

a. High Ammonia Loading

All of the ammonia carried over in the steam to the turbines was assumed to show up in the hotwell and to be converted to ammonium hydroxide on dissolution in water. The concentration of ammonia carried over to the hotwell, during ammonia addition is 37.3 ppm NH_3 (2.2×10^{-3} moles/liter). Using the equilibrium constant $K_b = 1.85 \times 10^{-5}$, the ammonium ($NH_4+$) ion concentration is 1.95×10^{-4} moles/liter. With this ammonium ion concentration, it is possible to calculate the time to ammonia breakthrough of the cation resins, and to judge whether to operate with resins in the ammonium form, the degree of regeneration required for nominal condenser leaks, bed life with a nominal condenser leak, and the amount of chemicals required to reach the desired degree of regeneration. A summary of the calculational results is presented in Table 3-13. The effects of high pH operation are summarized in Table 3-14.

b. Anion Resins

Similar calculations for the effect upon the anion resin of the high hydroxide ion concentration were completed. The equilibrium is shifted by the hydroxyl ion to a point where only a small fraction of the nominal anion exchange capacity is available. The results of the calculations of effects on the anion resins are also presented in Table 3-14.

c. Ionic Species Evaluated

Sodium and chloride were the ionic species chosen for evaluating the effects of additive injection, since definite limits exist for these species in the reactor water. As may be noted from Table 3-14, the capacity of the cation resin for sodium is very low for both the

Table 3-13

DEMINERALIZER SYSTEM SUMMARY

		Dresden	Quad Cities
A.	Condensate flow, kg/s	1.23×10^3	1.23×10^3
	(lb/hr)	9.77×10^6	9.77×10^6
	Type of Condensate Demineralizer	Deep Bed	Powdered
	Number of Vessels	6 + 1 spare	6 + 1 spare
	Volume of Exchange Resin/Vessel, m^3 (ft^3)	5.1 (180)	---
	Area of Holding Element/Vessel, m^2 (ft^2)	---	74 (800)
	Weight of Dry Resin/Vessel, kg (lb)	2040 (4,500)	73 (160)
	Volume Ratio of Ion-Exchange Resin, Cation:Anion	2:1	2:1
B.	Reactor Water Cleanup System (RWCU) flow, kg/s	82	13
	(lb/hr)	6.5×10^5	1.03×10^5
	Type of RWCU Demineralizer	Deep Bed	Powdered
	Number of Vessels	3	2
	Flow/Vessel, kg/s	82	8.2
	Volume of Resin/Vessel, m^3, (ft^3)	5.1 (180)	---
	Area of Holding Element/Vessel, m^2 (ft^2)	---	9 (93)
	Weight of Dry Resin/Vessel, kg	2050	8.5
	Volume Ratio of Ion-Exchange Resin, Cation:Anion	2:1	2:1

condensate and reactor water treatment systems. Typically, the affinity (selectivity coefficient) of ammoniated cation resins for sodium is approximately 0.77 (for NH_4 = 1.0). The resin is more selective for ammonia than for sodium and would require a higher degree of regeneration to prevent sodium slough than would be necessary for hydrogen form cation resins in neutral water.

A somewhat different procedure was used to determine the ammonia effect upon powdered resin systems. Extrapolated values for sodium capacity at the stream pH, 10.3 for condensate and 9.98 for reactor water, were applied to actual test data for powdered resin systems operating with [NH_4R-ROH] resins. The capacity of the cation resin for sodium to a 10% leak value varied nearly linearly with the influent sodium concentration but was affected to a greater extent by the system pH. The cation resin capacity was estimated to be

Table 3-14

EFFECT OF HIGH pH OPERATION ON DEEP-BED SYSTEMS

CONDENSATE TREATMENT	Cation Resin	Anion Resin
Time to ammonia break, hr/vessel	2.28	--
pH of influent water	10.3	10.3
Minimum active exchange sites required, %	99.82	97.
Maximum usable capacity, g/m^3 (as $CaCO_3$)	0.23	2.5
Operating capacity (assume 50% of above) g/m^3 (as $CaCO_3$)	0.12	1.3
Base level capacity (neutral) g/m^3 (as $CaCO_3$)	54	27
Run length, hr/vessel:	10	54
(With 12 gpm leak of cooling water containing 100 ppm NaC)		
Recommended regeneration levels, kg/m^3 resin	180 to 400 H_2SO_4	210 to 240 NaOH
Recommended NH_3 wash or purge, kg m/m^3 resin	110	80 to 100

Table 3-14

EFFECT OF HIGH pH OPERATION ON DEEP-BED SYSTEM (Continued)

REACTOR WATER CLEAN-UP

	Cation Resin	Anion Resin
Time to ammonia break, hr/vessel	21.4	--
pH of influent water	10	10
Minimum active exchange sites required,%	99.4	90.5
Maximum usable capacity, kg/m^3 as $CaCO_3$	4.7	20
Operating capacity (assume 50% of above), kg/m^3 (as $CaCO_3$)	2.4	10
Base level capacity (neutral) kg/m^3 (as $CaCO_3$)	84	39
Run length, hr/vessel (if condensate contains 10 ppb Na^+ and 12 ppb Cl^-)	84	218

decreased by a factor of 4 with an increase of 0.7 pH units. The anion resin capacity for chlorides appeared to be only dependent upon the concentration of the ionic species according to the test data with ammonium-hydroxyl form powdered resins. The calculated results of ammonia addition on powdered resin systems are presented in Table 3-15.

The effect of hydrazine was also evaluated. As the hydrazine breaks down, ammonia is formed and carried over with the steam to the hotwell. The amount of ammonia appearing in the condensate stream is approximately the same as for direct ammonia addition (36.7 ppm from hydrazine versus 37.3 ppm from ammonia). It is assumed that the values obtained for ammonia addition are applicable for hydrazine injection also.

3.7 TASK B-6. RADWASTE SYSTEM IMPACT (J. M. Jackson, T. Yuoh)

Objective. Predict the radwaste loads (amount and composition) accompanying the potential changes in water chemistry. Evaluate the effect of these

Table 3-15

EFFECT OF HIGH pH OPERATION ON POWDERED RESIN SYSTEMS

CONDENSATE TREATMENT	Cation Resin	Anion Resin
Time to ammonia break, hr/vessel	0.08	---
Influent water pH	10.3	10.3
Minimum active exchange sites required, %	99.97	99.5
Usable capacity to 10% break through, kg equivalents/kg resin	6×10^{-6}	2×10^{-3}
Run length, hr/vessel (with 5×10^{-4} m^3/s (8 gpm) cooling water leak at 40 ppb Na^+)	0.53	Controlled by Cation
REACTOR CLEANUP SYSTEM		
Time to ammonia break, hr/vessel	0.09	---
Influent water pH	10	10
Minimum active exchange sites required, %	99.4	90.5
Usable capacity to 10% leak, kg equivalents/kg	2.6×10^{-4}	2×10^{-3}
Run length, hr/vessel (if feed water contains 1.6 ppb Na^+)	9.4	Controlled by Cation

loads on equipment capacity, construction materials, processing sequence, etc. Determine the cost of the resulting, modified radwaste system.

This task has been delayed pending the optimization of the demineralizer systems as a result of the insights gained from the calculations reported in Task B-5 (Demineralizer Performance). Use of current standard performance criteria for GE BWR's such as ability to operate with a cooling water leak of 6×10^{-5} m^3/s (1 gpm) of sea water (or the equivalent amount of total salts if brackish or fresh water coolant is used) is clearly impossible for the high pH flow sheets with any reasonable radwaste volume. Consequently, additional constraints on leakage rate and composition are being formulated to determine whether a system with compatible and realistic condenser leak rate, condensate quality, and radwaste volumes can be achieved. Because of the greatly reduced resin capacity and increased regenerant strength, a nearly zero-leakage condenser will certainly be required. Immediate condenser tube repair will be necessary whenever a leak is detected; the plant will not have capacity for continued operation with even the slightest leak.

3.8 TASK B-7. INJECTION AND CONTROL EQUIPMENT

Objective. Identify the proper system locations for injecting the potential additives and the appropriate equipment for this purpose. Similarly, select the position for obtaining a representative sample of the additive concentration and the correct instrumentation for the measurement.

3.8.1 System Requirements (D. T. Snyder)

In response to queries from the design personnel assigned to do the detailed design of these systems, these criteria were established for the additive systems based on a plant with a thermal power rating of 2500 MW:

3.8.1.1 Location of the Injection Point

Hydrogen

The optimum injection point, in terms of water chemistry, is the suction of the reactor feed pumps. A secondary location would be the suction to the condensate booster pumps.

Ammonia

The optimum injection point is the suction of the condensate booster pumps.

Hydrazine

Because of the rapid decomposition of hydrazine at feedwater temperature, injection must be made as close to the reactor inlet nozzle as possible.

3.8.1.2 Flow Rate Ranges

Hydrogen

The system should be capable of injecting and dissolving up to 4×10^{-3} kg/s (30 lb/hr) of hydrogen in the feedwater.

Ammonia

The system should be capable of maintaining a flow of up to 0.22 kg/s (1,750 lb/hr) of ammonia (NH_3) into the feedwater.

Hydrazine

The system should be capable of maintaining a flow rate up to 0.19 kg/s (1500 lb/hr) of hydrazine in the feedwater to the core. (Injection of hydrazine to maintain small concentrations >8 ppb in the core exit water is not practical due to high thermal and radiolytic decomposition rates in the BWR environment.)

3.8.1.3 Space Limitation

The injection systems must be compatible with normal building and equipment layout.

3.8.1.4 Control Requirements

Hydrogen

The system should be designed to inject hydrogen into the feedwater proportionately with feedwater flow (i.e., directly related to plant feedwater flow signals). A reactor and feedwater sample system for dissolved H_2 will be required to calibrate and monitor the process. Several dissolved H_2 analyzers have been developed for special test use and could be reconstructed if no commercial systems are available.

Ammonia

The system should be designed to maintain a selected conductivity in the feedwater by ammonia addition. The conductivity controller sensor should be located downstream of the last feedwater heater. Ammonia and pH sampling equipment for reactor water and feedwater will be required to calibrate and monitor the system.

Hydrazine

Control of the hydrazine system would be similar to ammonia.

3.8.1.5 Degree of Automation

Hydrogen

The system should be automated to maintain an injection rate in direct proportion to feedwater flow. Special precautions should be included to ensure that no significant amount of free gas will be introduced to the pump suction. The system should be capable of operating unattended with weekly maintenance. A reactor scram must close off the hydrogen supply.

Ammonia

The system should be automated similarly to hydrogen with additional "scram" capabilities based on pH. Care should be taken to ensure that the system will not operate beyond limit conditions, as these conditions could cause an extreme change in water chemistry.

Hydrazine

Since this system is, for all practical purposes, an alternate method of ammonia addition, the same degree of automation is required as the ammonia system.

3.8.1.6 Comments on Hydrogen Addition Systems

Tests involving addition of both hydrogen and oxygen to the feedwater at the Humboldt Bay Plant of Pacific Gas and Electric Company were run in 1968-1969. The tests showed that bubbling the gas into the feedwater line through a 7-μm frit was not effective. The small bubbles coalesced to form large bubbles reducing the gas/water interface. This problem can be eliminated by injecting water with a high concentration of dissolved gas. Thus, dispersion of H_2 becomes a case of dilution. A system of this type is shown in Figure 3-37.

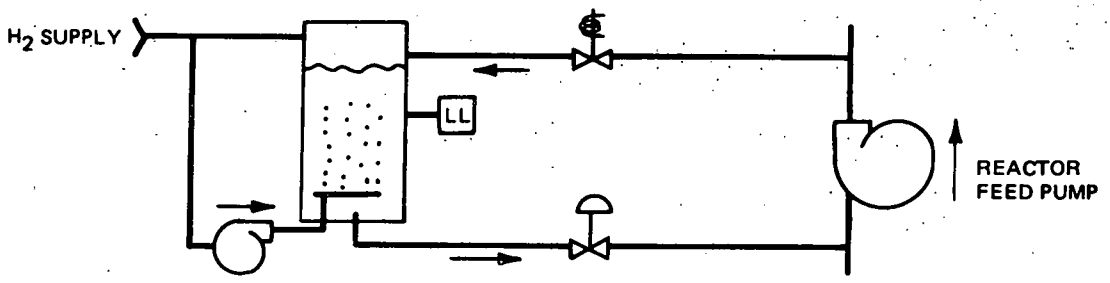

Figure 3-37. H_2 Addition System

The discharge of the plant reactor feed pumps (RFP) or condensate booster pumps (CBP) supplies water to the tank which is maintained near pump pressure. Liquid level control is made by injecting or venting H_2 gas. Hydrogen-saturated water is injected proportionately to feedwater flow into the suction of the pump. The table below indicates the desirability of the reactor feed pumps (RFPs) for gas injection:

Pump	MPa	Pressure (psig)	Water Vapor Pressure MPa	Temperature (°C)	Equilibrium Liquid Concentration (ppm H_2)	Percent of Total Feedwater Flow Required
RFP	8.6	(1250)	0.46	150	185	1.2
CBP	2.1	(300)	0.0055	34	31	6.9

3.8.2 Hydrogen Addition System Design (J. D. Seymour, N. A. Fedrick)

An extensive literature search has been performed to find data on the solubility and rate of solution of hydrogen in water at elevated temperatures and pressures, and design correlations for sizing the necessary mass transfer equipment.

The literature reveals little information other than the fact that a bubble column (versus a packed tower) seems to be the equipment of choice. The mass transfer coefficient is higher and the column more efficient when the gas solubility is very low and the gas-to-liquid ratio is small, as is the case with hydrogen. In a separate telecon with Berkeley Chemical Engineering Department, this finding was independently confirmed.

Many specialty gas and mass transfer equipment manufacturers were contacted also regarding physical data for hydrogen at high temperatures and pressures. Most of the contacts were futile as the physical data required for computation, e.g., solubility in water, diffusivity, etc., seem to be nonexistent at the temperatures and pressures of interest. Several of the vendors have agreed to send what data they have.

Currently, sizing of the bubble column is proceeding with the design correlations and data available. Most of the correlations and data have been extracted from standard texts, and are applicable at a variety of conditions and for a variety of gas-liquid systems. This approach will allow a preliminary sizing of the column which will be revised and supplemented if and when new physical and design data are received.

3.9 TASK B-8. OPERATIONAL CONSIDERATIONS - SAFETY/TOXICITY HAZARDS (R. Stevens)

Objective. Consider the effect of each of the additive approaches on normal plant operation, e.g., additional manpower requirements, subcontracted service work, special safety or toxicity precautions, employee acceptance, etc. Enter these factors into the selection criteria.

3.9.1 Ammonia, Hazards and Precautions

At room temperature ammonia is a colorless alkaline gas with a pungent odor detectable in air down to about 20 ppm by volume. To meet the consumption rates presently predicted, the ammonia would be purchased and stored in bulk as liquid anhydrous ammonia at a pressure of 0.89 MPa (129 psia) at 21°C (70°F). The following subjects present the hazards and some of the precautions for use and storage of anhydrous ammonia.

3.9.1.1 Pressurized System

Liquid anhydrous ammonia is stored under pressure usually in the saturation range of 0.89 MPa. The storage and transport systems should be designed for these

pressures. Materials of construction should be steels. Copper, tin, zinc or their alloys should be avoided since water-ammonia mixtures readily attack and corrode these materials. Joints should be welded where possible to help eliminate leakage problems. Ammonia systems should be pressurized and leak tested prior to use.

3.9.1.2 Compressed Gas

The cooling due to vaporization of ammonia is sufficient to cause frostbite if personnel come in contact with the liquid ammonia due to spills or system leaks. Personnel should be alerted to these hazards.

3.9.1.3 Fire/Explosive Hazard

Ammonia gas is flammable in air in the range of 15 to 28 volume %. Therefore, precautions should be taken to avoid these mixtures and ignition sources in the areas where ammonia is stored and used.

Heat sources should be eliminated from the storage area for flammability control as well as to avoid pressurizing the storage vessel beyond design limits. Ventilation should be provided in these areas. The areas should also be monitored for high levels of ammonia (7% or higher) with automatic shut-offs in the ammonia supply. Ignition sources should be eliminated where possible. Ammonia fires may be extinguished by first shutting off the source of fuel (ammonia) and then smothering flames with carbon dioxide, or with a water spray.

3.9.1.4 Toxicity

Ammonia is classified as a highly toxic substance by skin contact, inhalation and ingestion. The recommended threshold limit value (TLV) as set by the American Conference of Governmental Industrial Hygenists (ACGIH) is 50 ppm in air by volume.

Personnel working with or in the area of an ammonia system should be trained in hazards and handling of ammonia. Personnel working with ammonia should wear rubber gloves, chemical goggles, and a rubber or plastic apron.

Areas where ammonia is used should be monitored for levels of NH_3 of 25 ppm or higher. For personnel safety, emergency eyewash and shower facilities should be available. Bureau of Mines approved gas masks or other emergency breathing apparatus should also be available for use in emergencies. Ventilation should be used to keep ammonia levels below the TLV.

3.9.1.5 Other Hazards

Ammonia reacts with mercury and silver to form explosive compounds, therefore, instrumentation containing mercury or silver should not be used in an ammonia environment.

3.9.2 Hydrazine, Hazards and Precautions (N_2H_g)

At room temperature hydrazine is a colorless, oily liquid with a vapor pressure of (1330 Pa (10 mm Hg). The vapor has an odor similar to that of ammonia. The bulk quantities required based on present estimates can be stored at room temperature as a liquid in an enclosed system with a nitrogen cover gas. The following subsections present hazards and associated precautions.

3.9.2.1 Fire/Explosion Hazards

Hydrazine in solution has a flash point which varies from 52°C at 100% hydrazine by weight (anhydrous) to 110°C at 40% hydrazine by weight. Below 40% hydrazine the solution will not flash. Heat sources should be eliminated from the immediate storage area. The solution temperature should be kept below 37°C, monitored, and alarmed if the temperature exceeds this valve.

Hydrazine vapor is flammable in air in the range of 4.67 to 100% by volume. Sources of ignition such as flame, or sparks from electrical equipment

should be eliminated in the hydrazine storage area. Hydrazine should be stored in closed containers under nitrogen cover gas. Hydrazine systems should be initially purged with nitrogen prior to the introduction of hydrazine to avoid explosive mixtures. Areas where hydrazine is used should be monitored and controlled at levels of 2.3% or lower hydrazine vapor by volume. To prevent formation of explosive mixtures, hydrazine storage and transport systems should be constructed of type 304 (or type 347) stainless steel since hydrazine will attack 316 stainless steel and mild steels.

Hydrazine fires can be smothered by the use of foam, carbon dioxide or dry chemicals. Water may also be used since it dilutes the hydrazine and provides cooling.

3.9.2.2 Toxicity

Hydrazine is classified as a high personnel hazard by skin contact, inhalation or ingestion for both short term and chronic exposure. The ACGIH recommends TLV is 1 ppm by volume in air. As reported in the July 19, 1978 issue of Chemical Week, recent findings on cancer producing effects of hydrazine and its derivatives* have led The National Institute for Occupational Safety and Health to Recommend the much lower limit of 30 ppb by volume.

To meet present limits, hydrazine usage areas should be monitored to maintain vapor at 500 ppb or lower. If the new lower limit of 30 ppb is invoked, the monitoring should be for 15 ppb or lower.

Areas should be well ventilated. The Bureau of Mines approved gas masks or emergency breathing apparatus should be provided in hydrazine storage and use areas.

Rubber gloves, chemical goggles and protective aprons should be provided for personnel working with hydrazine systems. Emergency eyewash and showers should also be readily available.

*"Hydrazine Limits", Chem. Week, July 19, 1978, p. 24

3.9.3 Hydrogen Hazards and Precautions

At ambient pressure and temperature hydrogen is a colorless odorless gas. In the quantities required for this program, it would be purchased and stored in liquified form at about 0.83 MPa (120 psia) and -253°C. The liquid hydrogen would be vaporized by drawing a portion of the liquid into an ambient vaporizer.

The hazards associated with such a hydrogen system are explained in the following subsections.

3.9.3.1 Fire/Explosive Hazard

The flammability limits of mixtures of hydrogen gas in air are 4.0% (lower) to 74.2% (upper) by volume. The precautions to prevent ignition or detonation in the atmosphere are three-fold:

a. Eliminate Leaks from Hydrogen Storage and Transport Systems - these systems should be constructed of austenitic stainless steel (types-304, -304L, -308, -316, and -321). Back-welded threaded joints should be used in the piping system to prevent leaks. Piping and storage systems should be helium leak checked prior to initial introduction of hydrogen.

b. Provide Ventilation and Monitor Interior Areas to Avoid Explosive Mixtures - the storage system including the liquid storage vessel and the vaporizer should be located outdoors. Any cover provided should not have inverted pockets where rising hydrogen might collect, and should be open for natural ventilation.

   Indoor areas in which hydrogen is transported or injected should be monitored and maintained by use of ventilation below a level of 2% by volume in air.

c. Eliminate Sources of Ignition. Potential sources of ignition are friction or impact sparks, electrical sparks (including static

electricity) and heat or flame sources. These hazards should be reduced as much as possible.

(1) Friction and Impact Sparking. No work should be done in hydrogen storage and transport/injection areas if it can be moved and completed elsewhere. Work that must be done in these areas on equipment other than the hydrogen system, can be done provided assurance is made that the ventilation and monitoring systems are in operation and that the hydrogen level is maintained below 2%. (Note: welding or torch cutting should never be done in hydrogen system areas, without first shutting down the system, emptying the hydrogen vessel or lines and then thoroughly purging with helium. Note: Nitrogen may be used on gas lines.) Work should be done on the hydrogen system only after it has been shut off and purged with nitrogen, or helium for the cryogenic portions of the system. Without shutdown, work may be done on the hydrogen system provided that it will not affect the system integrity. When work is done in hydrogen areas, care should be taken to prevent sparking caused by rough contact or handling of tools or equipment. "Spark proof" tools are available, and should be used, though their effectiveness has been questioned by the National Aeronautics and Space Administration (NASA).*

(2) Electrical Sparks. Static electrical sparking may be reduced by grounding all metal parts and connections and using conductive belting on rotary machinery. Personnel while working in these areas should wear cotton clothing rather than synthetic fabrics, should not comb hair, and should ground themselves before entering the area. Outdoor hydrogen storage and transport facilities should be protected by use of lightning rods, aerial cables, and ground rods.*

*NASA Technical Memorandum TMX-52454, 1968
**National Bureau of Standards Handbook 46, "Code for Lightning Protection"

(3) Electrical Equipment and Controls Should Be Avoided in the Storage Area. Pneumatic controls should be used wherever possible. If electrical controls are required, they should be constructed and enclosed in "Explosion Proof" housing in accordance with Article 501 of the National Electrical Code (NEC) for Class I, Division 2 locations. Electrical equipment in hydrogen transport or injection areas should meet Article 501 of NEC, Class I, Division 2.

(4) Heat or Flame Sources. Heating for vaporization should be provided by steam or hot water, avoiding direct flame or electrical heating. Absolutely no welding, brazing or torch cutting should be permitted in hydrogen storage or usage areas without first shutting down and purging the involved portion of the hydrogen system with helium. Nitrogen may be used for gas phase portions of the system.

(5) Instrumentation or equipment which uses or generates high temperatures should be eliminated from hydrogen storage, transport and injection system areas.

(6) System internal explosion and fire hazards should also be avoided. This may be done by purging all storage and transport systems prior to introduction of hydrogen. Gas-phase portions of the system may be purged with nitrogen. Helium should be used to purge storage and vaporization systems. The cryogenic portion of the system (the storage tank and vaporizer) must be particularly protected from trace amounts of air since the extreme low temperatures could freeze the air, forming a solid which could block valves and prevent venting, and which also would have the potential for explosive recombination with the hydrogen. Nitrogen will also freeze and potentially plug vents and valves at the temperature of liquid hydrogen, and should not be used for final purging or pressurization of the storage vessel or vaporization system.

3.9.3.2 Cryogenic System Hazards

In addition to the explosive hazards, the extreme low temperature system offers other hazards. Ambient heat leakage into the storage vessel constantly vaporizes hydrogen liquid, so the system must provide vents to avoid pressure buildup in the vessel. These vents shall be located such that they do not offer additional hazards.

3.9.3.3 Personnel Hazards

Hydrogen is not considered a toxic substance. The personnel hazards associated with hydrogen are:

a. Hydrogen may replace oxygen in an enclosed area and cause asphyxiation. Enclosed areas should be monitored and controlled to maintain below 2% hydrogen by volume.

b. Super-cooled surfaces and gases due to leaks in cryogenic systems. Liquid hydrogen spills offer extreme personnel hazard from possible contact with the liquid of supercooled vapor in the area of the spill as well as the explosive hazard.

c. Hydrogen burns with an invisible flame and personnel should be alerted to approach areas of potential hydrogen accumulation with caution.

3.9.3.4 Fire Fighting

Extreme care must be taken in methods for extinguishing hydrogen fires, since an erroneous approach could increase the hazard and potential damage. Before any attempt is made to extinguish flames, the flow of hydrogen should be stopped. If the flow has not been stopped, and the flame is extinguished, a combustible mixture will probably buildup and the resulting explosion would cause more damage and reignite the fire. Prior to shutoff of hydrogen source and extinguishment of hydrogen flame, a water spray should be used to extinguish secondary fires and cool surrounding equipment.

3.10 TASK B-9. ADDITIVE CONSUMPTION AND SOURCE - (T. L. Wong)

Objective. Predict the consumption of each additive as a function of required coolant concentration and the consequent increase in plant operating cost from the use of each of the chemicals.

The effort on the additive-consumption task has been directed toward obtaining data on costs, recommended form and availability for the proposed additives and sizing a hydrogen-separation adsorption system.

3.10.1 Additive Consumption and Cost

The cost, form and availability information for the presently estimated usage quantities are tabulated in Table 3-16 for the three additive candidates.

3.10.2 Hydrogen Recycle

Preliminary calculations were made to size a swing-cycle adsorption system for hydrogen separation. A simplified schematic of the hydrogen separation system is shown in Figure 3-38. The major components of the system are:

a. Recombiner. This unit will be used to recombine all the oxygen produced radiolytically or obtained from air inleakage with a portion of the hydrogen. The effluent stream from the recombiner will be (0.032 m^3/s (69 scfm) consisting essentially of 76.7 and 23.3 vol % hydrogen and nitrogen, respectively. These values are for the 10 ppb oxygen case.

b. Gas Pretreatment. Impurities such as nitrogen oxides and carbon oxides will be removed as needed. In addition, bulk water removal and fine drying with a desiccant dryer will be accomplished in this portion of the system prior to routing the gas stream to the hydrogen separation portion of the system.

Table 3-16

COST, FORM AND AVAILABILITY DATA

1. Ammonia

   A. Estimated usage: 0.13 kg/s (1000 lb/hr)

   B. Form: Anhydrous ammonia - available in bulk, pressurized liquid in tank truck or railroad car

   C. Cost: $0.11/kg ($100/short ton)

   D. Availability: Bulk anhydrous is readily available via rail tank cars, tank truck (also pipeline in the Midwest)

2. Hydrazine

   A. Estimated usage: 0.13 kg/s (1000 lb/hr)

   B. Form: Aqueous hydrazine - 64, 54.4, or 35% N_2H_4 solution

   C. Cost: $2.20/kg ($1.00/lb) of 54.4% hydrazine by weight

   D. Availability: Hydrazine is not presently produced in the bulk rates which would be required according to estimated consumption rate

3. Hydrogen

   A. Estimated usage: 3×10^{-3} kg/s (21 lb/hr)

   B. Form: The recommended method of handling the large quantity required would be to store as liquid hydrogen in a rechargeable vessel.

   C. Cost: $0.28/$m^3$ at STP ($0.80/100 standard cubic feet)

   D. Availability: Bulk hydrogen is generally available, including ability to recharge liquid hydrogen storage facilities

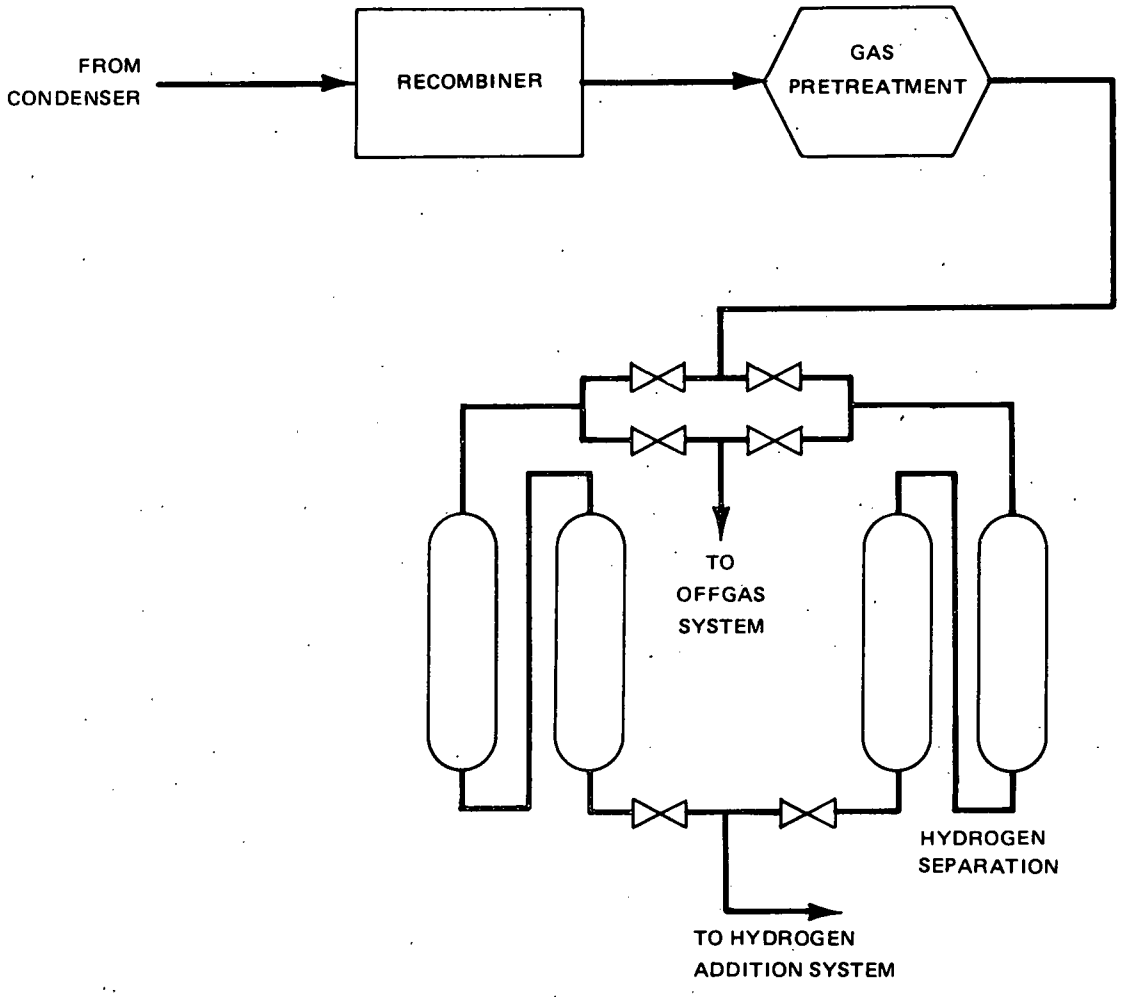

Figure 3-38. Swing-Cycle Adsorption Hydrogen Recycle System

c. Hydrogen Separation. This portion of the system will separate the hydrogen from the nitrogen, using a pressure cycle for regeneration. The steps in the hydrogen separation process are:

(1) Adsorption Cycle. Nitrogen is adsorbed at low temperature and high pressure on an adsorbent such as activated carbon until breakthrough. At that point, the feed gas is diverted to a fresh column and the saturated column is regenerated at low pressure. The relatively clean hydrogen gas obtained during the adsorption cycle is used for hydrogen addition to the reactor feedwater.

(2) Desorption Cycle

(a) The nitrogen adsorbed on the adsorbent (which is still maintained at low temperature) is removed by depressurization of the column. The depressurization is conducted in the reverse direction of flow. During this regeneration period, the nitrogen gas containing low levels of hydrogen which has been coadsorbed on the adsorbent during the adsorption cycle is routed to the offgas treatment system.

(b) The second desorption step is used to clean up the column in preparation for the next adsorption cycle. This is accomplished by purging the bed with clean hydrogen from the parallel adsorbing column. The purge flow rate is small and the purge operation is conducted with the column at low temperature and low pressure. The effluent gas generated during this operation is recycled back to the parallel column. Calculated results for a hydrogen separation adsorption system using a 2-hour cycle show that ∿7300 kg of activated carbon are required. This requirement is based on an adsorption-cycle temperature of -79°C and pressure of 1 ata (The adsorption coefficient for nitrogen on activated carbon at these operating conditions is about 80 cc (STP)/gm

of carbon). The quantity of activated carbon required would be reduced at a higher adsorption pressure. For the 1-ata case, the desorption cycle will be conducted under vacuum and -79°C during both the nitrogen recovery and purge steps.

The results discussed are presented as an illustration. If an adsorption system appears to be an attractive choice for hydrogen separation, experimentation will be required to define system parameters such as temperature, adsorption pressure, desorption pressure, cycle time and adsorbent type.

4. REFERENCES

1. E. L. Burley, Alternate Water Chemistry Program - Quarterly Report 2, January 1 to March 31, 1978, to be published (NEDC-23856-1).

2. F. Carlson, "Experiment RZ-S519, Radiochemical Studies Concerning the Cooling Medium under BWR Conditions", AE-MK-592, ASEA-Atom.

3. L. Hammar, et al., "Water Chemistry Research at the Halden Boiling Heavy Water Reactor (HBWR)", HPR55 (June 1967).

4. W. G. Burns, and P. B. Moore, "Radiation Enhancement of Zircaloy Corrosion in Boiling Water Systems: A Study of Simulated Radiation Chemical Kinetics", International Conference BNES, Bournemouth, October 24-27, 1977.

5. V. Kolba, "EBWR Test Reports", AN66229 (November 1960)

6. R. J. Law, "Off-Gas Baseline Impurity Studies - Test Plan and Procedure", TP 521.0393, August 16, 1978.

7. A. K. Agrawal, et al., Paper No. 187, "Stress Corrosion of Sensitized and Quench Annealed 304 S/S In High Purity Water," Corrosion '78 Conference, Houston, Texas, March 1978.

8. M. E. Indig and A. R. McIlree, High Temperature Electrochemical Studies of the Stress Corrosion of Type-304 Stainless Steel, May 1978 (NEDO-12709).

Uncited References (Subsection 3.9)

1. N. I. Sax, "Dangerous Properties of Industrial Materials", Van Nostrand-Reinhold Co. - New York 3rd Edition, 1968.

2. "Hydrogen Safety Manual", NASA Technical Memorandum TMX-52454, NASA, Washington, DC, 1968.

3. "Matheson Gas Data Book", Matheson Gas Products, East Rutherford, New Jersey, 5th Edition, 1971.

4. "Storage and Handling of Aqueous Hydrazine Solutions", Olin Chemicals, Stamford, Connecticut, 1975.

5. P. G. Stecher, "The Merck Index", Merck & Co., Rahway, New Jersey, 8th Edition, 1968.

6. H. F. Coward, and G. W. Jones, "Limits of Flammability of Gases and Vapors", Bureau of Mines Bulletin 503, 1952.

7. M. G. Zabetakis, "Flammability Characteristics of Combustible Gases", Bureau of Mines Bulletin 627, 1965.

8. "Cryogenics Safety Manual - A guide to Good Practice". British Cryogenics Council 1970.

DISTRIBUTION

Name	M/C
L. D. Anstine	V04
R. G. Bock	110
E. L. Burley (25)	585
R. N. Carter	H02
J. D. Clark	772
R. L. Cowan	407
W. R. DeHollander	110
C. F. Falk	165
P. Ford	SCH
B. M. Gordon	138
G. M. Gordon	138
R. Hanneman	SCH
H. R. Helmholz	V04
M. Indig	V17
C. E. Kent	772
R. J. Law	V15
J. C. Lemaire	138
W. L. Lewis	772
M. F. Lyons	110
W. G. Myers	154
L. E. Nesbitt	761
G. F. Palino	V04
H. H. Paustian	151
H. Pellow	110
W. Pitt	195
D. R. Rogers	165
R. R. Roof	870
C. P. Ruiz	V04
M. Siegler	585
J. M. Skarpelos	110
L. L. Sundberg	585
J. S. Wiley	110
C. D. Wilkinson	164

DISTRIBUTION (Continued)

Name	M/C
T. L. Wong	585
J. C. Blomgren (10 Commonwealth Research Corp. 1319 S. First Ave. Maywood, IL 60153	
NEG Library (5)	328
VNC Library (1)	V01